Multiscale Models for Sea Ice

Ken Golden, University of Utah

Mechanical & Civil Engineering Seminar
Caltech, December 4, 2025

Sea ice is a multiscale fluid-solid composite.

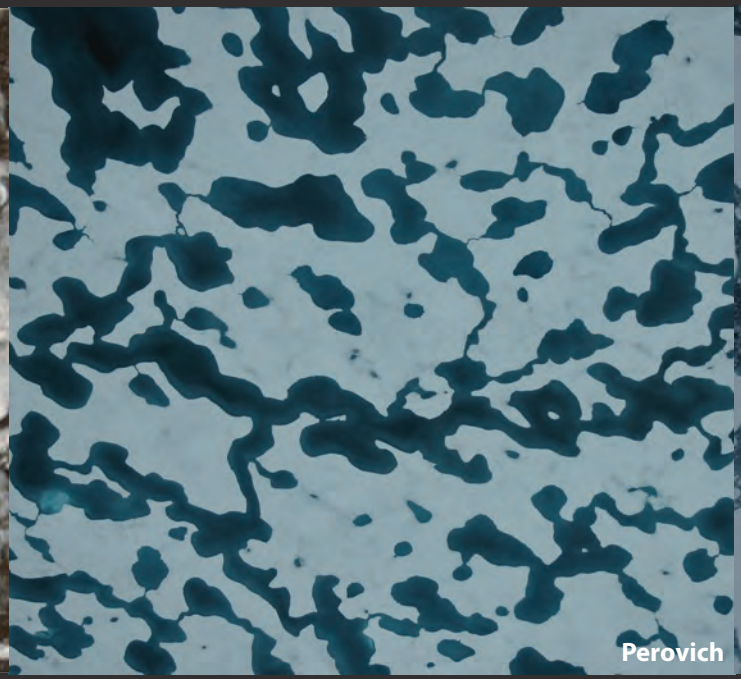

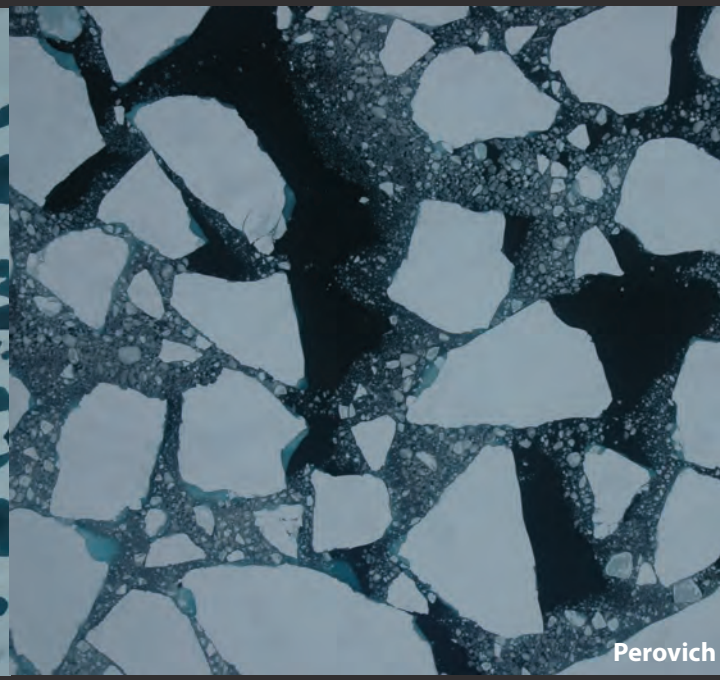

micro meso macro

composites & metamaterials

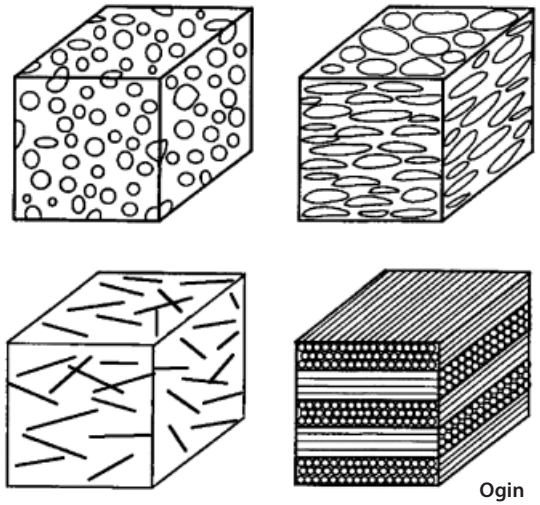

Ogin

negative index of refraction metamaterials

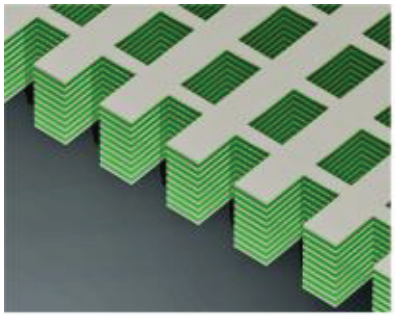

UC Berkeley

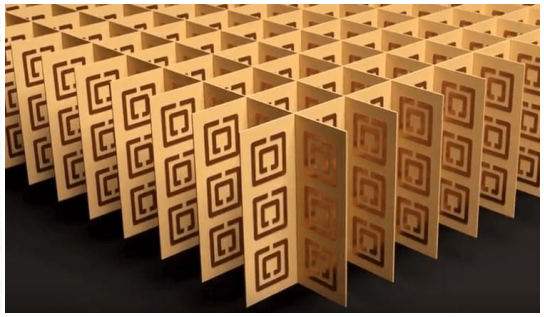

AccSci

porous rock

Gaspari

porous sea ice

Weeks

acoustic and seismic metamaterials

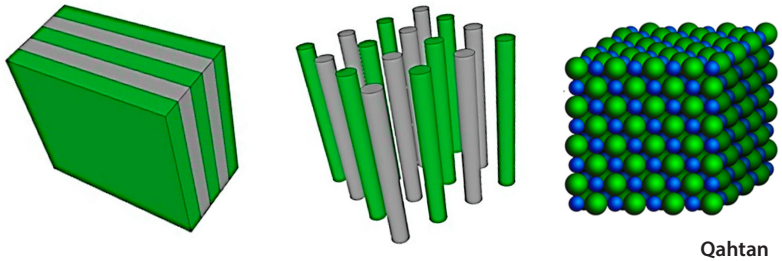

Qahtan

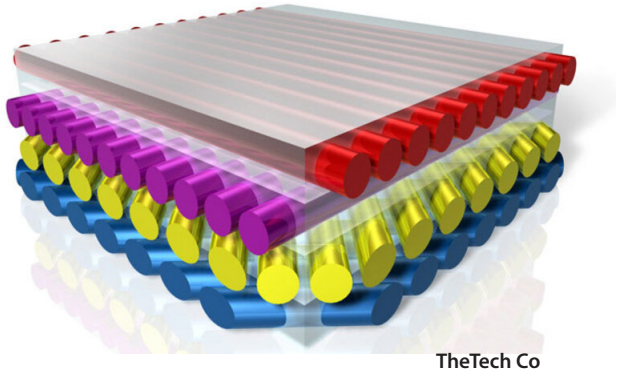

TheTech Co

invisibility cloak

Warner Bros.

structural cloak

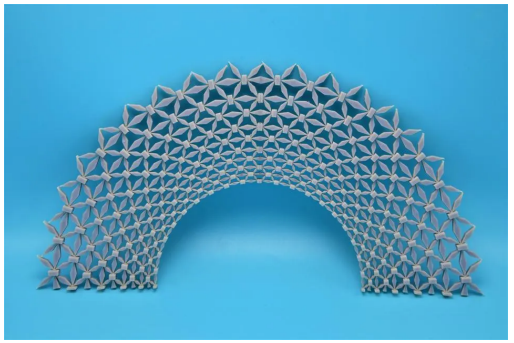

U. Missouri

Central theme:

How do we use "small scale" information to find effective behavior relevant to large-scale sea ice physics and ecology models?

HOMOGENIZATION for Composite Materials

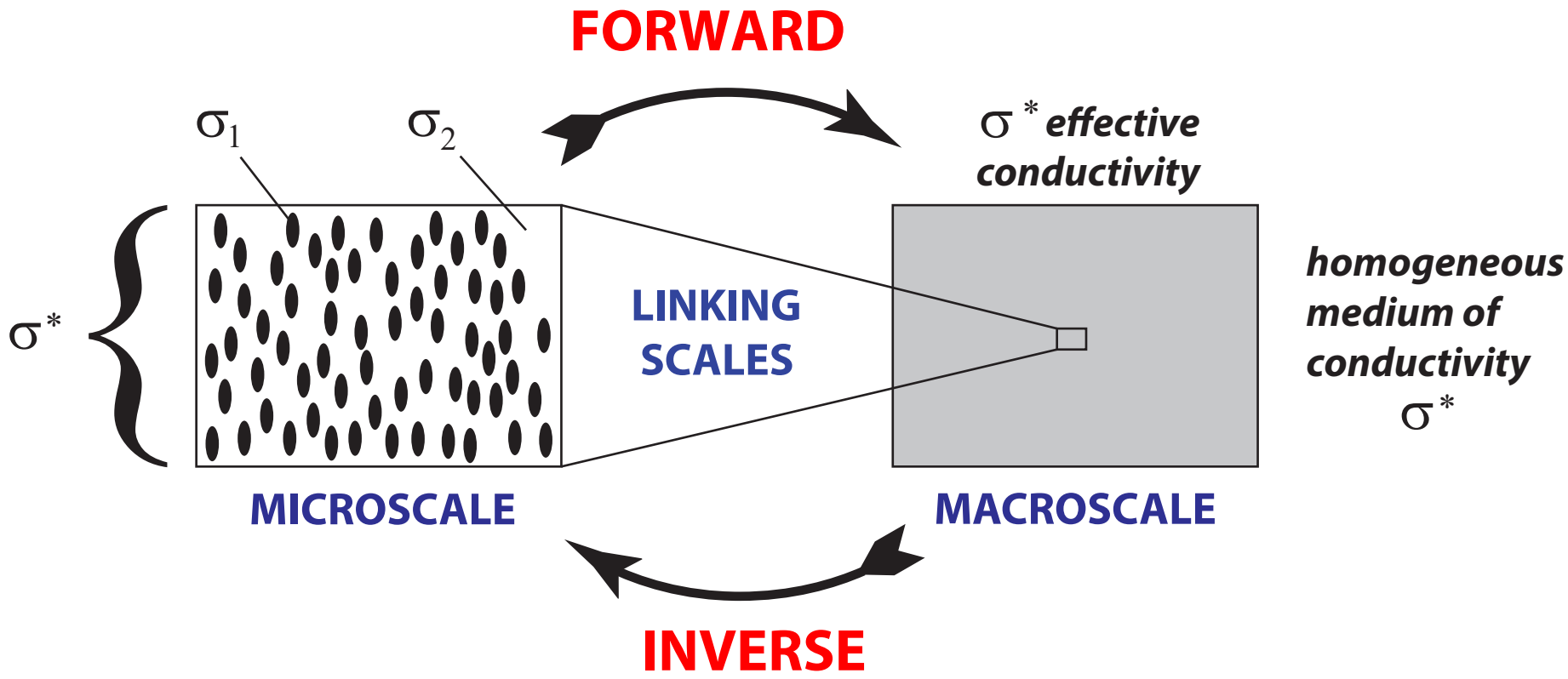

Maxwell 1873

Einstein 1906

Wiener 1912, Hashin & Shtrikman 1962

resistors in series

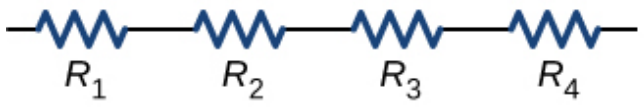

resistors in parallel

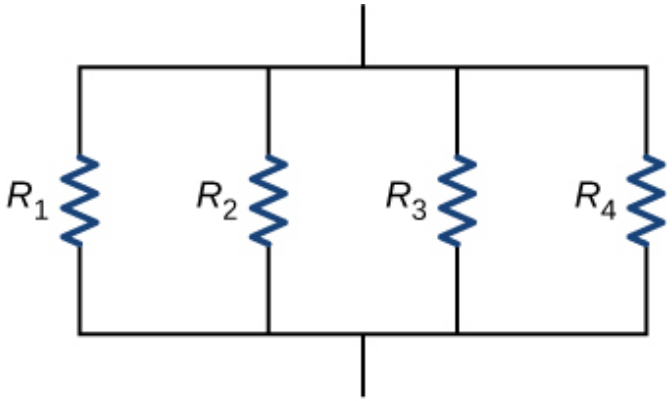

equivalent resistance

$$R_{eq} = R_1 + R_2 + R_3 + R_4$$

$$\frac{1}{R_{eq}} = \frac{1}{R_1} + \frac{1}{R_2} + \frac{1}{R_3} + \frac{1}{R_4}$$

random resistor network

percolation model

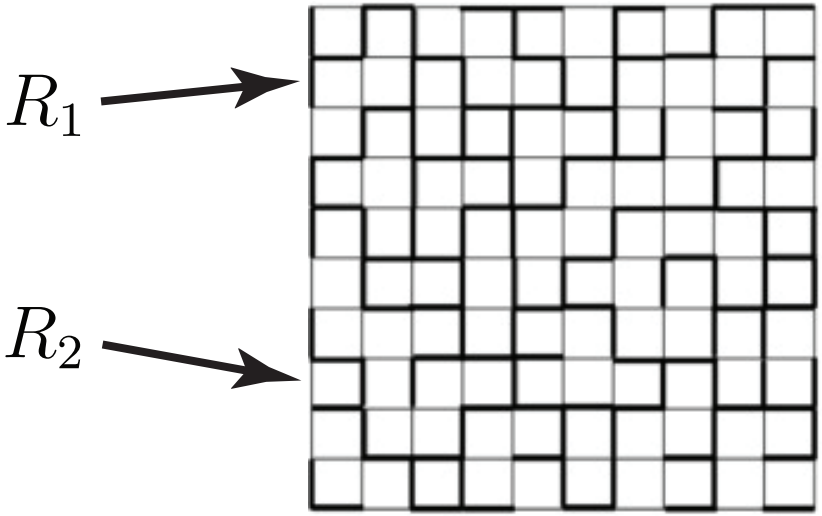

R_{eq} = ??

infinite lattice ?

discrete homogenization

STATISTICAL PHYSICS

How do microscopic laws determine macroscopic behavior?

Banwell, Burton, Cenedese, Golden, Astrom, Physics of the Cryosphere, *Nature Reviews Physics* 2023

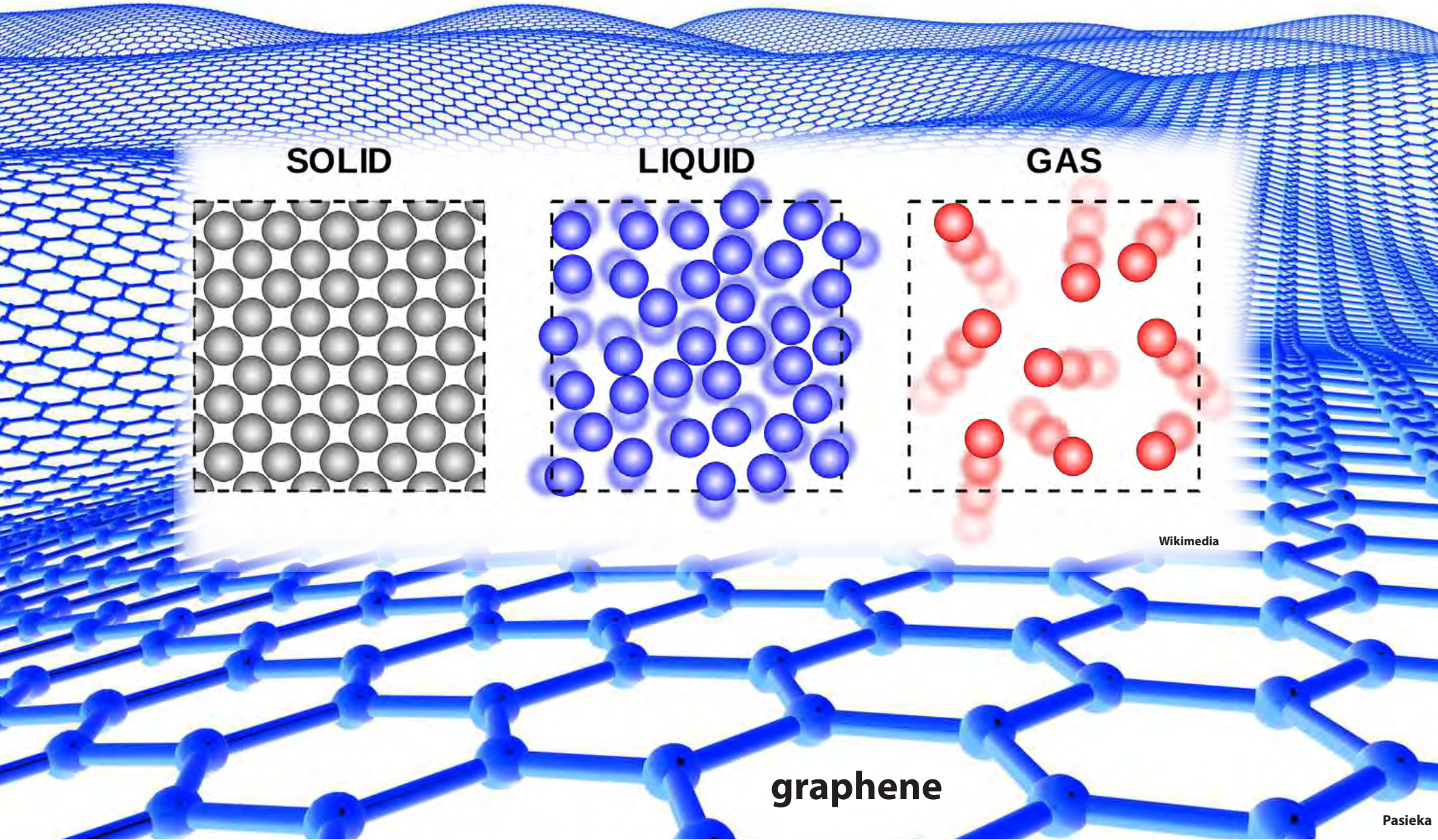

Polar Ecology and the Physics of Sea Ice

How do sea ice properties affect the life it hosts?

How does life in and on sea ice affect its physical properties?

Pekelo/iStockphoto

Golden

Arrigo

What is this talk about?

A tour of recent results on multiscale modeling of physical and biological processes in the sea ice system.

microscale

mesoscale

macroscale

through the lens of several areas of mathematics

microscale

brine inclusions in sea ice (mm)

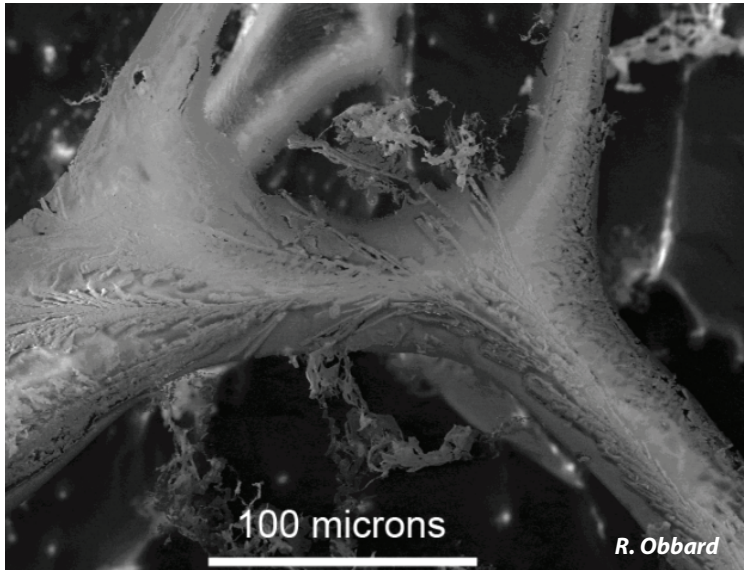

micro - brine channel (SEM)

sea ice is a porous composite

pure ice with brine, air, and salt inclusions

brine channels (cm)

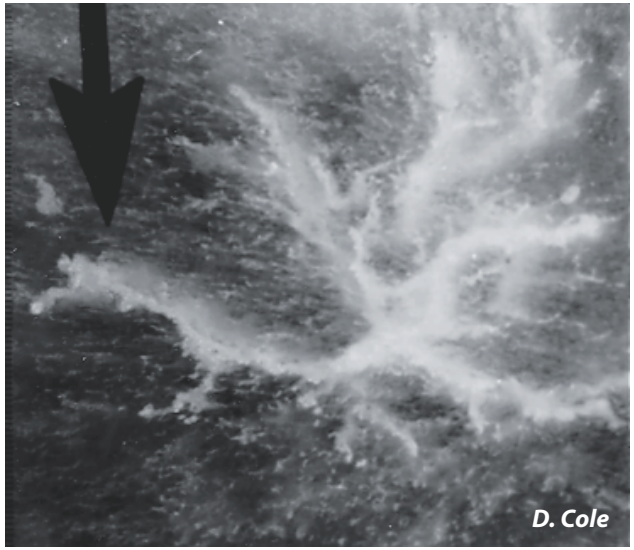

horizontal section

vertical section

fluid flow through the porous microstructure of sea ice governs key processes in polar climate and ecosystems

evolution of Arctic melt ponds and sea ice albedo

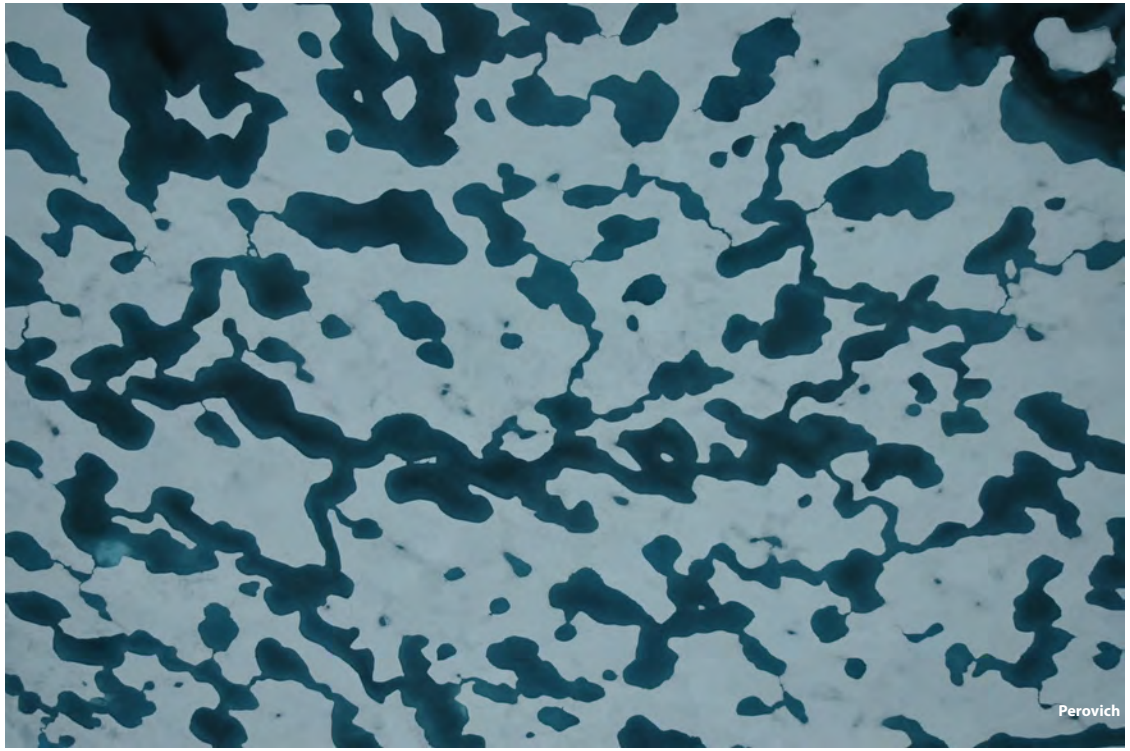

nutrient flux for algal bloom

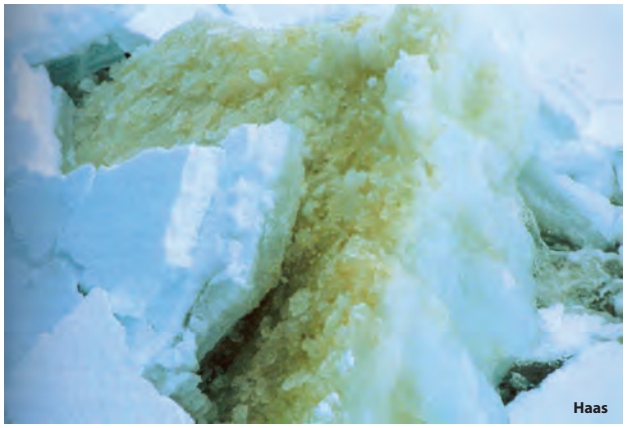

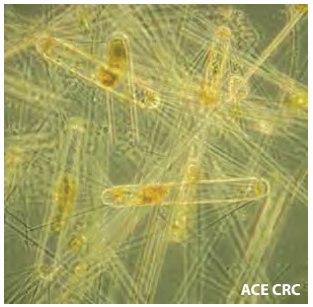

brine volume fraction and ***connectivity*** increase with temperature

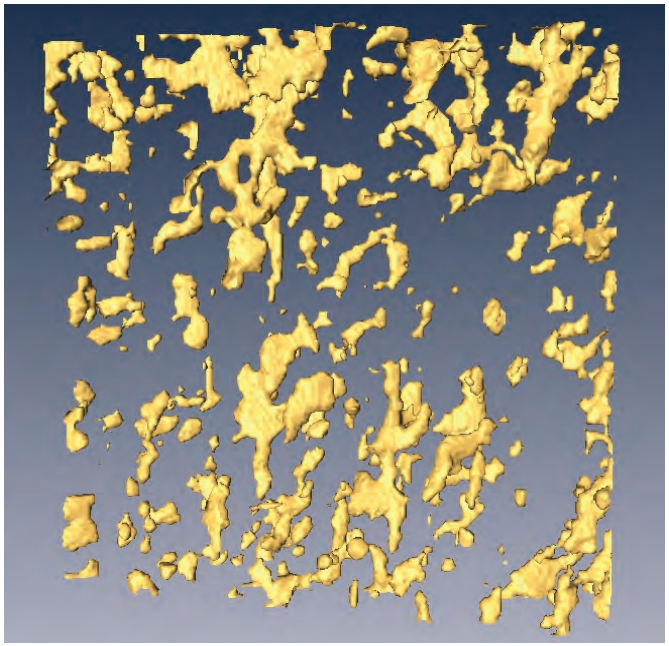

T = -15 °C, $\phi = 0.033$

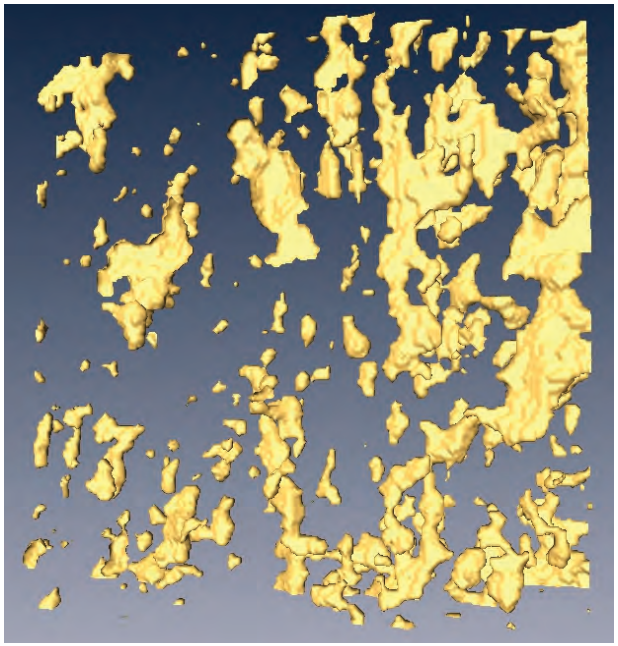

T = -6 °C, $\phi = 0.075$

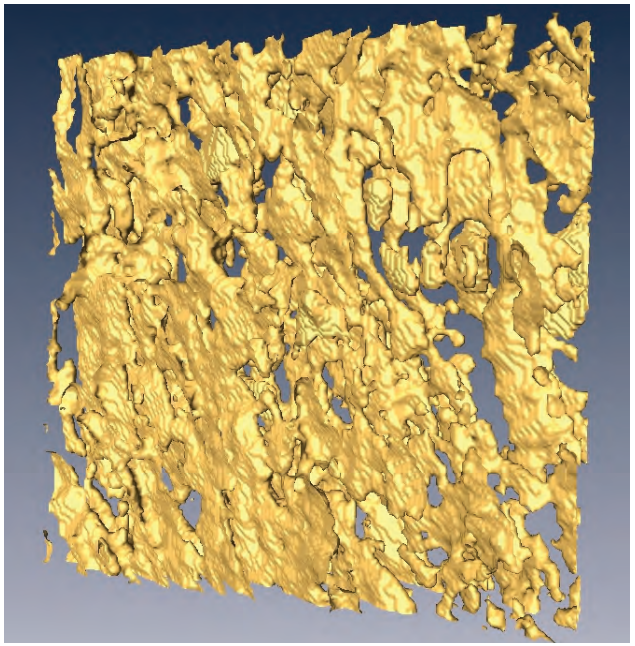

T = -3 °C, $\phi = 0.143$

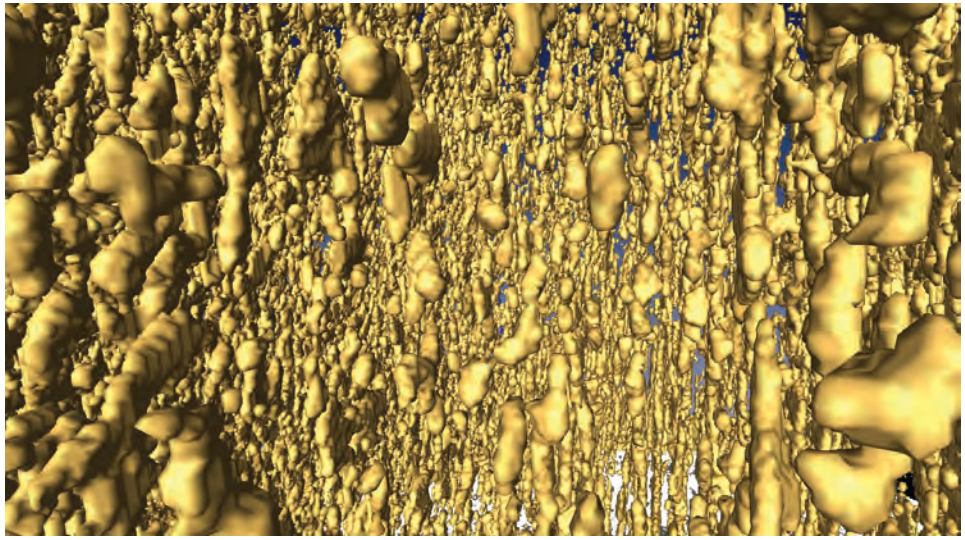

T = -8 °C, $\phi = 0.057$

X-ray tomography for brine in sea ice

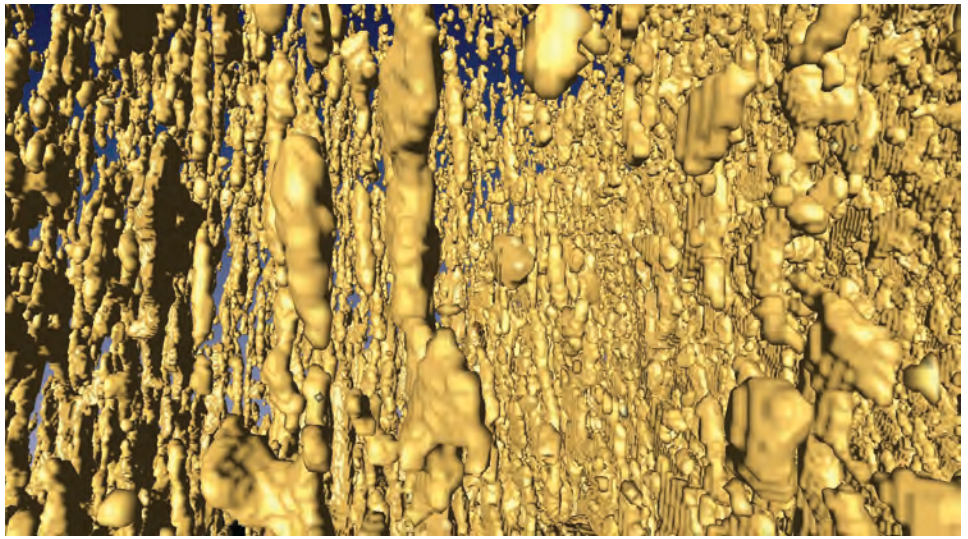

T = -4 °C, $\phi = 0.113$

Golden *et al.*, *Geophysical Research Letters*, 2007

percolation model

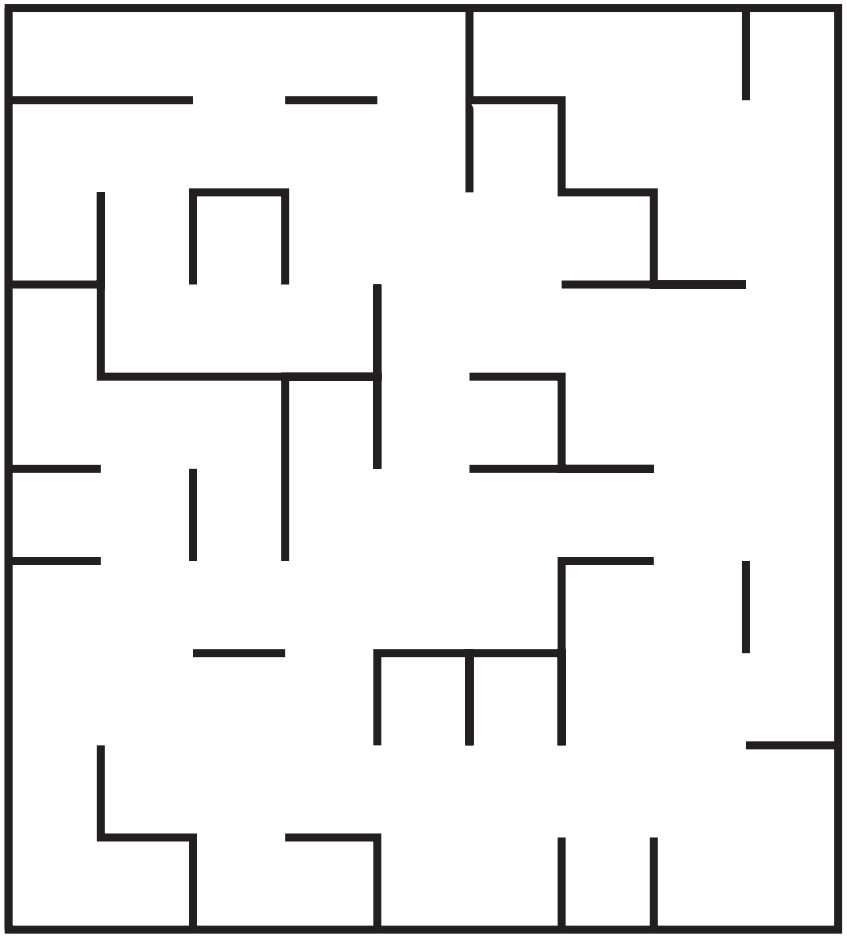

$p = 1/3$

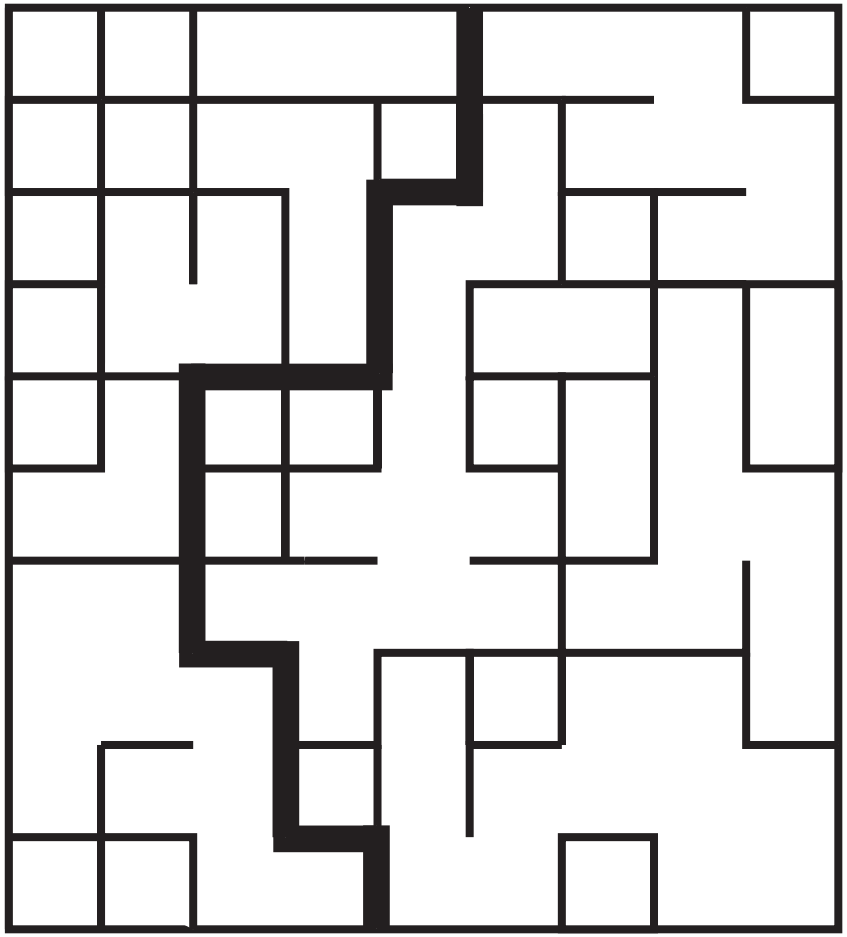

$p = 2/3$

$p_c = ?$

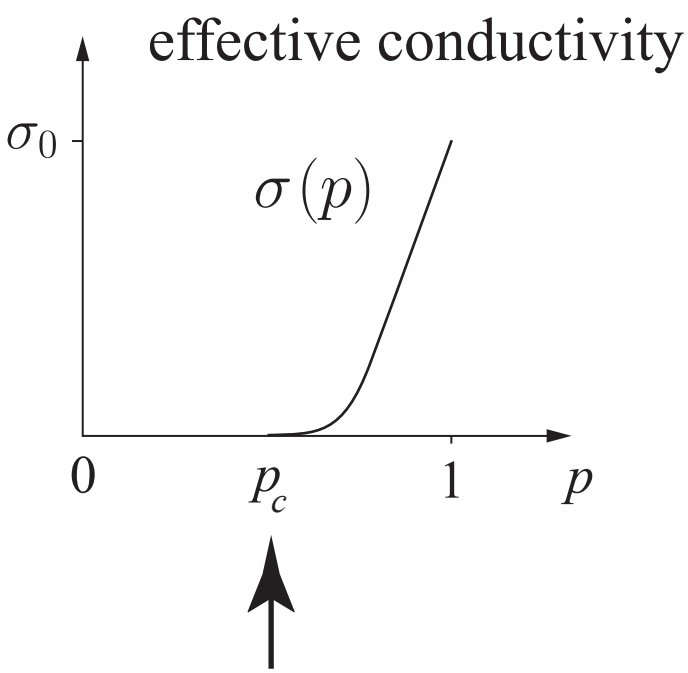

Critical behavior of transport near percolation threshold

conductivity

$$\sigma(p) \sim \sigma_0 (p - p_c)^t, \quad p \to p_c^+$$

permeability

$$\kappa(p) \sim \kappa_0 (p - p_c)^e, \quad p \to p_c^+$$

conductivity critical exponent t

UNIVERSAL for lattices

depends only on dimension, $e = t$

$d = 3$	**numerical**	$t \approx 2$
$d = 2$		$t \approx 1.3$

rigorous bound $1 \leq t \leq 2$

Golden PRL 1990, CMP 1992

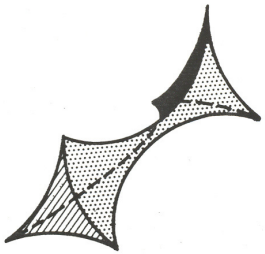

continuum exponents can be ***non-universal***

SWISS CHEESE ***Halperin, Feng, Sen PRL 1985***

Critical behavior of fluid transport in sea ice

impermeable permeable

off on

"on - off" switch for bulk fluid flow

Arctic field data

vertical fluid permeability k (m^2)

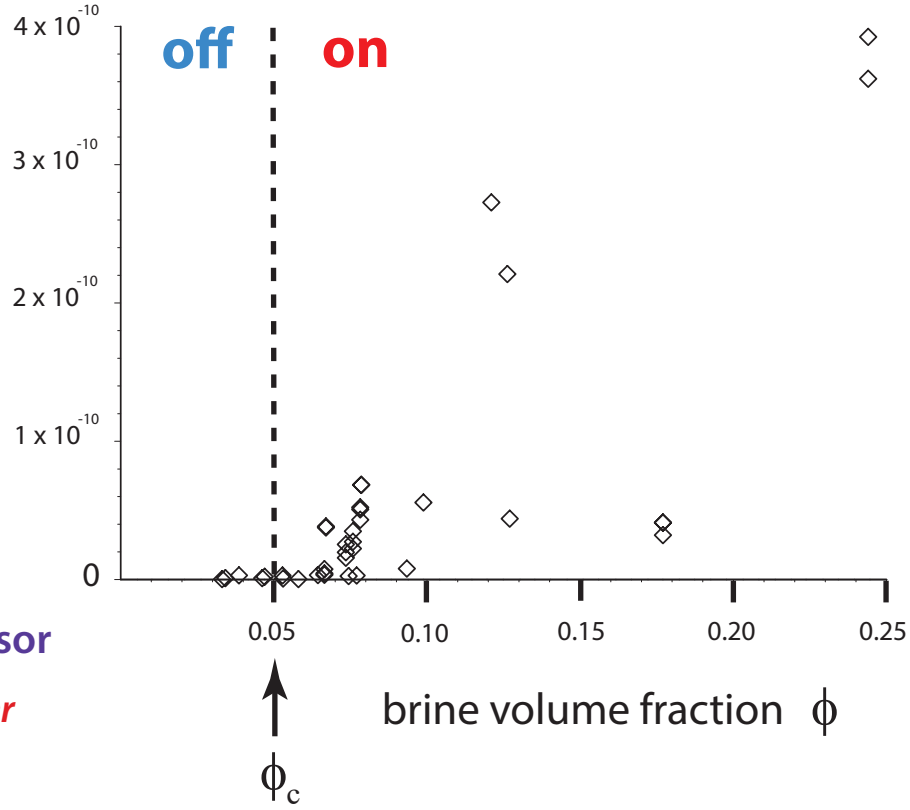

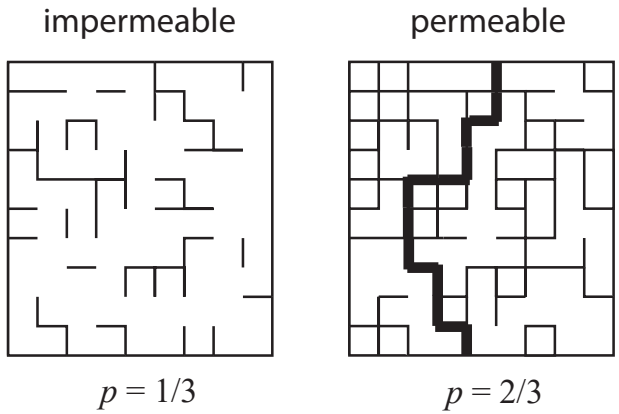

Darcy's Law

$$\mathbf{v} = -\frac{\mathbf{k}}{\eta}\nabla p$$

$\mathbf{k}$ = fluid permeability tensor

homogenized parameter

PERCOLATION THRESHOLD $\phi_c \approx 5\% \longleftrightarrow T_c \approx -5^\circ\mathrm{C},\ S \approx 5$ ppt

RULE OF FIVES

Golden, Ackley, Lytle Science 1998
Golden, Eicken, Heaton, Miner, Pringle, Zhu GRL 2007
Pringle, Miner, Eicken, Golden J. Geophys. Res. 2009

sea ice algal communities

D. Thomas 2004

nutrient replenishment
controlled by ice permeability

biological activity turns on
or off according to
rule of fives

Golden, Ackley, Lytle ***Science 1998***

Fritsen, Lytle, Ackley, Sullivan ***Science 1994***

critical behavior of microbial activity

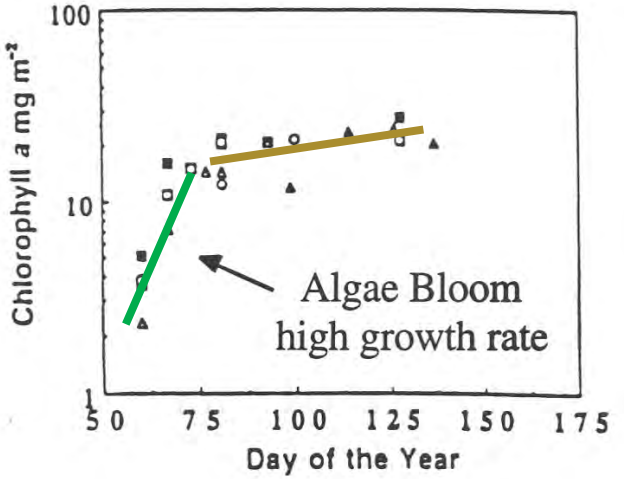

Convection-fueled algae bloom
Ice Station Weddell

stealth

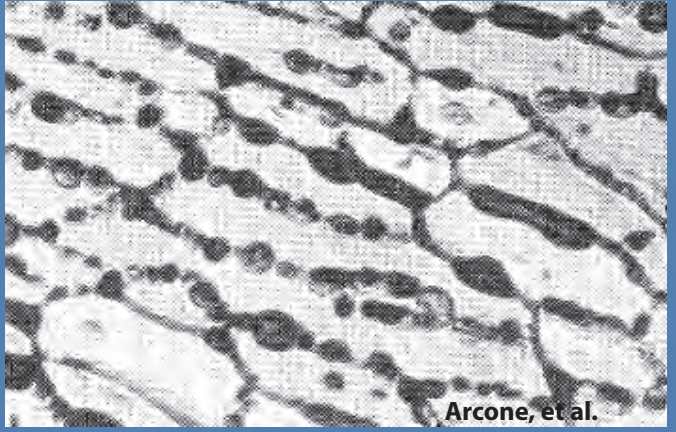

Arcone, et al.

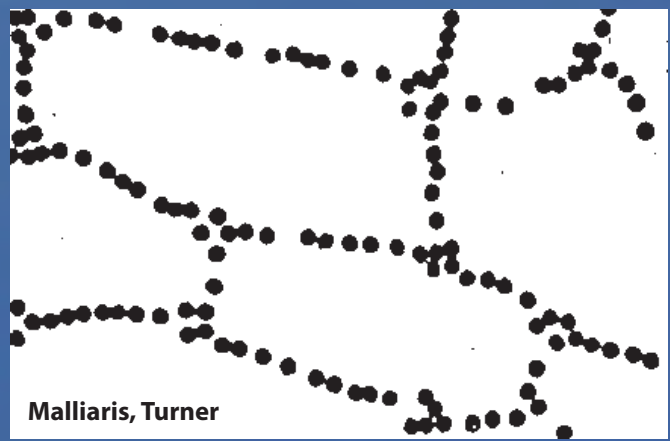

Malliaris, Turner

NW Florida Daily News, Wikimedia

cross-pollination

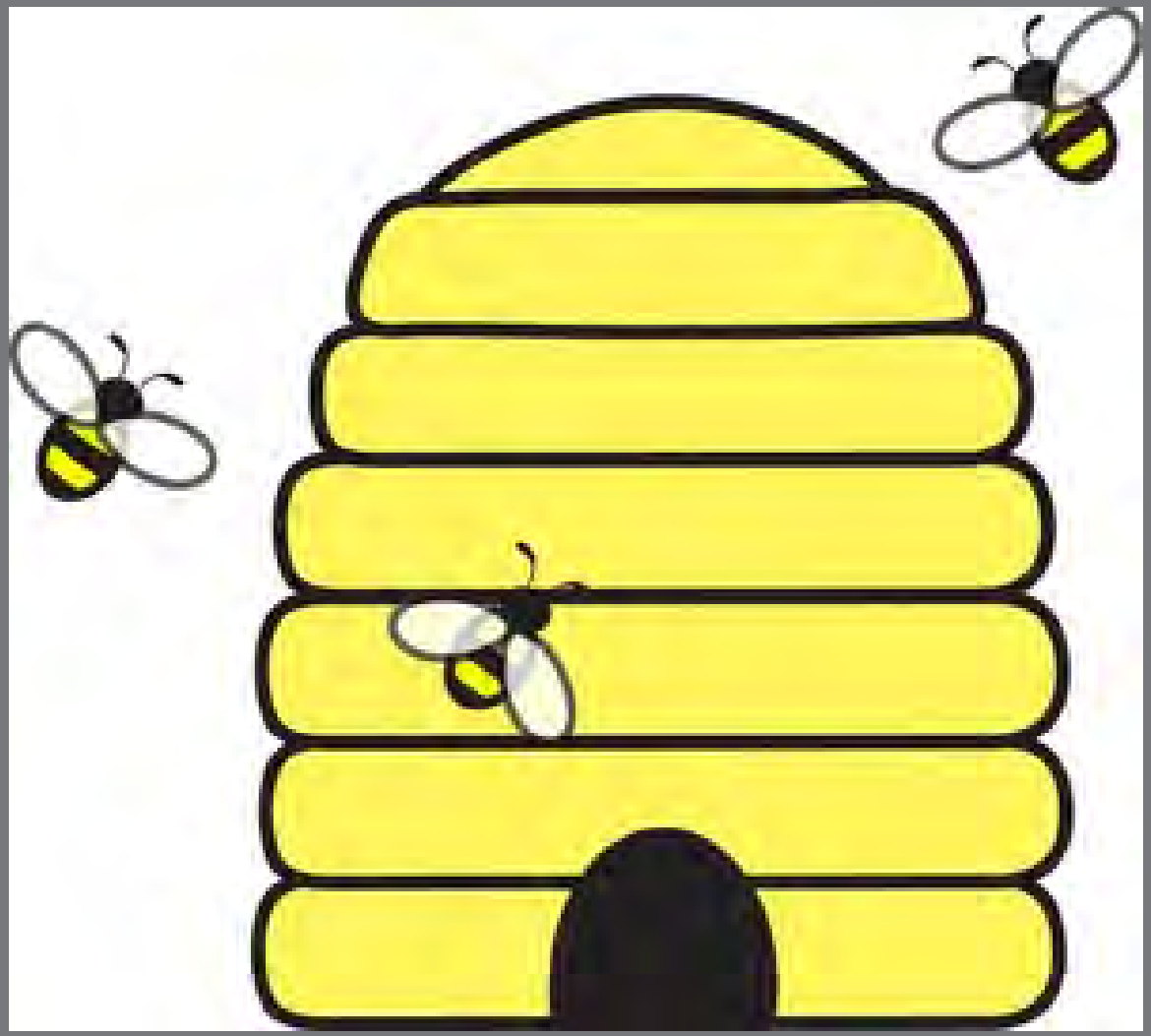

sea ice

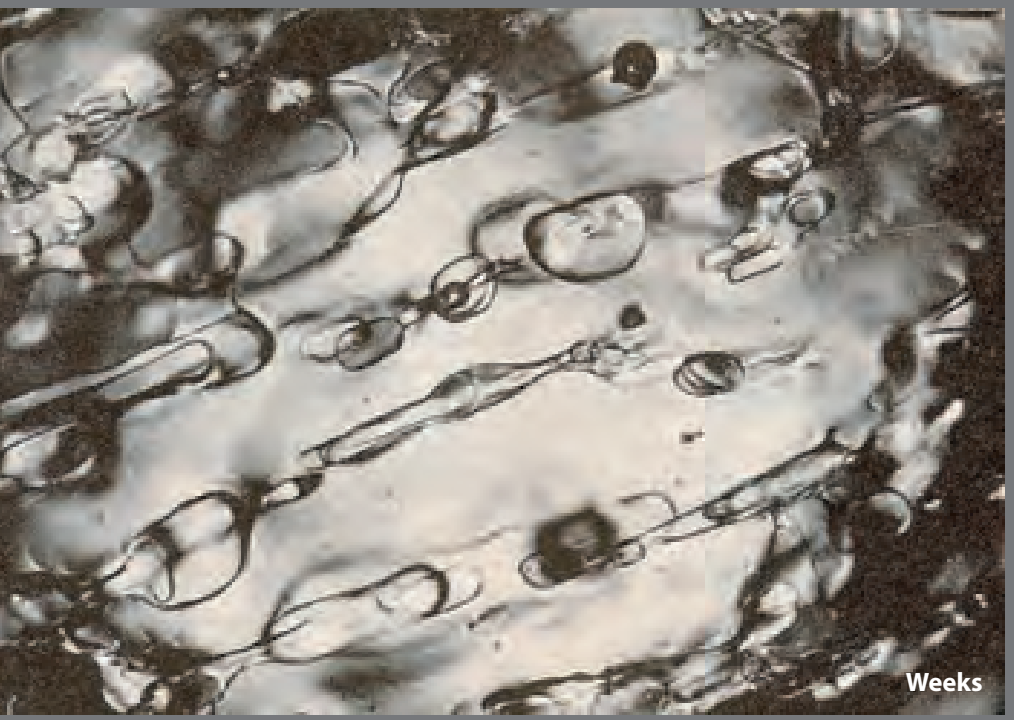

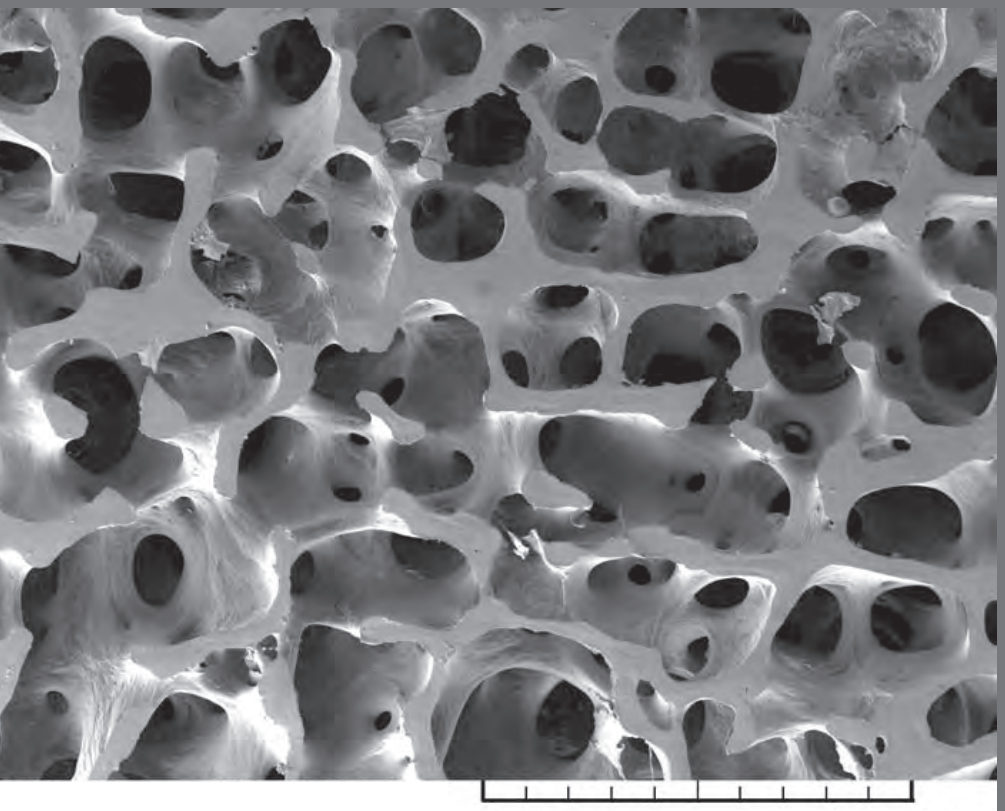

human bone

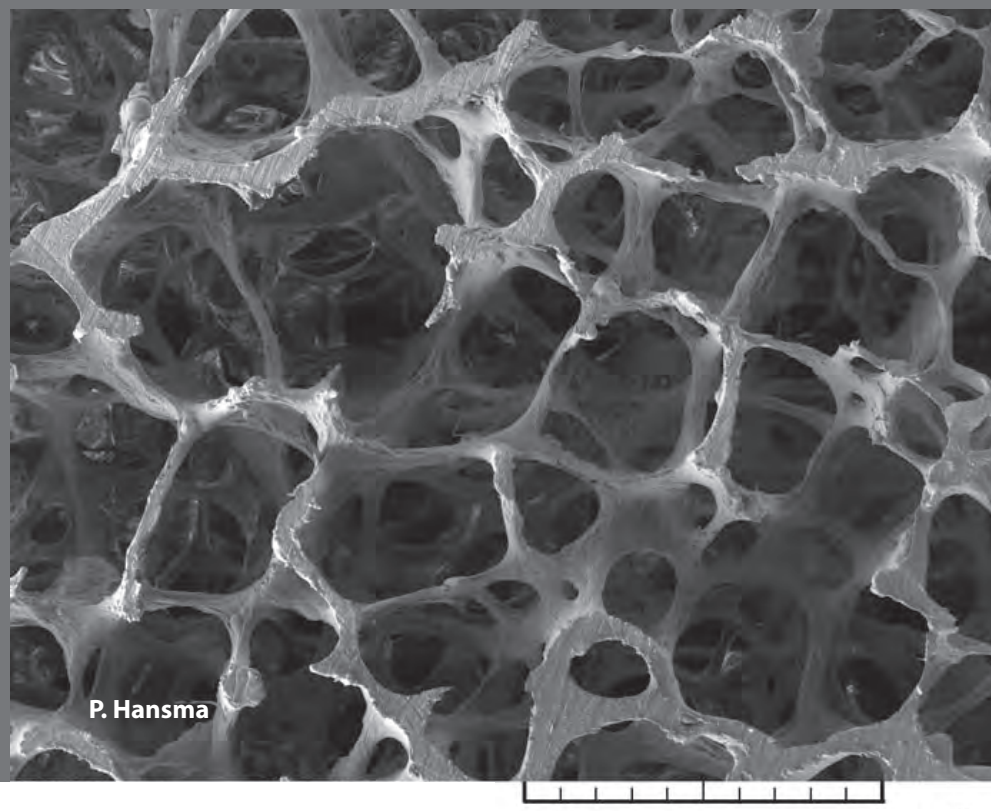

Thermal evolution of permeability and microstructure in sea ice

Golden, Eicken, Heaton, Miner, Pringle, Zhu, Geophysical Research Letters 2007

percolation theory
for fluid permeability

$$k(\phi) = k_0 (\phi - 0.05)^2$$

$$k_0 = 3 \times 10^{-8} \text{ m}^2$$

critical exponent ***t***

critical path analysis

microscale

governs

mesoscale
processes

X-ray CT

confirms rule of fives

Pringle, Miner, Eicken, Golden
J. Geophys. Res. 2009

theory agrees closely
with field data

ISSN 0002-9920

Notices

of the American Mathematical Society

May 2009 Volume 56, Number 5

photo by Jan Lieser

Real analysis in polar coordinates (see page 613)

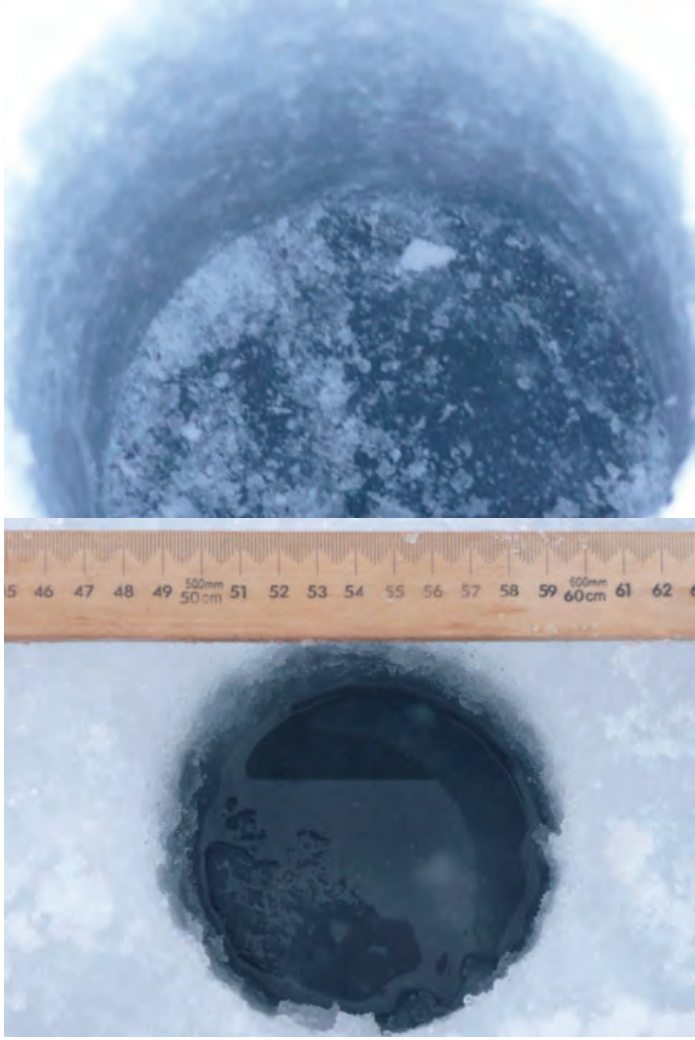

measuring fluid permeability of Antarctic sea ice

SIPEX 2007

electrical measurements

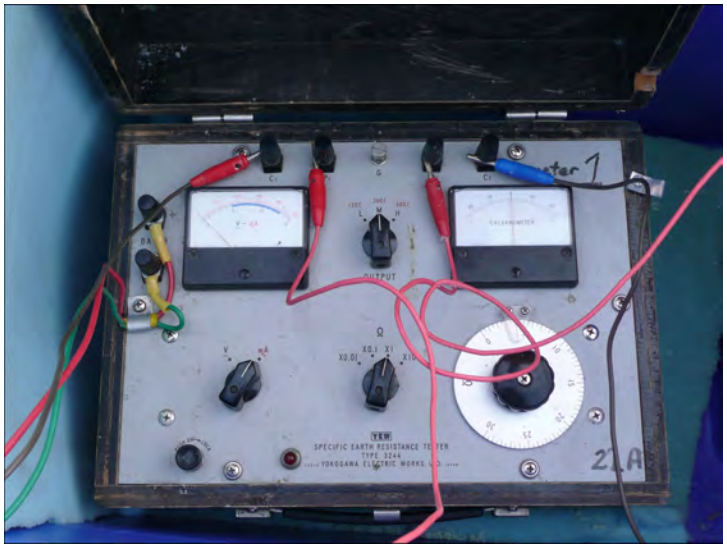

Wenner array

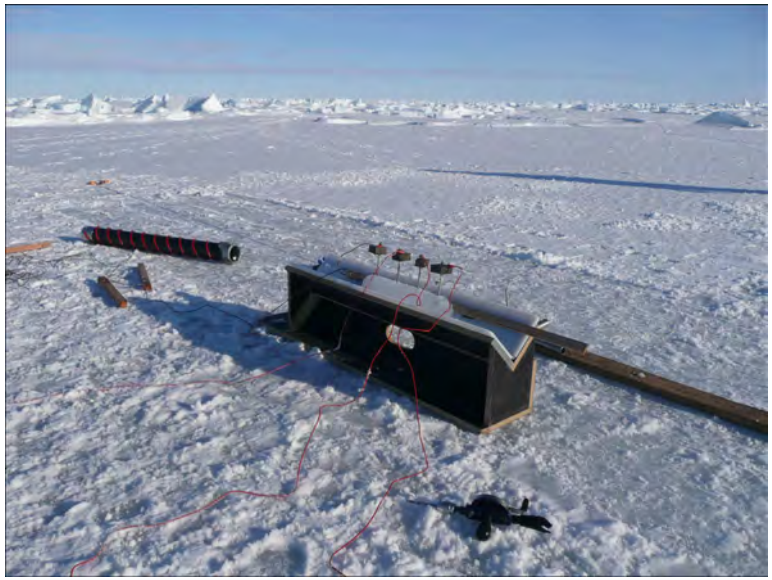

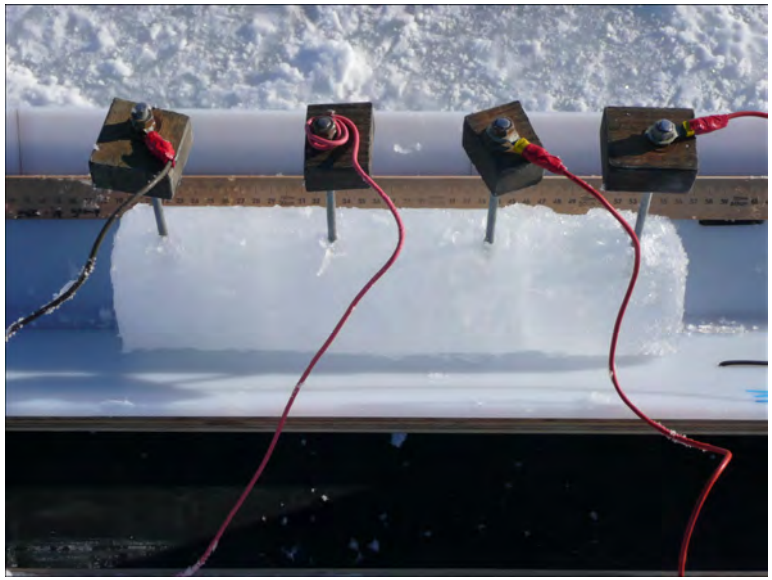

vertical conductivity

Zhu, Golden, Gully, Sampson ***Physica B*** 2010
Sampson, Golden, Gully, Worby ***Deep Sea Research*** 2011

Sea ice algae secrete exopolymeric substances (EPS) affecting evolution of brine microstructure.

How does EPS affect fluid transport? How does the biology affect the physics?

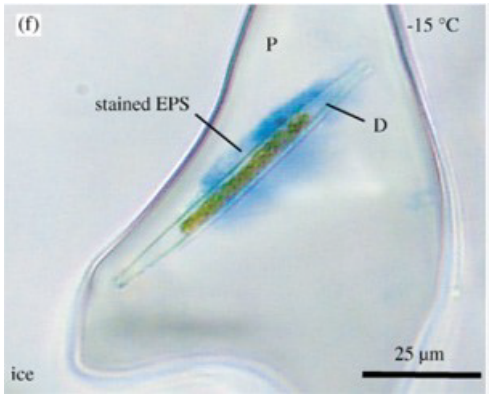

Krembs

FRACTAL

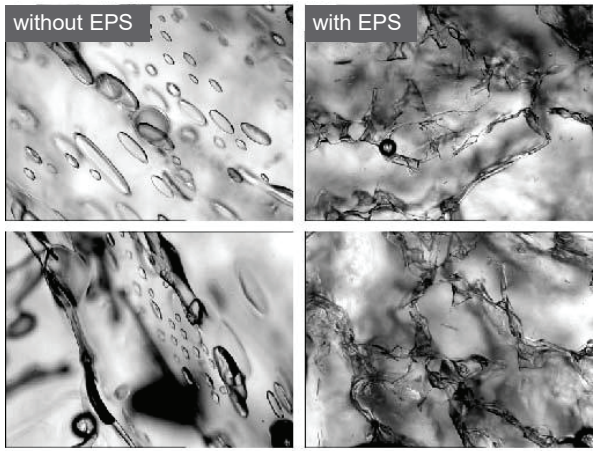

Krembs, Eicken, Deming, PNAS 2011

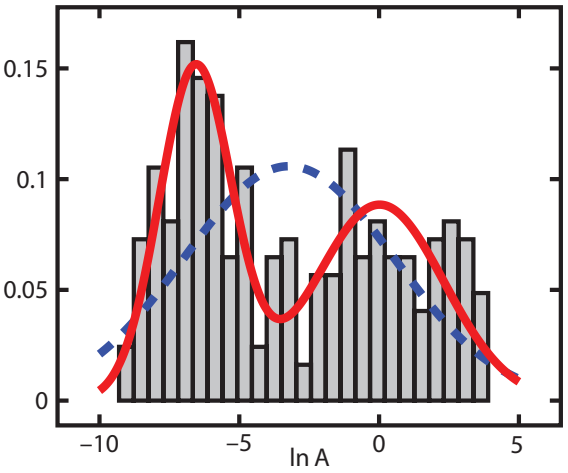

RANDOM PIPE MODEL

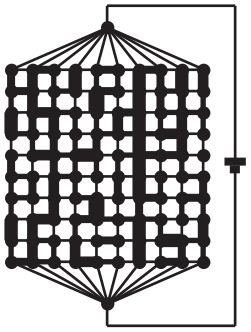

- 2D random pipe model with bimodal distribution of pipe radii

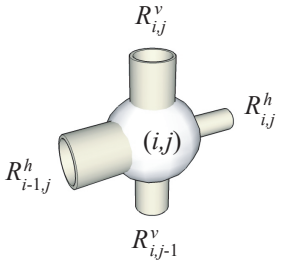

- Rigorous bound on permeability *k;* results predict observed drop in *k*

Steffen, Epshteyn, Zhu, Bowler, Deming, Golden
***Multiscale Modeling and Simulation*, 2018**

Zhu, Jabini, Golden, Eicken, Morris
***Ann. Glac.* 2006**

SIAM News
June 2024

EPS - Algae Model Jajeh, Golden, Deming, Reimer 2025

brine skeletonization

Manav Arora, Lou Kondic, Darrren Skolnik, Ken Golden

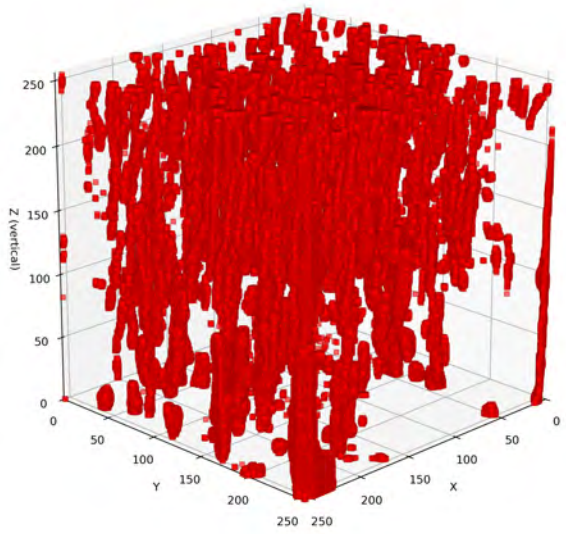

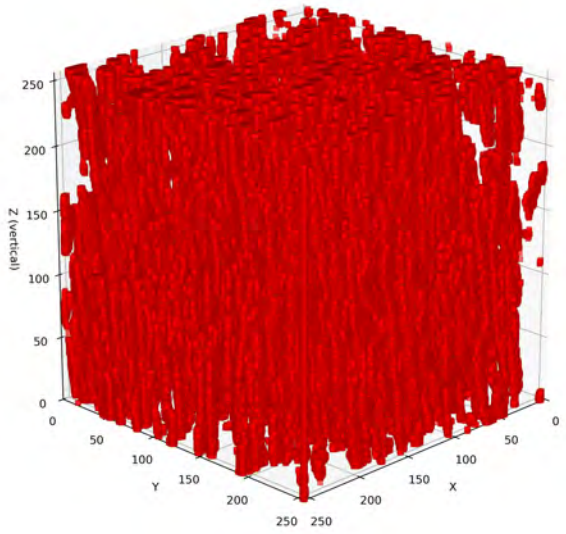

porosity = 0.022

porosity = 0.114

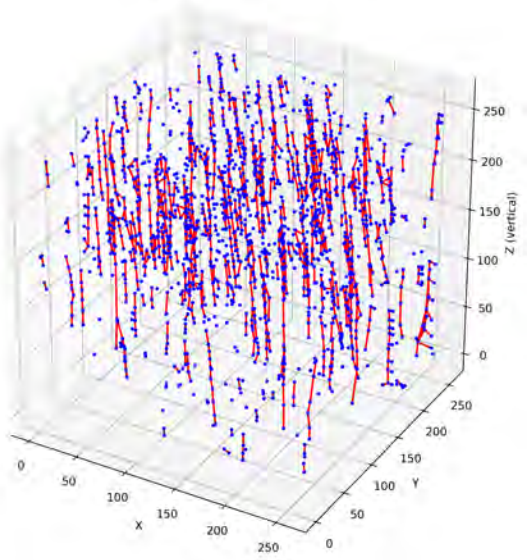

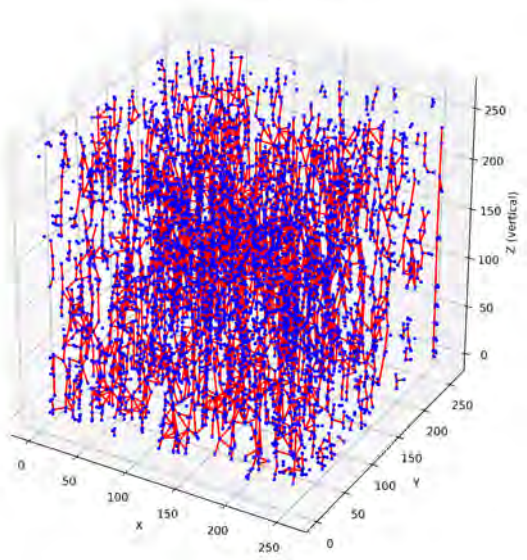

skeletonization of porous brine microstructures

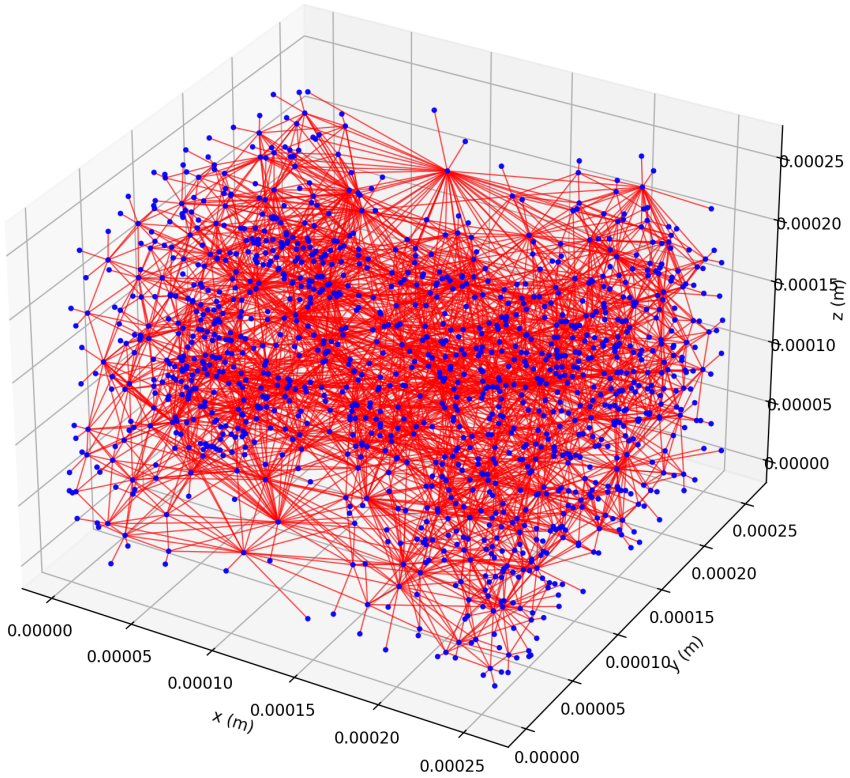

porosity = 0.028

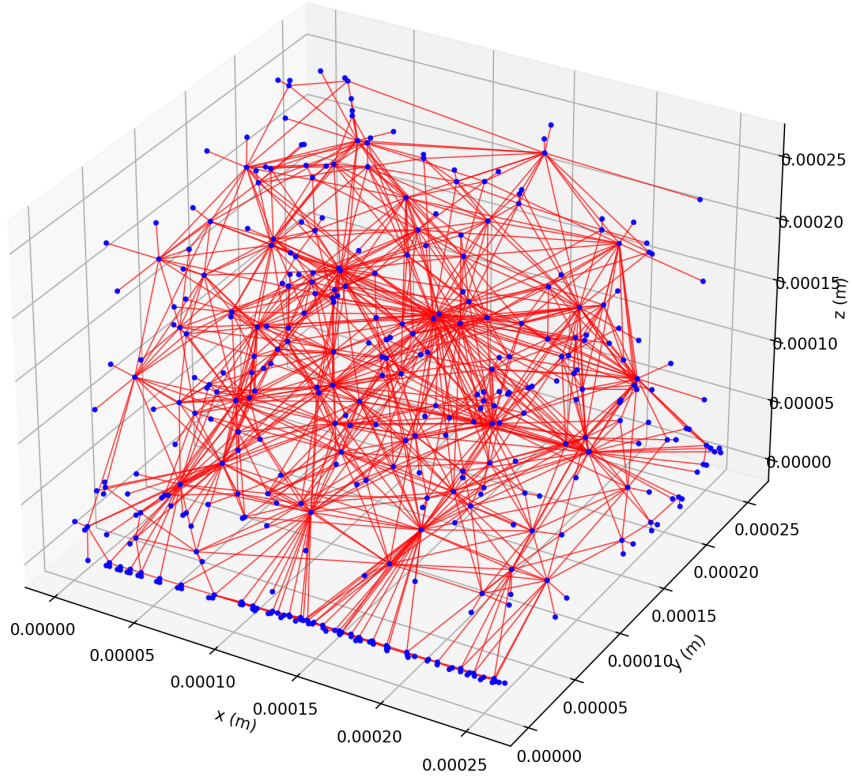

porosity = 0.004

Thermal Evolution of Brine Fractal Geometry in Sea Ice

Nash Ward, Daniel Hallman, Benjamin Murphy, Jody Reimer,
Marc Oggier, Megan O'Sadnick, Elena Cherkaev and Kenneth Golden, 2024

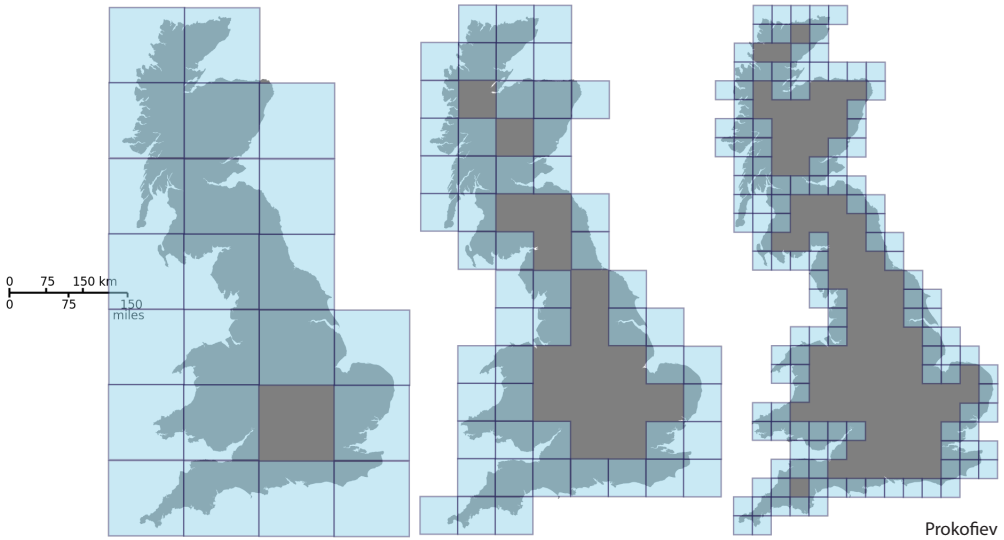

fractal dimension of the coastline of Great Britain by box counting

$$N(\epsilon) \sim \epsilon^{-D}$$

brine channels and inclusions "look" like fractals (from 30 yrs ago)

$T = -12^\circ$ C, $\phi = 0.033$ $T = -8^\circ$ C, $\phi = 0.057$

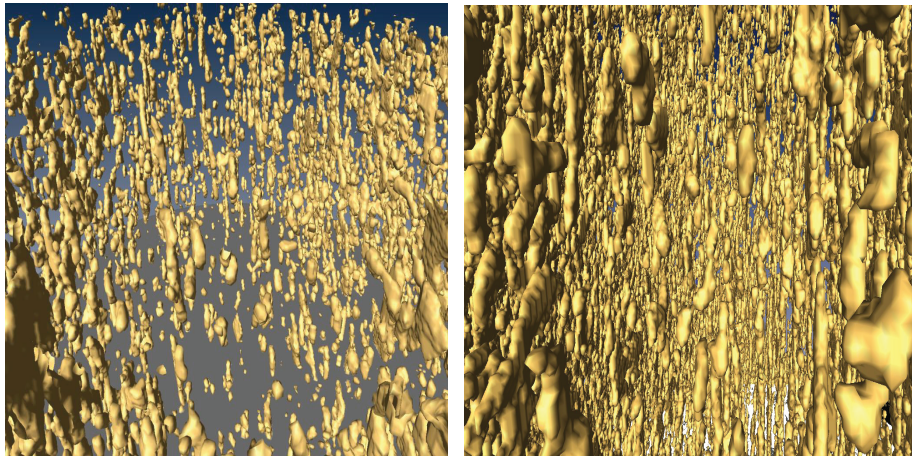

Golden, Eicken, et al. *GRL*, 2007

X-ray computed tomography of brine in sea ice

columnar and granular

The first quantitative study of the fractal dimension of brine in sea ice and its strong dependence on temperature and porosity.

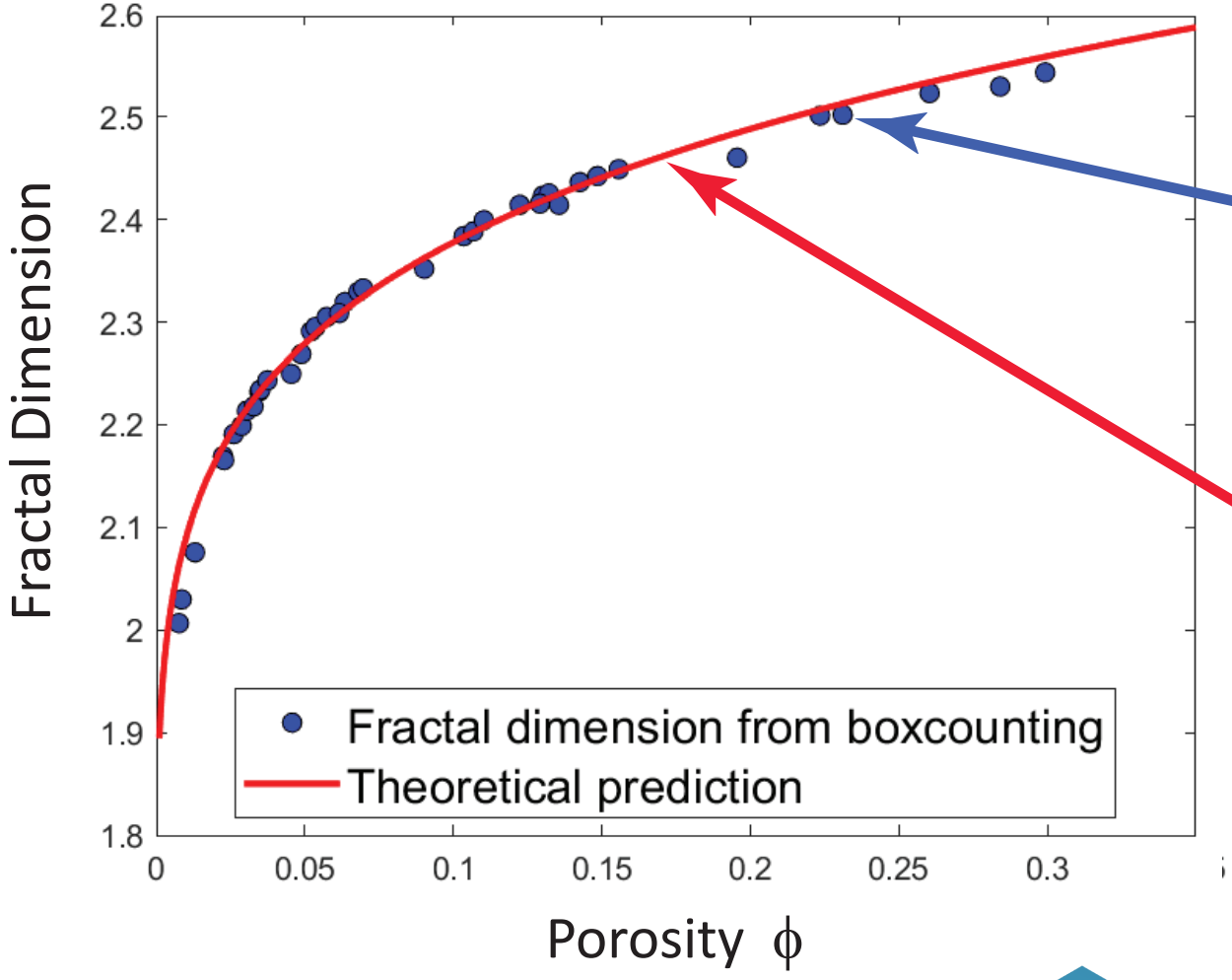

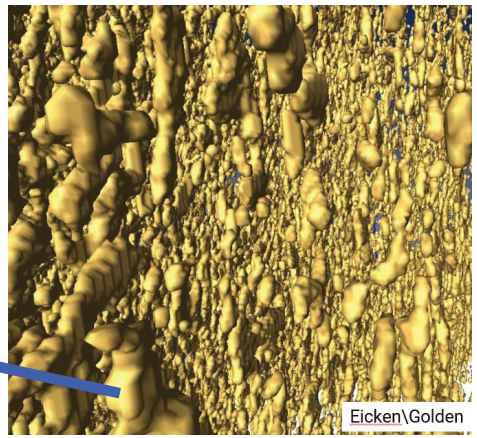

Follows same curve as exactly self-similar Sierpinski tetrahedron

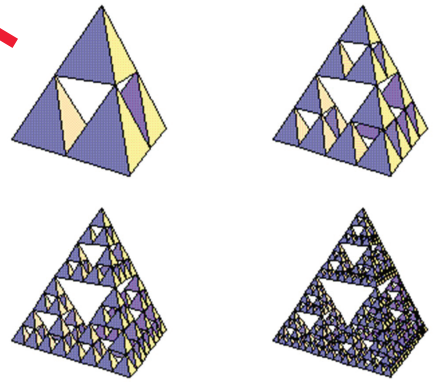

D. Eppstein

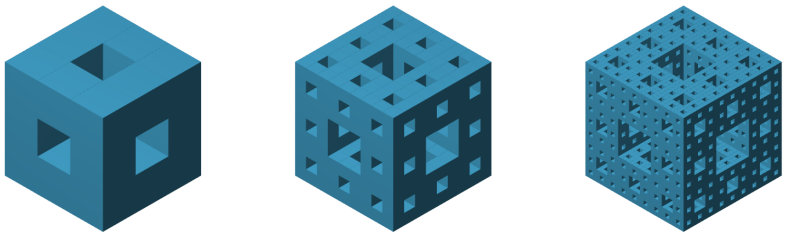

red curve $$F_d = d_E - \frac{\ln \phi}{\ln(\lambda_{min}/\lambda_{max})}$$

Katz and Thompson,1985; Yu and Li, 2001

discovered for sandstones
statistically self-similar porous media

Fractal geometry of brine in sea ice, Ward, *et al.* 2024

Implications of brine fractal geometry on sea ice ecology and biogeochemistry

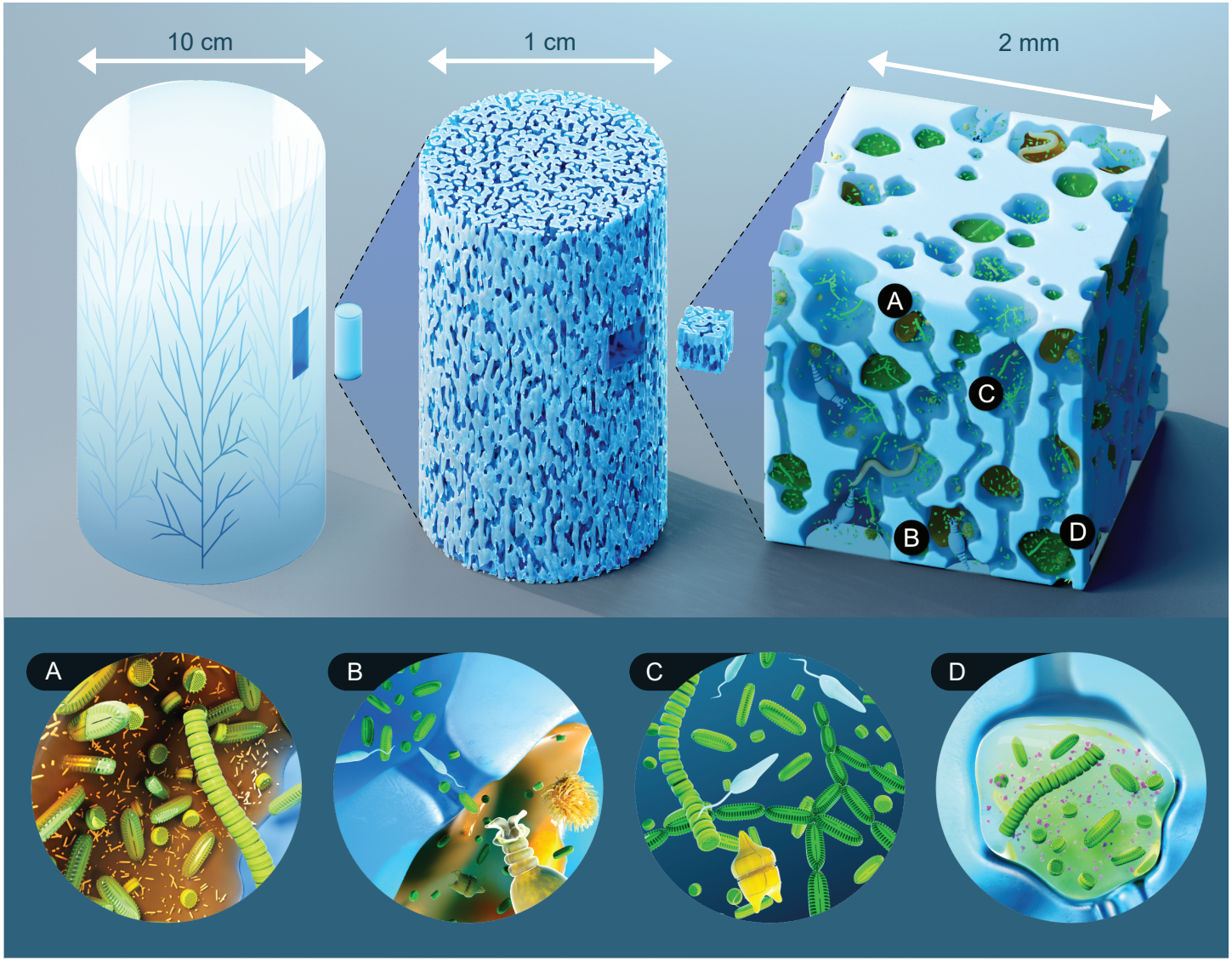

Brine inclusions are home to ice endemic organisms, e.g., bacteria, diatoms, flagellates, rotifers, nematodes.

The habitability of sea ice for these organisms is inextricably linked to its complex brine geometry.

(A) Many sea ice organisms attach themselves to inclusion walls; inclusions with a higher fractal dimension have greater surface area for colonization.

(B) Narrow channels prevent the passage of larger organisms, leading to refuges where smaller organisms can multiply without being grazed, as in (C).

(D) Ice algae secrete extracellular polymeric substances (EPS) which alter incusion geometry and may further increase the fractal dimension.

Remote Sensing of Sea Ice

with radar, microwaves, ...

interaction of EM waves with brine and polycrystalline microstructures, rough surfaces

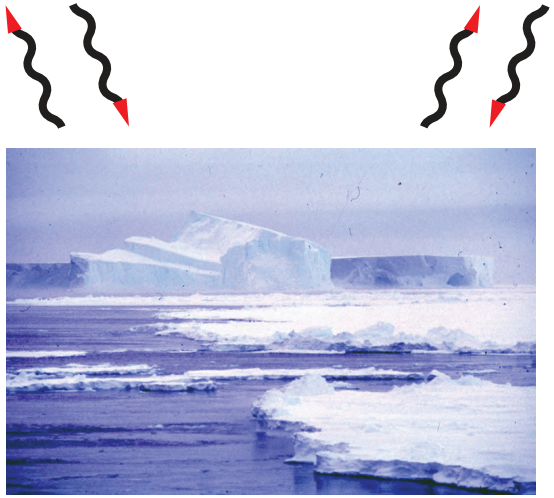

INVERSE PROBLEM

Recover sea ice properties from electromagnetic (EM) data ε^*

Effective complex permittivity of a composite in the quasistatic (long wavelength) limit

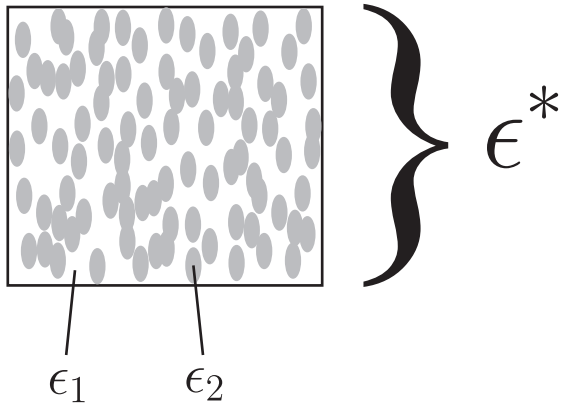

$$D = \epsilon E$$

$$\nabla \cdot D = 0$$

$$\nabla \times E = 0$$

$$\langle D \rangle = \epsilon^* \langle E \rangle$$

p_1 , p_2 = volume fractions of the components

electrical conductivity
thermal conductivty
magnetic permeability
diffusivity

$$\epsilon^* = \epsilon^* \left(\frac{\epsilon_1}{\epsilon_2} \text{ , composite geometry} \right)$$

What are the effective propagation characteristics of an EM wave (radar, microwaves) in the medium?

Analytic Continuation Method for Homogenization

Bergman 1978, Milton 1979, Golden & Papanicolaou 1983, Milton 2002

Stieltjes integrals for homogenized parameters

$$F(s) = 1 - \frac{\epsilon^*}{\epsilon_2} = \int_0^1 \frac{d\mu(z)}{s - z} \qquad s = \frac{1}{1 - \epsilon_1/\epsilon_2}$$

geometry

material parameters

- μ = **spectral measure** of $\Gamma\chi$ (operator, matrix)

$$\Gamma = \nabla(-\Delta)^{-1}\nabla\cdot$$

χ = characteristic function of the brine phase

- rigorous forward bounds; approximations; inverse bounds to recover porosity, connectivity

complexities of mixture geometry

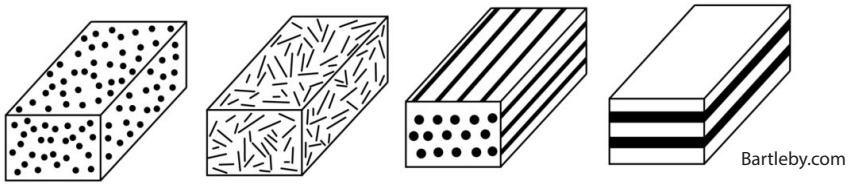

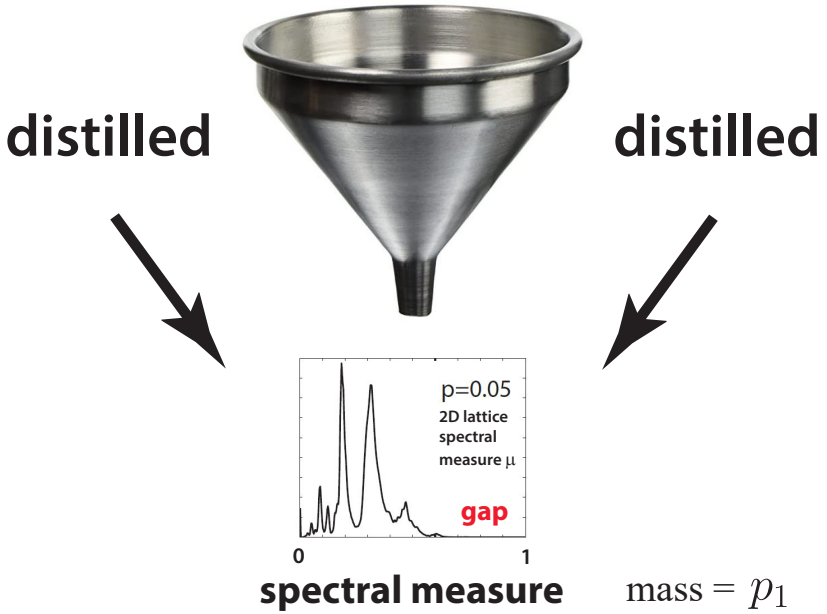

quantum mechanics

fractal geometries

forward and inverse bounds on the complex permittivity of sea ice

forward bounds

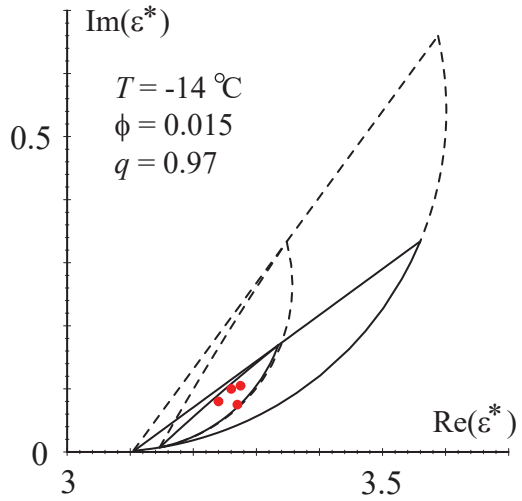

4.75 GHz data

matrix particle

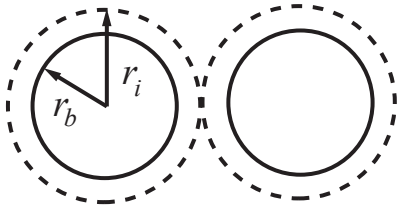

$$q = r_b / r_i$$

$$0 < q < 1$$

Golden 1995, 1997

Bruno 1991

inverse bounds

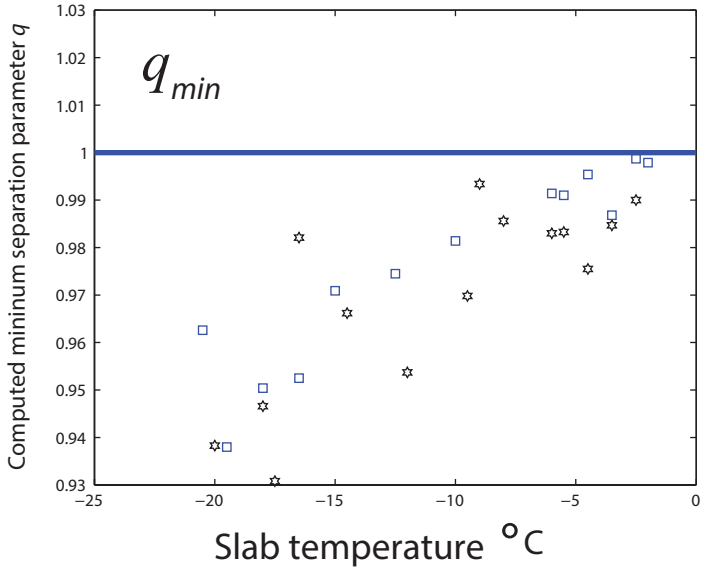

Inverse Homogenization

Cherkaev and Golden (1998), Day and Thorpe (1999), Cherkaev (2001), McPhedran, McKenzie, Milton (1982), *Theory of Composites*, Milton (2002)

ε^* ⟶ ***composite geometry*** (spectral measure μ)

inverse bounds and recovery of brine porosity

Gully, Backstrom, Eicken, Golden
Physica B, 2007

inversion for brine inclusion separations in sea ice from measurements of effective complex permittivity ε^*

rigorous inverse bound on spectral gap

construct algebraic curves which bound admissible region in (p,q)-space

Orum, Cherkaev, Golden
Proc. Roy. Soc. A, 2012

Uncertainty Quantification for Homogenization via Stieltjes Integral Representations

Clara Platt, Elena Cherkaev, Akil Narayan, Debdeep Bhattacharya, Ken Golden 2025

Classical bounds in the analytic continuation method assume fixed microstructural parameters, such as porosity, local permittivities, or inclusion separations.

But what if there is uncertainty, and they are random variables?

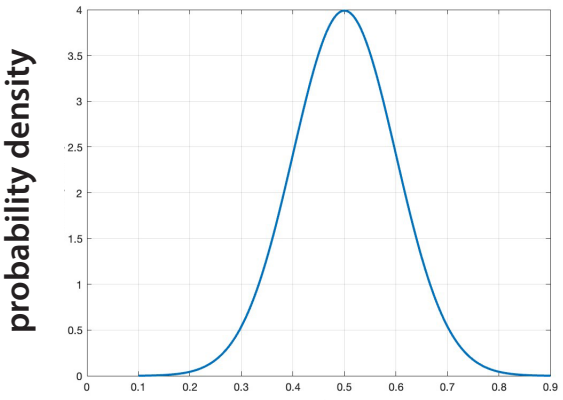

Hashin-Shtrikman bounds

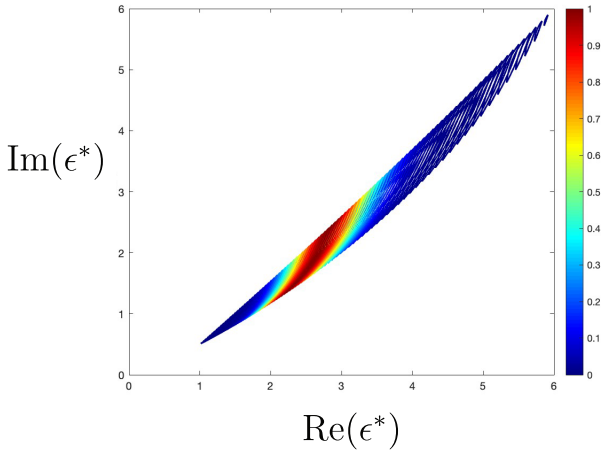

matrix-particle bounds

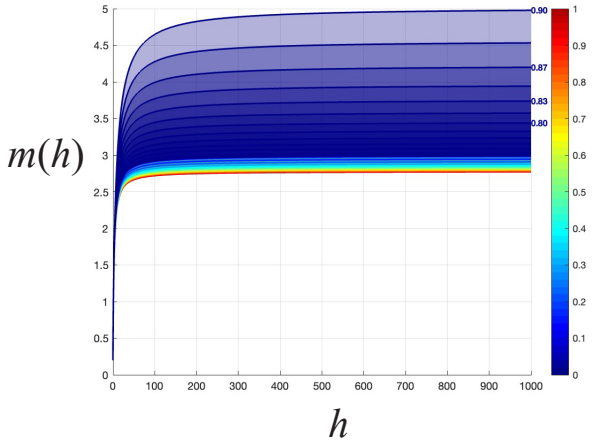

UQ for complex permittivity & thermal conductivity of sea ice

Bounds on the complex permittivity of polycrystalline materials by analytic continuation

Adam Gully, Joyce Lin,
Elena Cherkaev, Ken Golden

- **Stieltjes integral representation for effective complex permittivity**

  Milton (1981, 2002), Barabash and Stroud (1999), ...

- **Forward and inverse bounds**

  orientation statistics

- **Applied to sea ice using two-scale homogenization**

- **Inverse bounds give method for distinguishing ice types using remote sensing techniques**

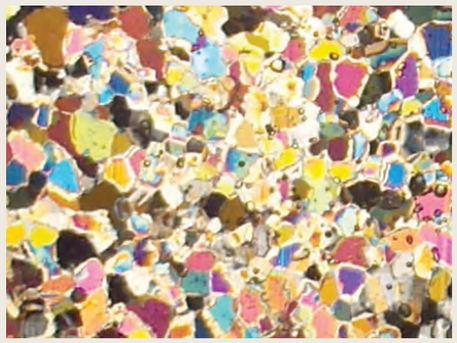

Proc. Roy. Soc. A 8 Feb 2015

ISSN 1364-5021 | Volume 471 | Issue 2174 | 8 February 2015

PROCEEDINGS A

350 YEARS OF SCIENTIFIC PUBLISHING

Proc. R. Soc. A | Volume 471 | Issue 2174 | 8 February 2015

An invited review commemorating 350 years of scientific publishing at the Royal Society

A method to distinguish between different types of sea ice using remote sensing techniques

A computer model to determine how a human should walk so as to expend the least energy

THE ROYAL SOCIETY PUBLISHING

21/01/15 1:47 PM

higher threshold for fluid flow in granular sea ice

microscale details impact "mesoscale" processes

nutrient fluxes for microbes
melt pond drainage
snow-ice formation

columnar granular

5%

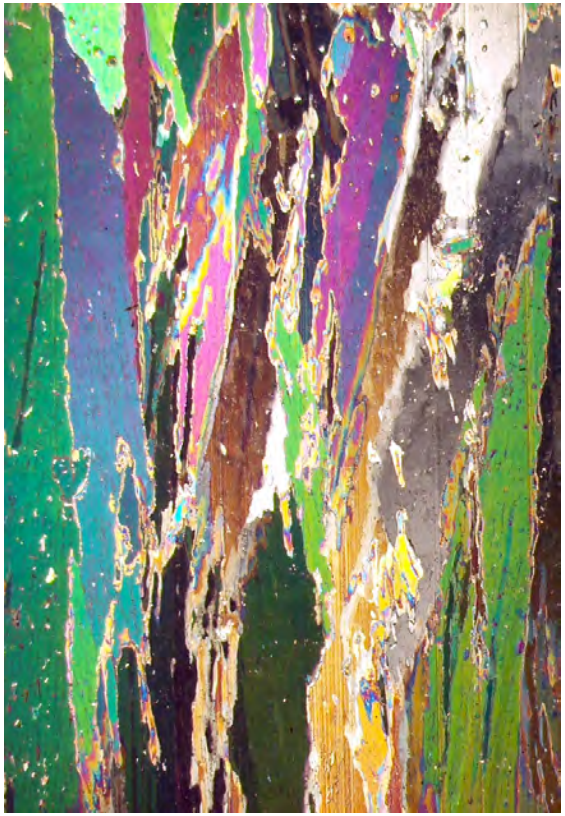

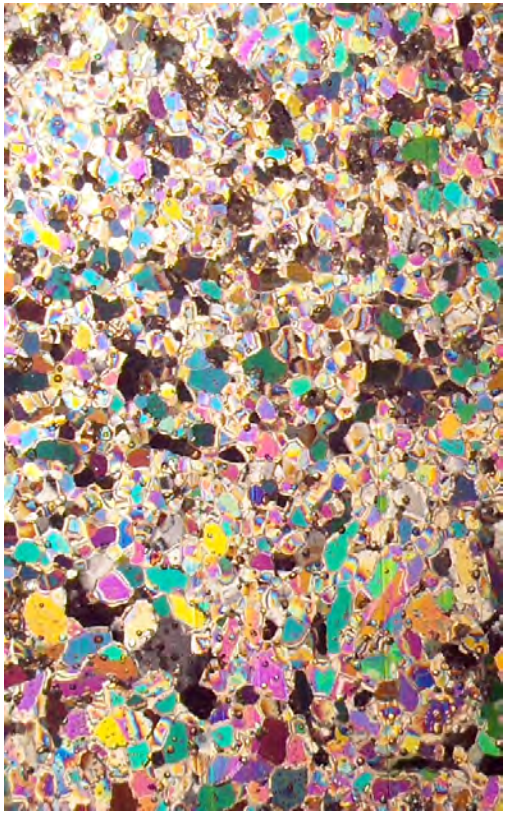

10%

Golden, Furse, Gully, Lin, Mosier, Sampson, Tison 2025

electromagnetically distinguish ice types
inverse homogenization for polycrystals

Spectral computations for sea ice floe configurations

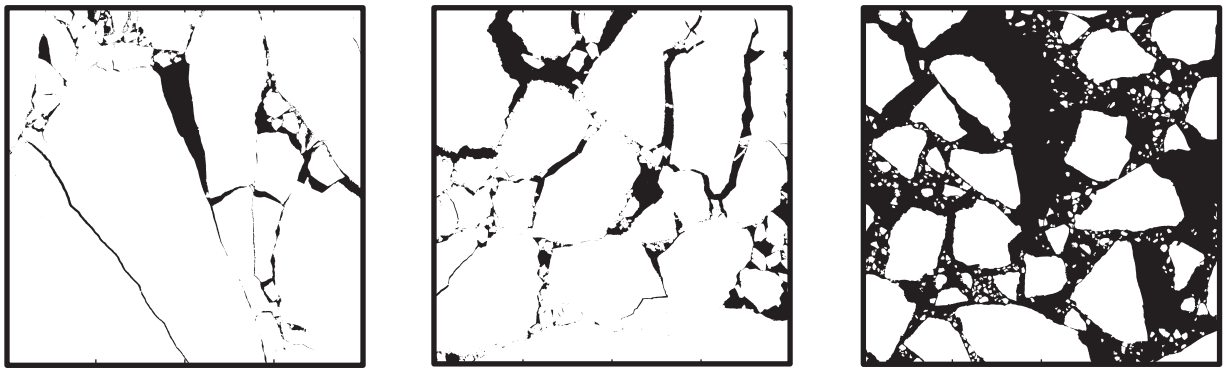

spectral measures

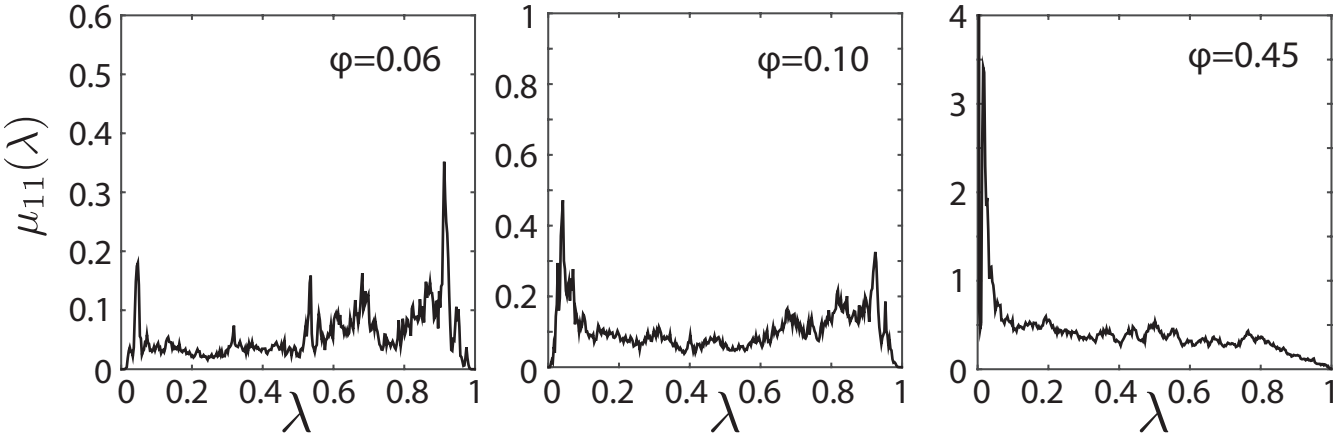

eigenvalue spacing distributions

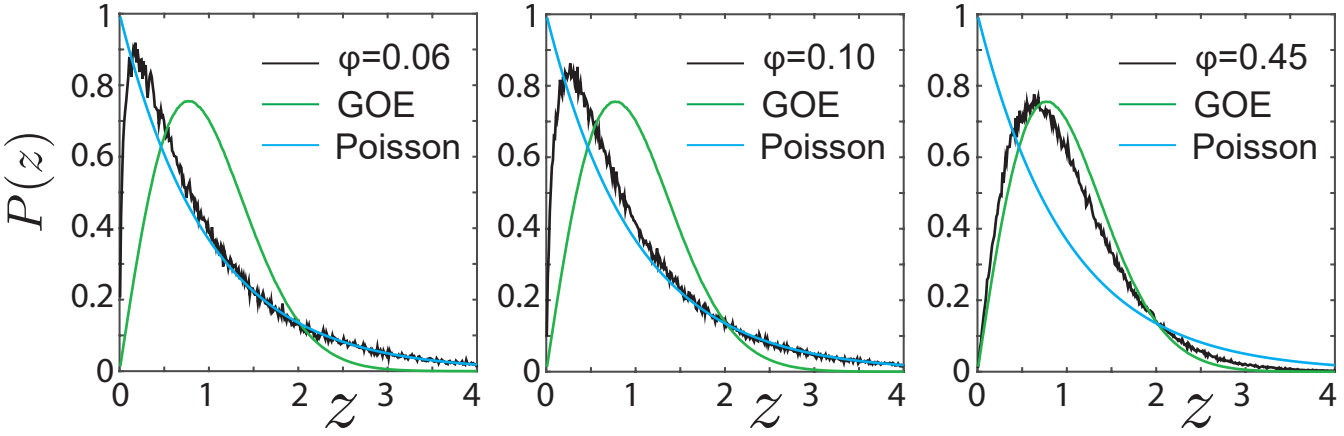

RANDOM MATRIX THEORY

uncorrelated → **level repulsion**

UNIVERSAL Wigner-Dyson distribution

Anderson localization transition

Murphy, Cherkaev, Golden, *Phys. Rev. Lett.* 2017; Murphy, Cherkaev, Hohenegger, Golden, *Comm. Math. Sci.* 2015

Eigenvalue Statistics of Random Matrix Theory

Wigner (1951) and Dyson (1953) first used random matrix theory (RMT) to describe quantized energy levels of heavy atomic nuclei.

$[\mathbf{N}]_{ij} \sim N(0,1)$, $\mathbf{A} = (\mathbf{N}+\mathbf{N}^T)/2$ ***Gaussian orthogonal ensemble (GOE)***

$[\mathbf{N}]_{ij} \sim N(0,1)+iN(0,1)$, $\mathbf{A} = (\mathbf{N}+\mathbf{N}^\dagger)/2$ ***Gaussian unitary ensemble (GUE)***

Short range and long range correlations of eigenvalues are measured by various eigenvalue statistics.

Spacing distributions of energy levels for heavy atomic nuclei

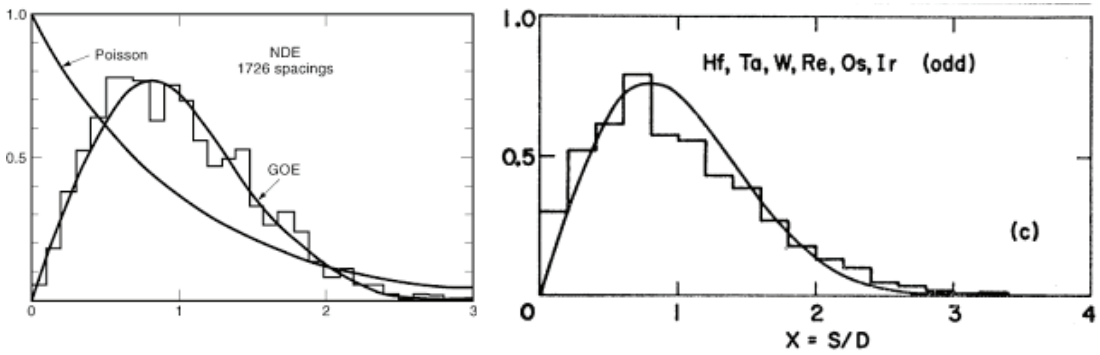

Spacing distributions of the first billion zeros of the Riemann zeta function

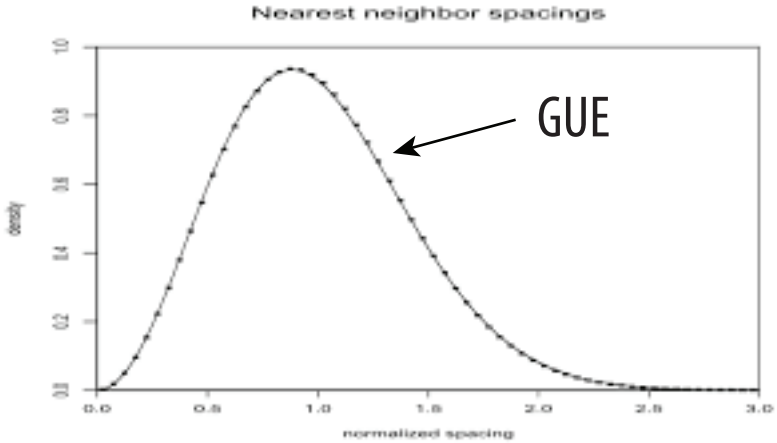

Universal eigenvalue statistics arise in a broad range of "unrelated" problems!

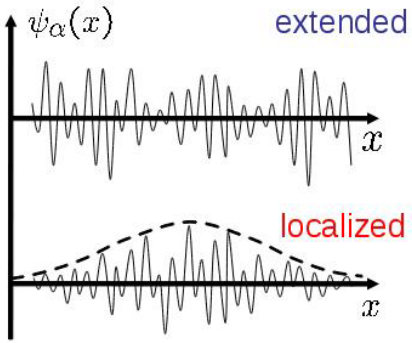

Anderson localization

disorder-driven

metal / insulator transition

Anderson 1958
Mott 1949
Evangelou 1992
Shklovshii et al 1993

propagation vs. localization in wave physics:
quantum, optics, acoustics, water waves

Wave equations

Laplace + Diffusion equations

we find percolation-driven

Anderson transition for classical transport in composites

mobility edges, localization, universal spectral statistics

Murphy, Cherkaev, Golden Phys. Rev. Lett. 2017

but no wave interference or scattering effects at play!

Order to Disorder in Quasiperiodic Composites

D. Morison (Physics), N. B. Murphy, E. Cherkaev, K. M. Golden, *Communications Physics* 2022

quasiperiodic crystal

quasicrystal

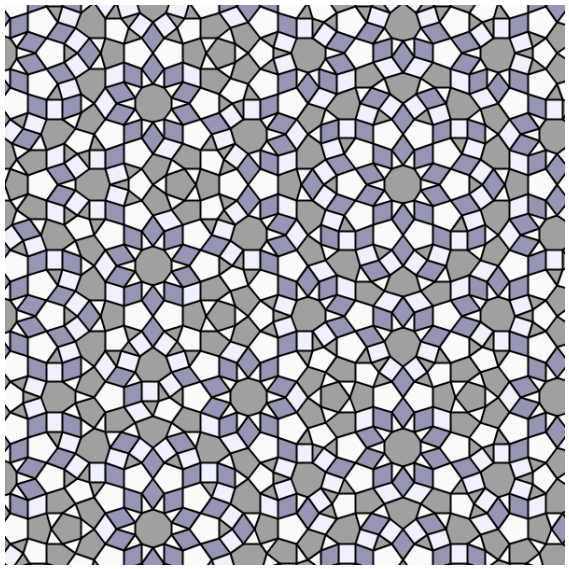

quasiperiodic checkerboard

Stampfli, 2013

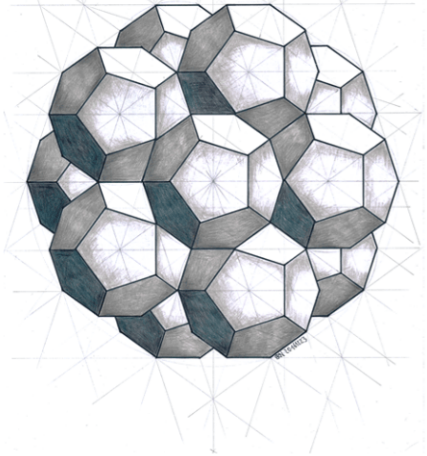

dense packing of dodecahedra

3D Penrose tiling Tripkovic, 2019

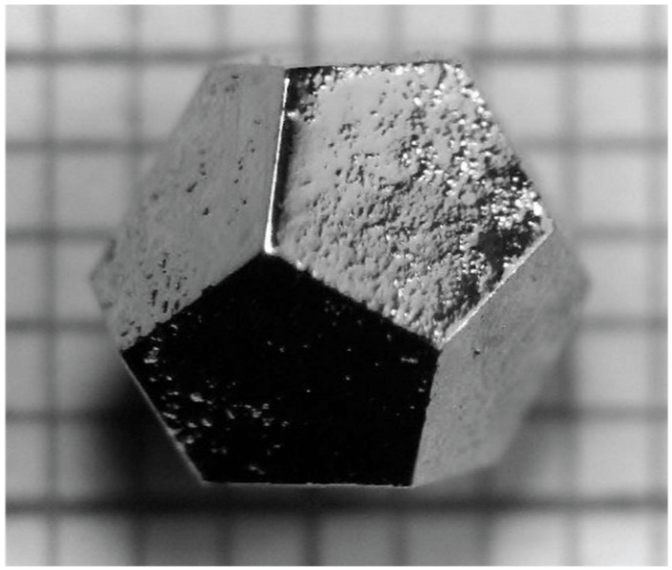

Holmium–magnesium–zinc quasicrystal

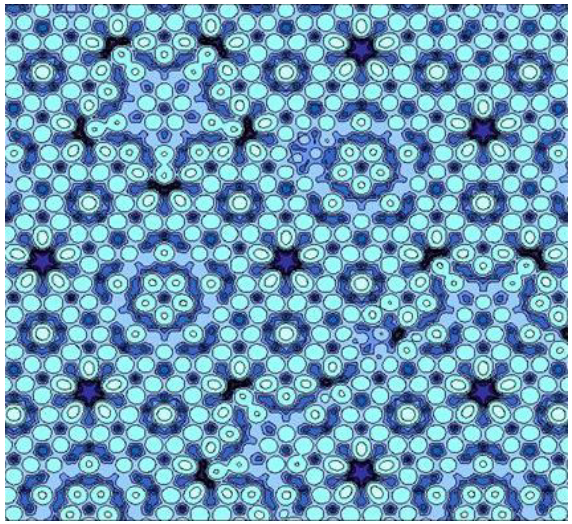

energy surface Al-Pd-Mn quasicrystal

Unal et al., 2007

ordered but aperiodic

lacks translational symmetry

Shechtman et al., *Phys. Rev. Lett.*, 1984

Levine & Steinhardt, *Phys. Rev. Lett.*, 1984

classical transport in quasiperiodic media

Golden, Goldstein & Lebowitz, *Phys. Rev. Lett.*, 1985

Golden, Goldstein & Lebowitz, *J. Stat. Phys.*, 1990

⋮

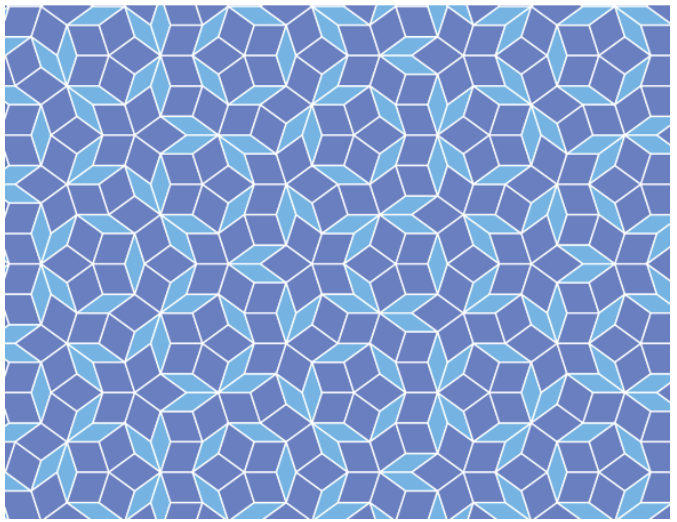

aperiodic tiling of the plane - R. Penrose 1970s

1D, 2D inhomogeneous materials - quasiperiodic

$$\sigma(x) = 3 + \cos x + \cos kx$$

effective conductivity

$$\sigma^*(k) = \begin{cases} \text{constant} & k \text{ irrational} \\ f(k) & k \text{ rational} \end{cases}$$

quasiperiodic

periodic

Golden, Goldstein, Lebowitz
Classical transport in modulated structures, ***Phys. Rev. Lett.*** **1985**

...

G. Bouchitté, S. Guenneau, F. Zolla, *SIAM Multiscale Modeling & Simulation*, 2010

E. Cherkaev, S. Guenneau, N. Wellander, *IEEE Metamaterials, 2017*

N. Wellander, S. Guenneau, E. Cherkaev, *Math. Methods in the Applied Sci.*, 2017

Classical transport in quasiperiodic media

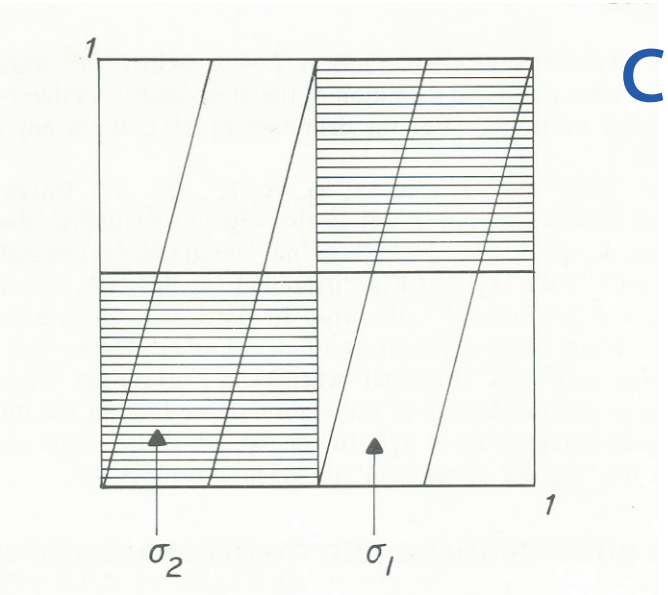

line of slope k through
an infinite checkerboard

Golden, Goldstein, and Lebowitz
***Phys. Rev. Lett.* 1985**
***J. Stat. Phys.* 1990**

1D two component composite material

effective conductivity $\sigma^*(k)$

effective resistivity $1/\sigma^*(k) = 1 - G(k)$

$$G(k) = \begin{cases} 0, & k \text{ irrational} \\ 1/pq, & k = p/q \text{ rational} \end{cases}$$

continuous at *k* irrational
discontinuous at *k* rational

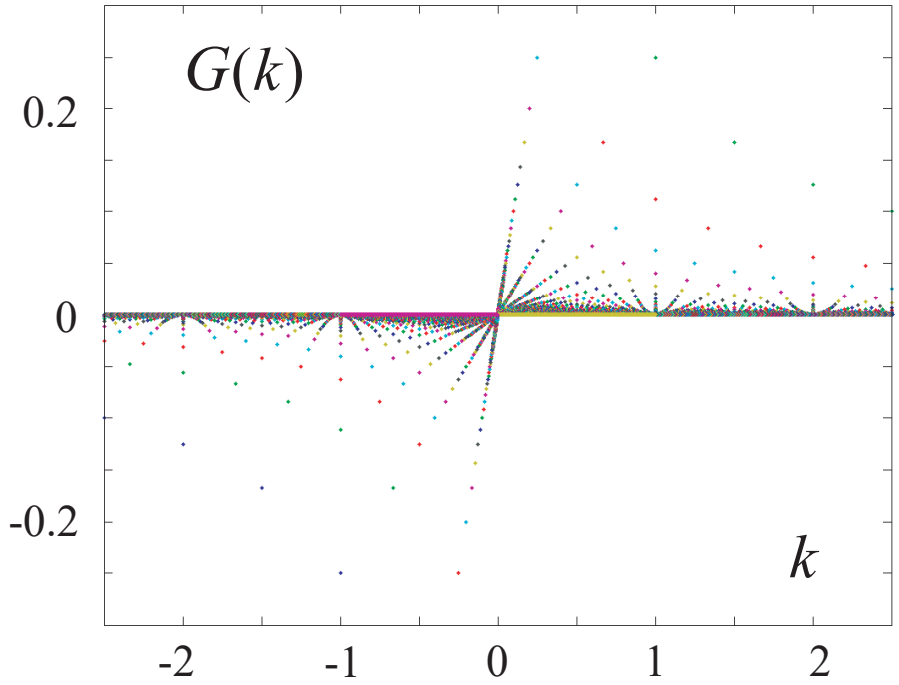

Moiré patterns generate two component composites **on any scale**

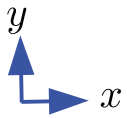

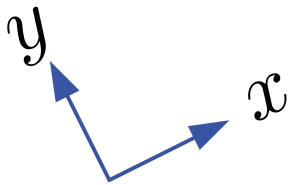

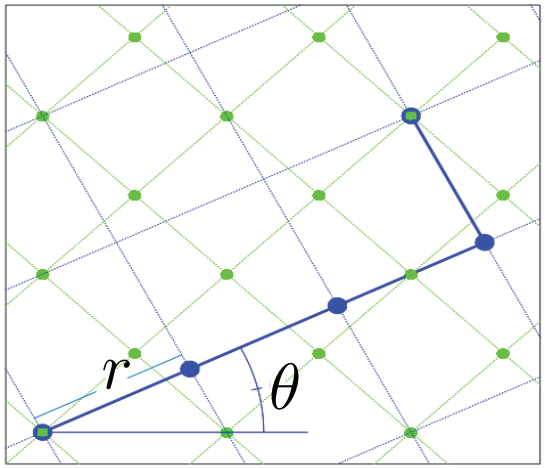

rotation
dilation

$$\begin{pmatrix} x' \\ y' \end{pmatrix} = r \begin{pmatrix} \cos\theta & -\sin\theta \\ \sin\theta & \cos\theta \end{pmatrix} \begin{pmatrix} x \\ y \end{pmatrix}$$

$$\psi\left(x', y'\right) = \cos 2\pi x' \cos 2\pi y'$$

$$\chi = \begin{cases} 1, & \psi \geq 0 \\ 0, & \psi < 0 \end{cases}$$

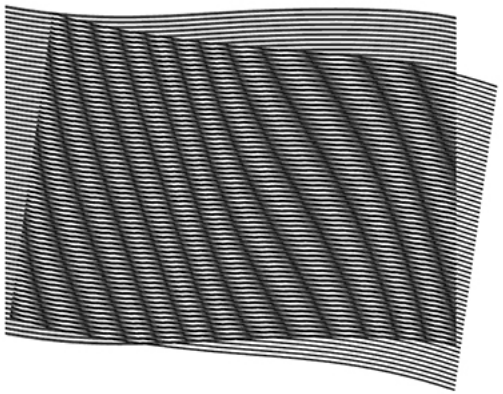

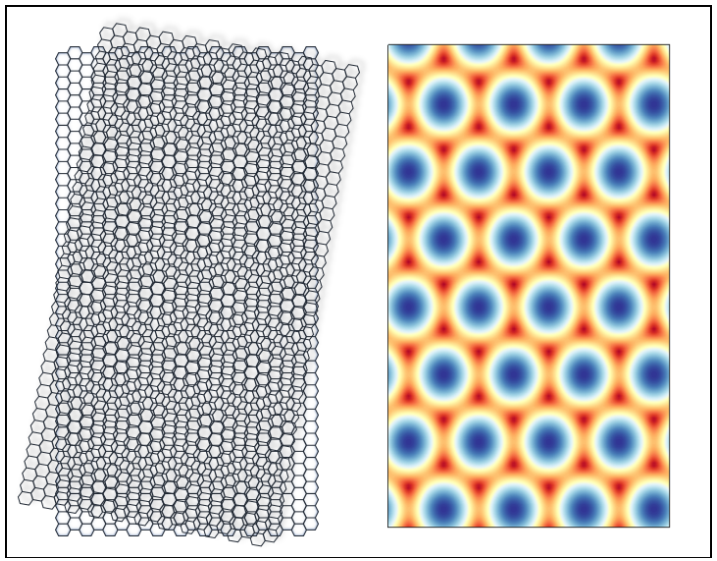

quantum dots
artificial atoms

Tran et al.
Nature 2019

TWISTRONICS

graphene

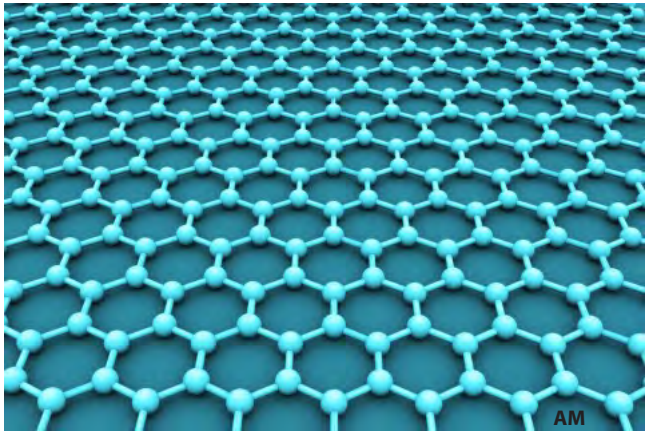

twisted bilayer graphene

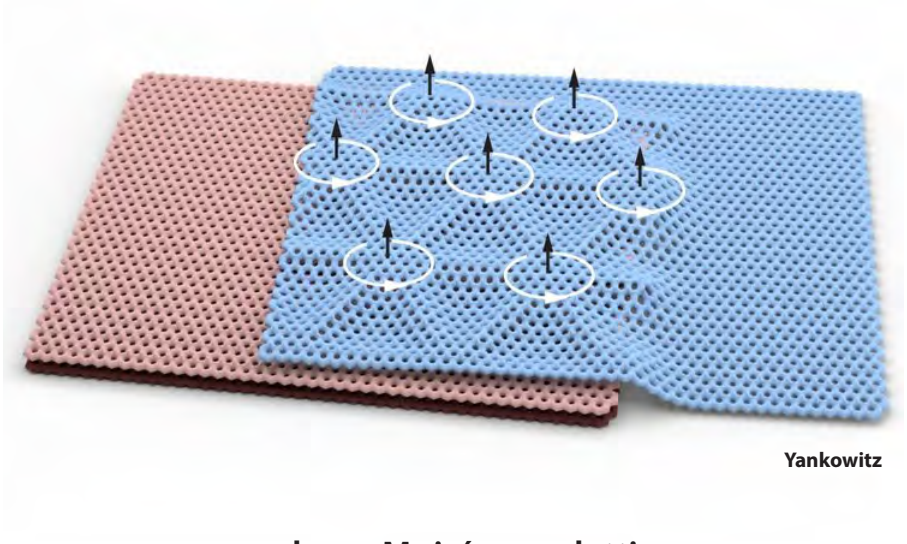

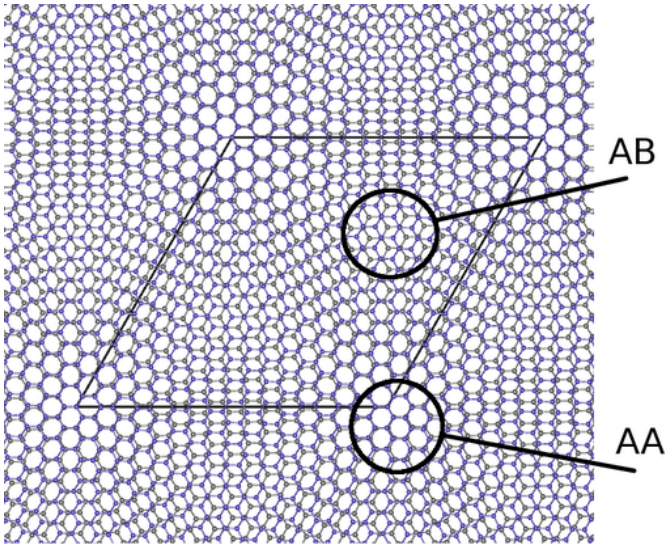

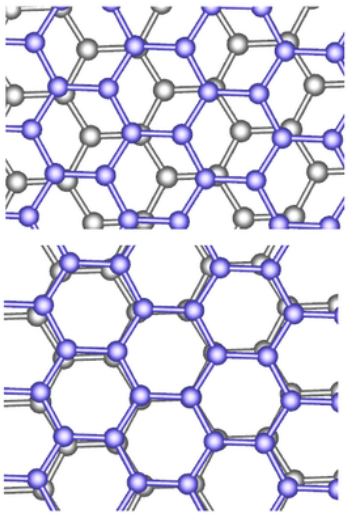

graphene Moiré superlattice

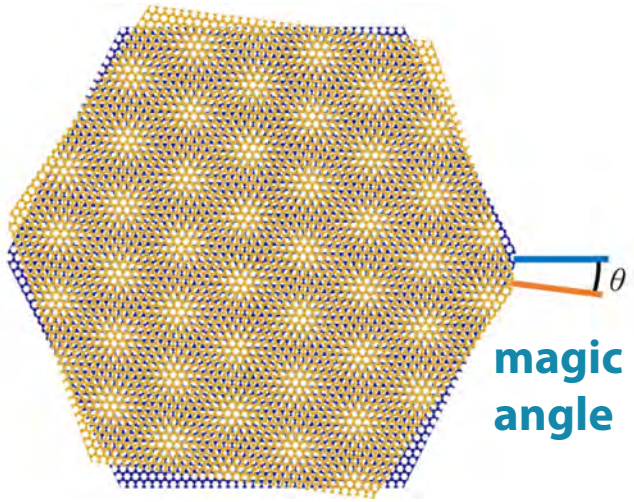

superconductivity, novel band topology

semiconductor quantum dots, acting as "artificial atoms"

Moiré patterns from "interference" of two periodic lattices

Moiré superlattices - condensed matter playground (Li et al, 2023)

Order to disorder in quasiperiodic composites

Morison, Murphy, Cherkaev, Golden, Comm. Phys. 2022

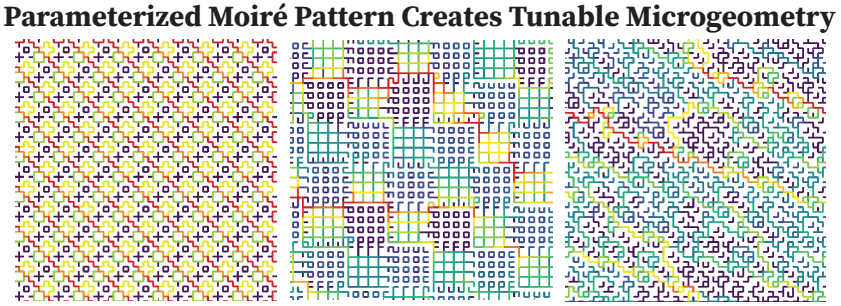

twisted bilayer composites

sea ice - inspired high tech spin off

tunable Moiré composites with exotic properties

(optical, electrical, thermal, ...), Anderson localization; our Moiré patterned geometries are similar to twisted bilayer graphene

but can be engineered on any scale!

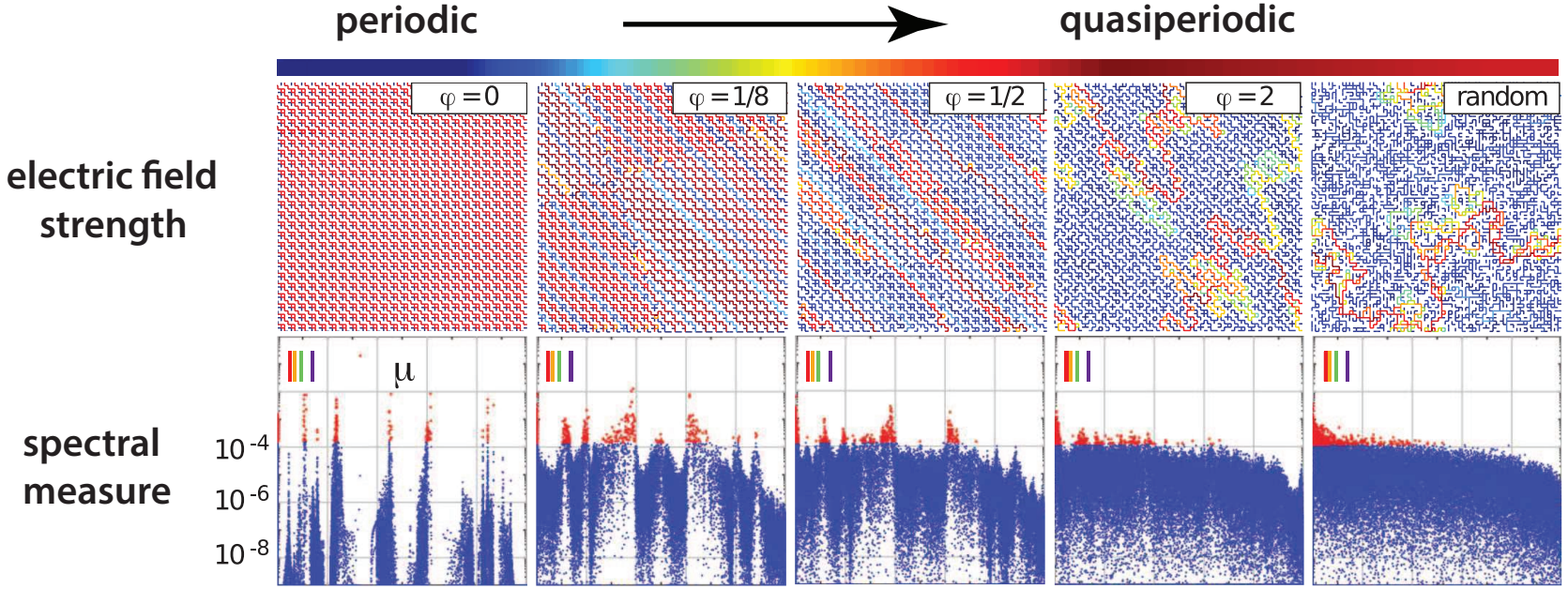

we bring the solid state physics framework for electronic transport and band gaps in semiconductors to classical transport in periodic and quasiperiodic composites

Anderson transition as twist angle is tuned

photonic crystals and quasicrystals

mesoscale

advection enhanced diffusion

effective diffusivity

nutrient and salt transport in sea ice
heat transport in sea ice with convection
sea ice floes in winds and ocean currents
tracers, buoys diffusing in ocean eddies
diffusion of pollutants in atmosphere

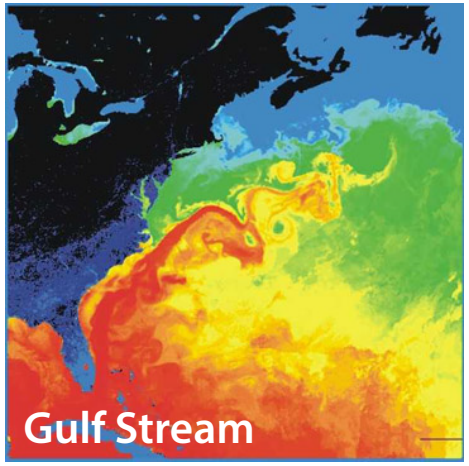

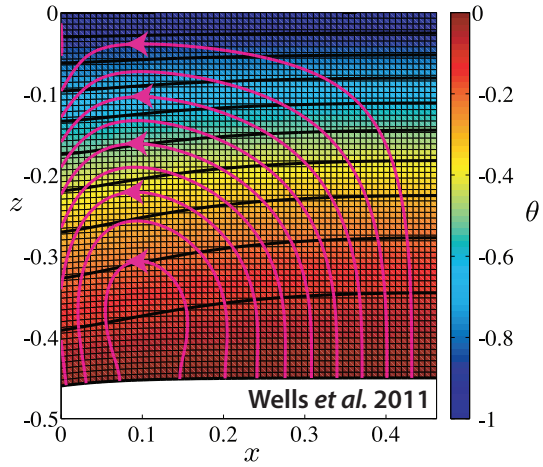

advection diffusion equation with a velocity field $\vec{u}$

$$\frac{\partial T}{\partial t} + \vec{u} \cdot \vec{\nabla} T = \kappa_0 \Delta T$$

$$\vec{\nabla} \cdot \vec{u} = 0$$

homogenize

$$\frac{\partial \overline{T}}{\partial t} = \kappa^* \Delta \overline{T}$$

κ^* *effective diffusivity*

Stieltjes integral for κ^* *with spectral measure*

Avellaneda and Majda, PRL 89, CMP 91

Murphy, Cherkaev, Xin, Zhu, Golden, *Ann. Math. Sci. Appl.* 2017
Murphy, Cherkaev, Zhu, Xin, Golden, *J. Math. Phys.* 2020

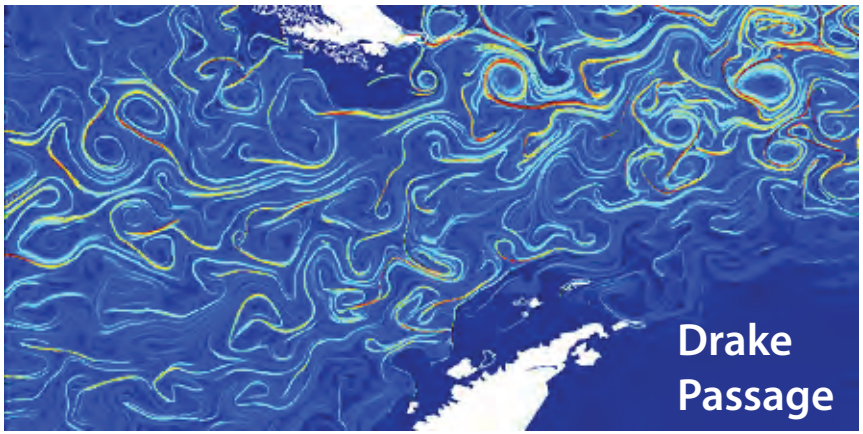

PROCEEDINGS
OF THE ROYAL SOCIETY A

MATHEMATICAL, PHYSICAL AND ENGINEERING SCIENCES

THE
ROYAL
SOCIETY
PUBLISHING

Homogenization for convection-enhanced thermal transport in sea ice

N. Kraitzman, R. Hardenbrook,
H. Dinh, N. B. Murphy, E. Cherkaev,
J. Zhu and K. M. Golden

August 2024

First rigorous mathematical theory of thermal conductivity of sea ice with convective fluid flow; captures data.

missing in climate models

tracers flowing through inverted sea ice blocks

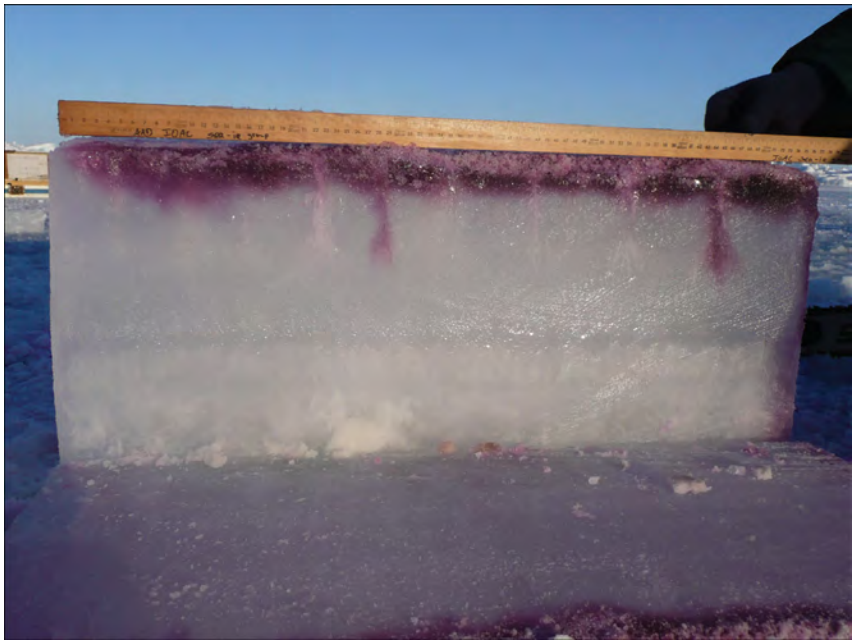

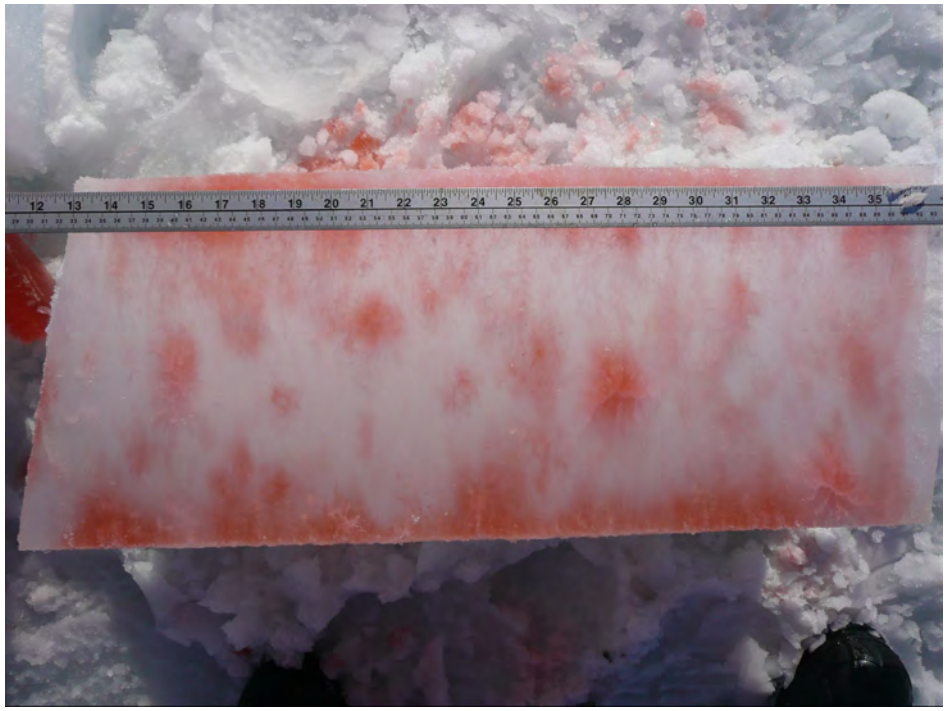

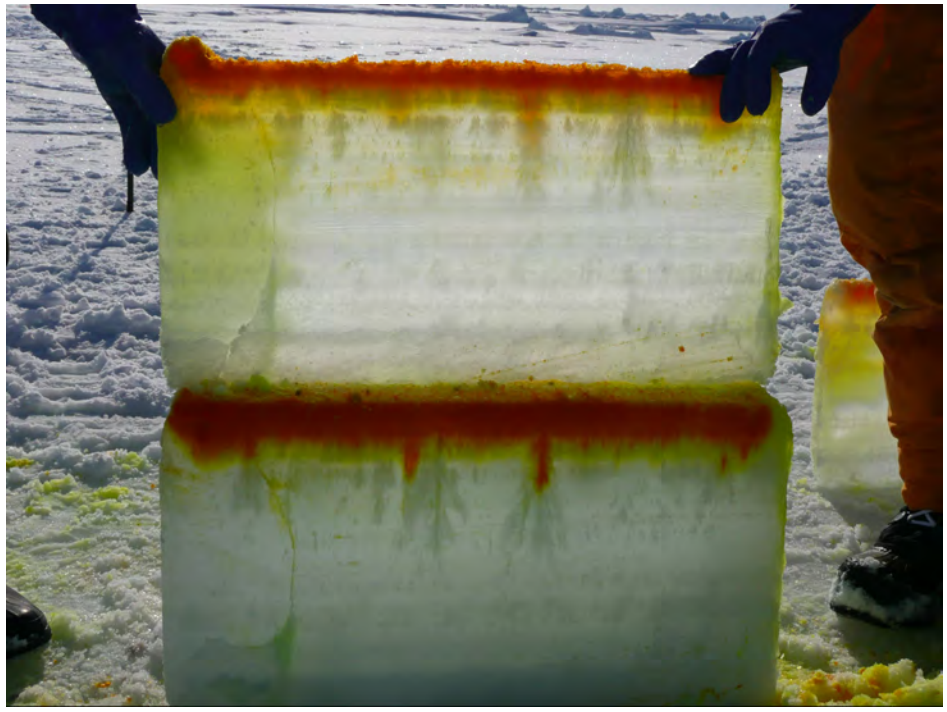

Stieltjes Integral Representation for Advection Diffusion

Murphy, Cherkaev, Zhu, Xin, Golden, *J. Math. Phys.* 2020

$$\kappa^* = \kappa\left(1 + \int_{-\infty}^{\infty} \frac{d\mu(\tau)}{\kappa^2 + \tau^2}\right), \quad F(\kappa) = \int_{-\infty}^{\infty} \frac{d\mu(\tau)}{\kappa^2 + \tau^2}$$

- μ is a positive definite measure corresponding to the spectral resolution of the self-adjoint operator $i\Gamma H\Gamma$
- $H =$ stream matrix , $\kappa =$ local diffusivity
- $\Gamma := -\nabla(-\Delta)^{-1}\nabla\cdot$, Δ is the Laplace operator
- $i\Gamma H\Gamma$ is bounded for time independent flows
- $F(\kappa)$ is analytic off the spectral interval in the κ-plane

rigorous framework for numerical computations of spectral measures and effective diffusivity for model flows

new integral representations, theory of moment calculations

separation of material properties and flow field

Bounds on Convection Enhanced Thermal Transport

simulations

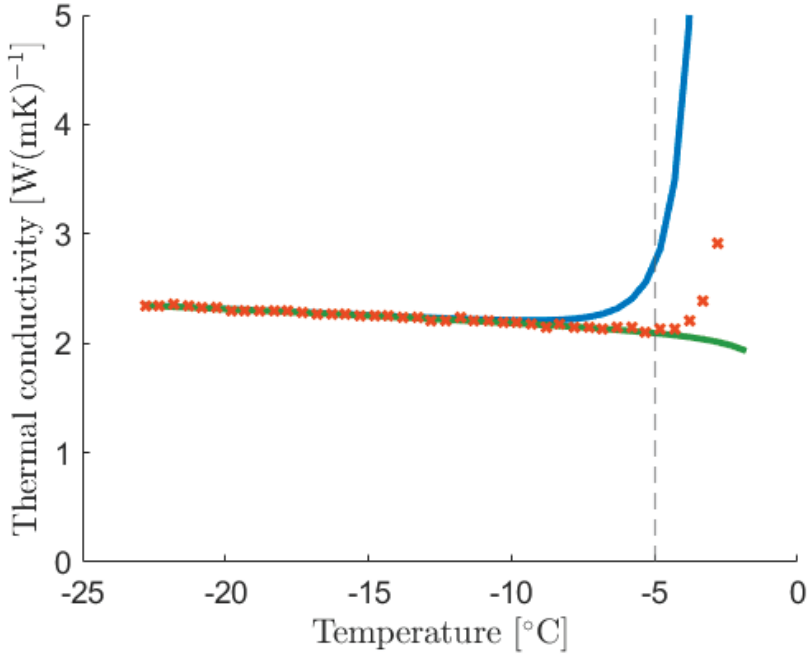

data [Trodahl et al., 2001]

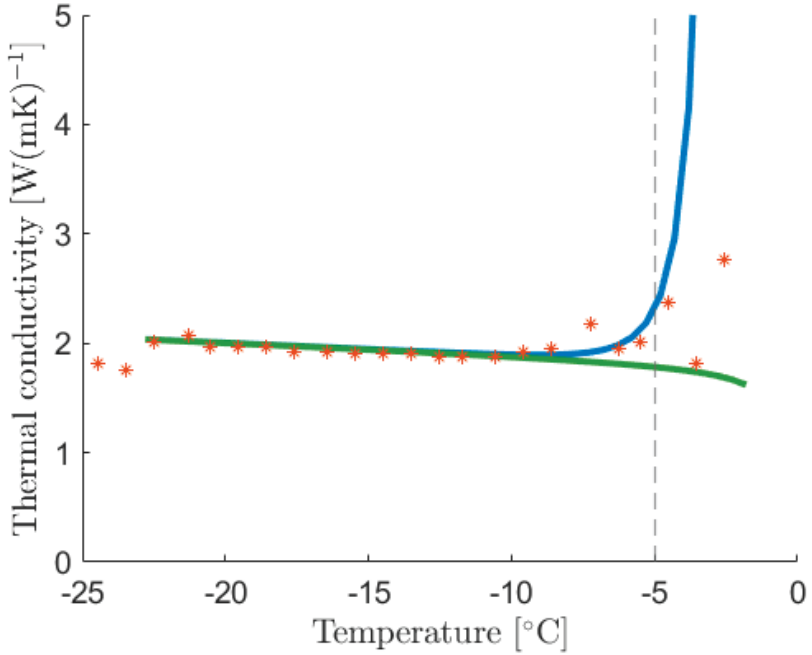

Monte-Carlo simulations of SDE with temperature dependent Péclet number P

strength of advection B = κP/2π

Euler-Maruyama and subsampling methods for SDE

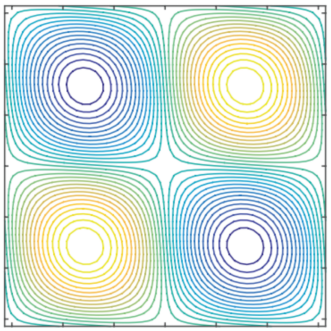

cat's eye flow model for brine convective flow

Rigorous Padé approximant bounds in terms of P using Stieltjes integral + analytic continuation method for the measure

Darcy velocity v = 0.5 [m/s]

Kraitzman, Hardenbrook, Dinh, Murphy, Cherkaev, Zhu, & Golden

***Proc. Royal Soc. A*, 2024**

ocean wave propagation through the sea ice pack

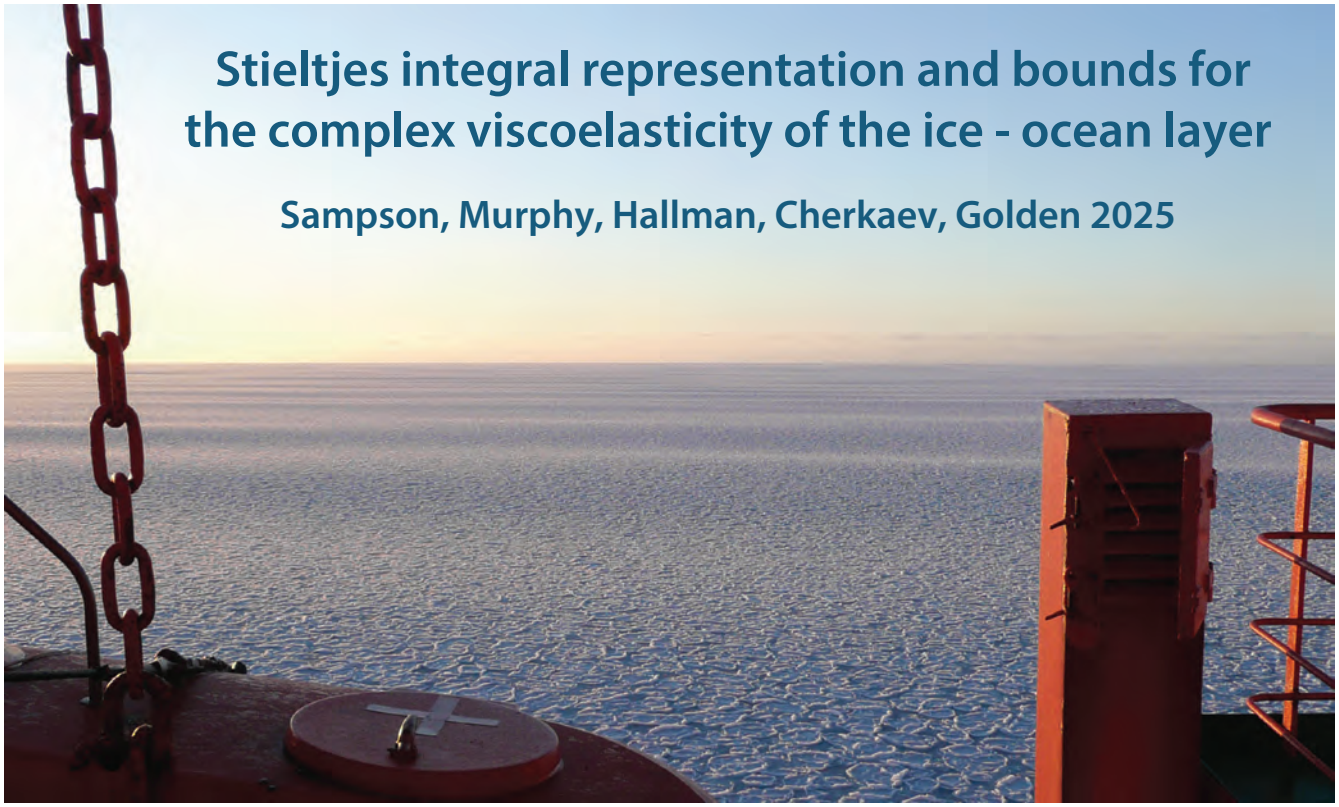

- wave-ice interactions critical to growth and melting processes
- break-up; pancake promotion floe size distribution

effective layer parameter previously fit to wave data

Keller 1998
Mosig, Montiel, Squire 2015
Wang, Shen 2012

Analytic Continuation Method

Bergman 1978, Milton 1979
Golden and Papanicolaou 1983
Milton, *Theory of Composites* 2002

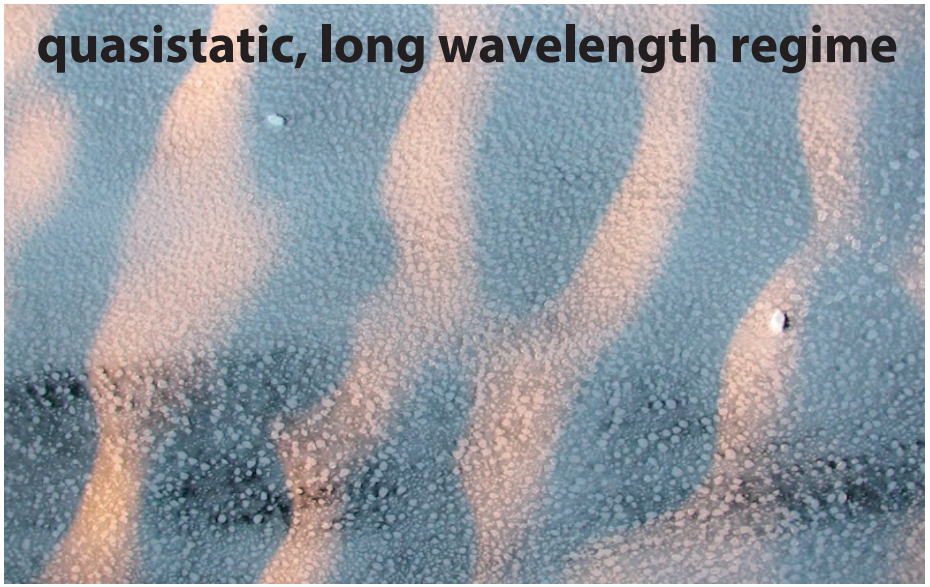

homogenized parameter depends on sea ice concentration and ice floe geometry

like EM waves

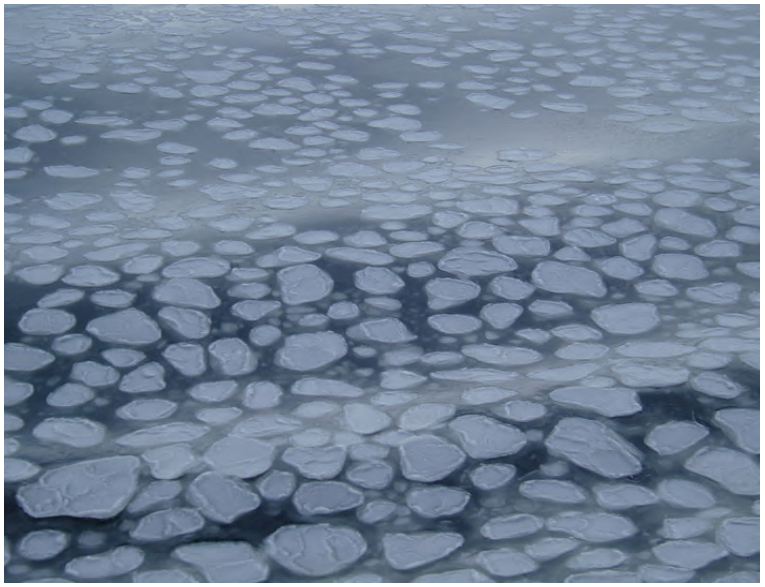

Waves in sea ice and solid state physics

Resolvent representation of the deviatoric strain field

$$\chi\epsilon_s = s\left(sI - \chi\Gamma^S\chi\right)^{-1}\chi\epsilon_s^0$$

Stieltjes integral representation of effective complex viscoelasticity

$$\frac{\nu^*}{\nu_2} = \int_0^1 \frac{d\mu(\lambda)}{s-\lambda}$$

Increasing geometric order →

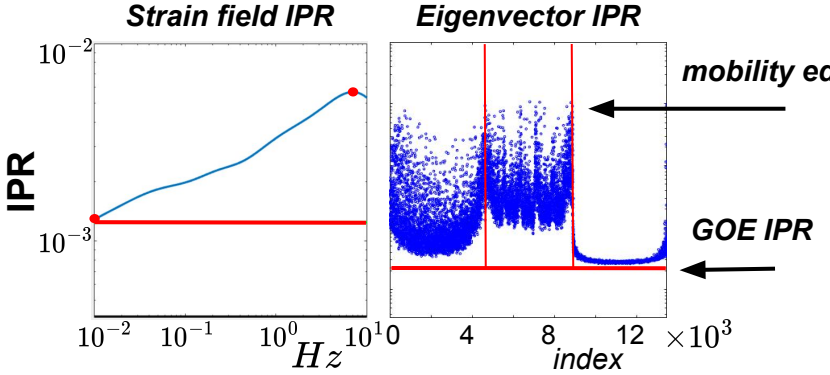

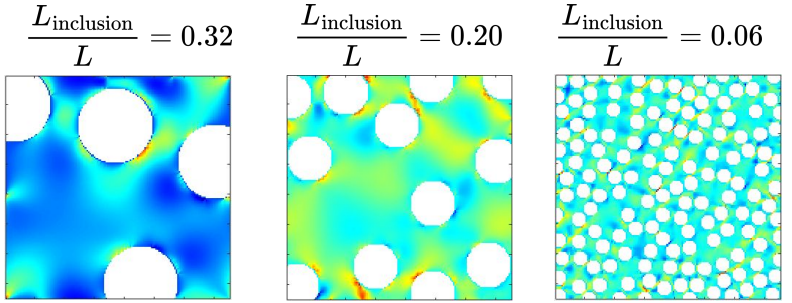

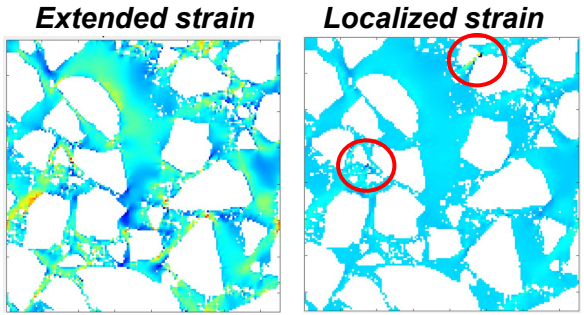

$f = 0.01Hz$ $f = 7.079Hz$

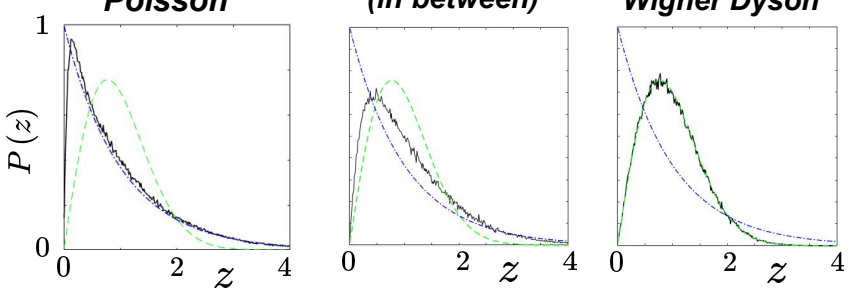

Transition in the eigenvalue spacing distribution of $\chi\Gamma^S\chi$

Large inclusions → ***Small inclusions***

"Local to collective deformation transition"

The sea ice pack has fractal structure.

Self-similarity of sea ice floes

Weddell Sea, Antarctica

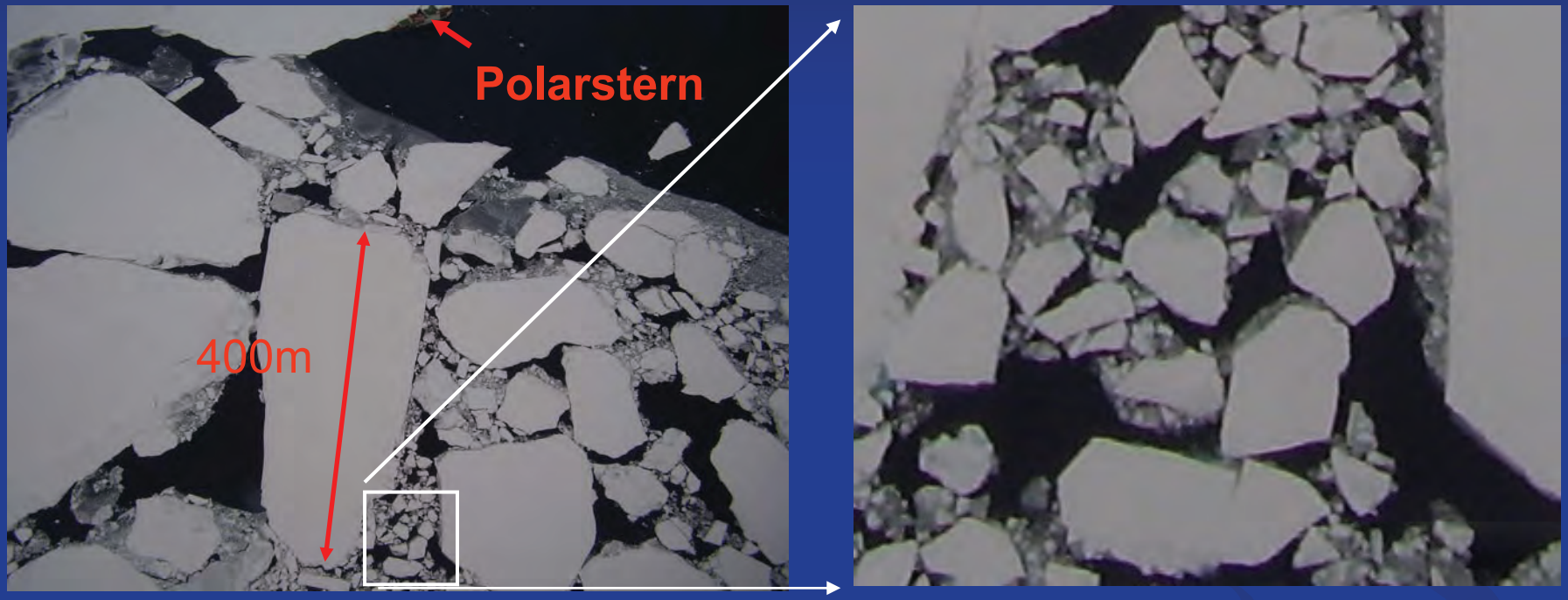

fractal dimensions of Okhotsk Sea ice pack
smaller scales D~1.2, larger scales D~1.9

fractal dim. *vs.* floe size exponent
Adam Dorsky, Nash Ward, Ken Golden 2024

Toyota, *et al. Geophys. Res. Lett.* 2006
Rothrock and Thorndike, *J. Geophys. Res. 1984*

SEA ICE ALGAE high level of local heterogeneity

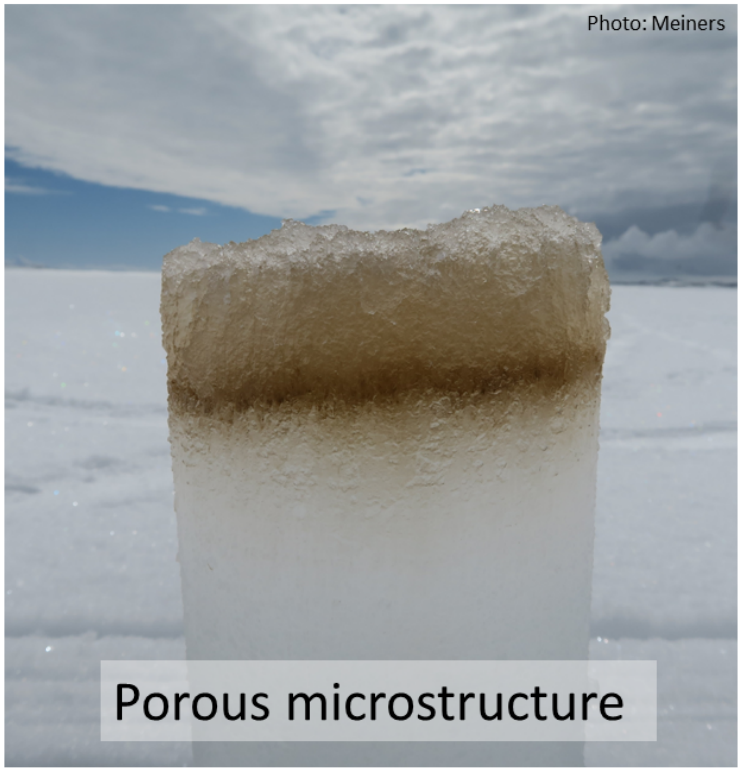

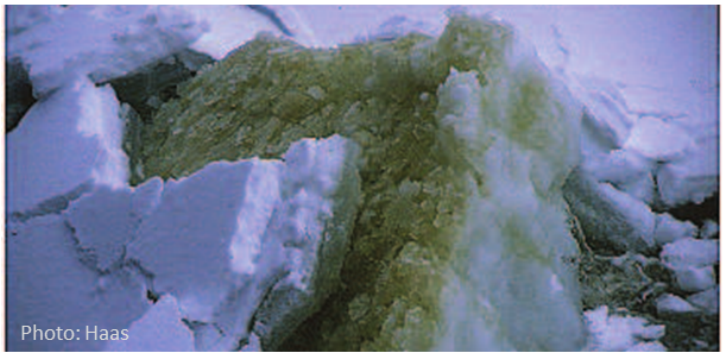

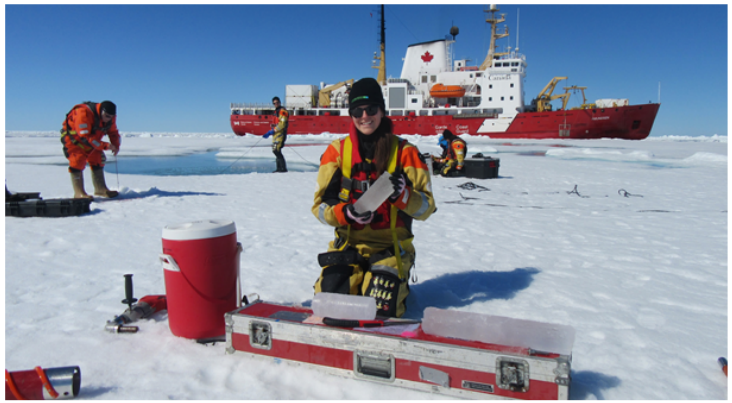

Can we improve agreement between algae models and data?

80% of polar bear diet can be traced to ice algae*.

* Brown TA, et al. (2018). *PloS one*, 13(1), e0191631

HETEROGENEITY in PARAMETERS & CONDITIONS

At each location within a larger region, consider

$$\frac{dN}{dt} = \alpha - BNP - \eta N$$

$$\frac{dP}{dt} = \gamma BNP - \delta P$$

treating parameters as random variables

$$N(0) = N_0, \qquad P(0) = P_0$$

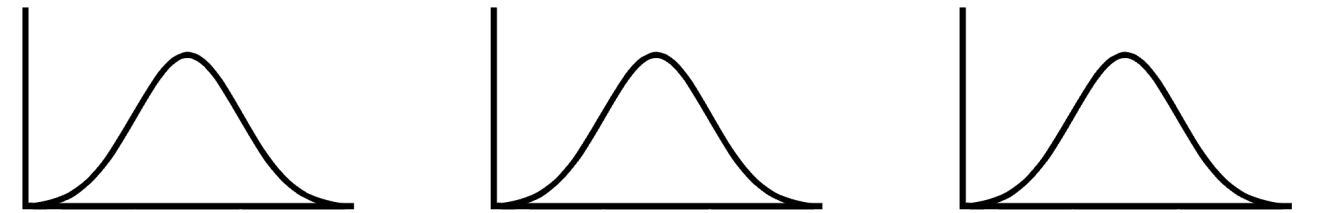

But, Monte Carlo for Full Algae Model: 8 hours X 10,000

Received: 7 June 2022 | Revised: 1 August 2022 | Accepted: 1 August 2022

DOI: 10.1111/ele.14095

ECOLOGY LETTERS cnrs WILEY

METHOD

Uncertainty quantification for ecological models with random parameters

Jody R. Reimer[1,2] | **Frederick R. Adler**[1,2] | **Kenneth M. Golden**[1] | **Akil Narayan**[1,3]

[1]Department of Mathematics, University of Utah, Salt Lake City, Utah, USA

[2]School of Biological Sciences, University of Utah, Salt Lake City, Utah, USA

[3]Scientific Computing and Imaging Institute, University of Utah, Salt Lake City, Utah, USA

Correspondences
Jody R. Reimer, Department of Mathematics and School of Biological Sciences, University of Utah, Salt Lake City, Utah, USA.
Email: reimer@math.utah.edu

Abstract

There is often considerable uncertainty in parameters in ecological models. This uncertainty can be incorporated into models by treating parameters as random variables with distributions, rather than fixed quantities. Recent advances in uncertainty quantification methods, such as polynomial chaos approaches, allow for the analysis of models with random parameters. We introduce these methods with a motivating case study of sea ice algal blooms in heterogeneous environments. We compare Monte Carlo methods with polynomial chaos techniques to help understand the dynamics of an algal bloom model with random parameters.

N-P Model

Introduce polynomial chaos approach to widely used ecological ODE models, but with random parameters.

Ecological insights

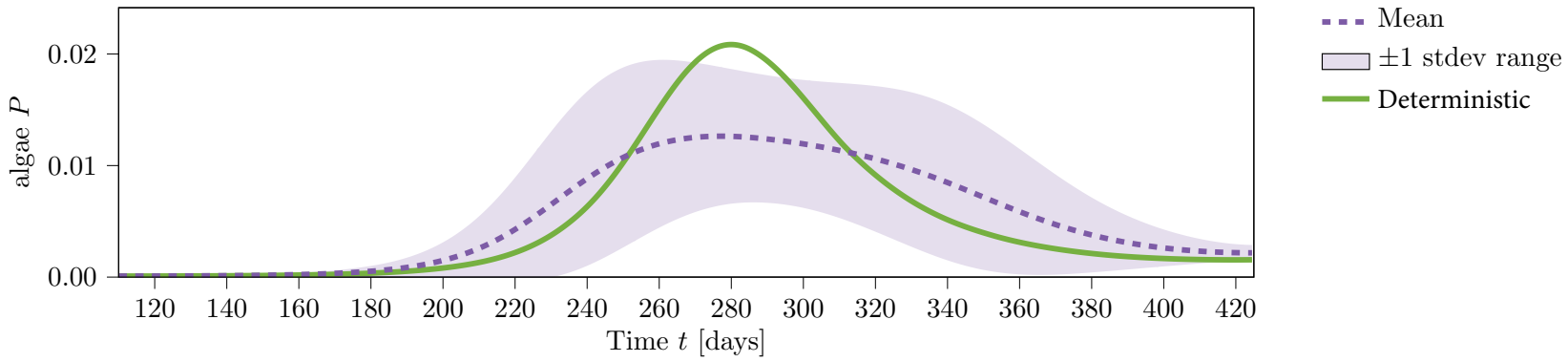

- lower peak bloom intensity
- longer bloom duration
- able to compare variance to data

Inverse Problem: given algal and nutrient data, recover growth rate distribution
Anthony Lee, Jody Reimer, Akil Narayan, Ken Golden 2024

Optimal Movement of a Polar Bear in a Heterogenous Icescape

Nicole Forrester, Rylie Gagne, Jody Reimer, Ken Golden 2025

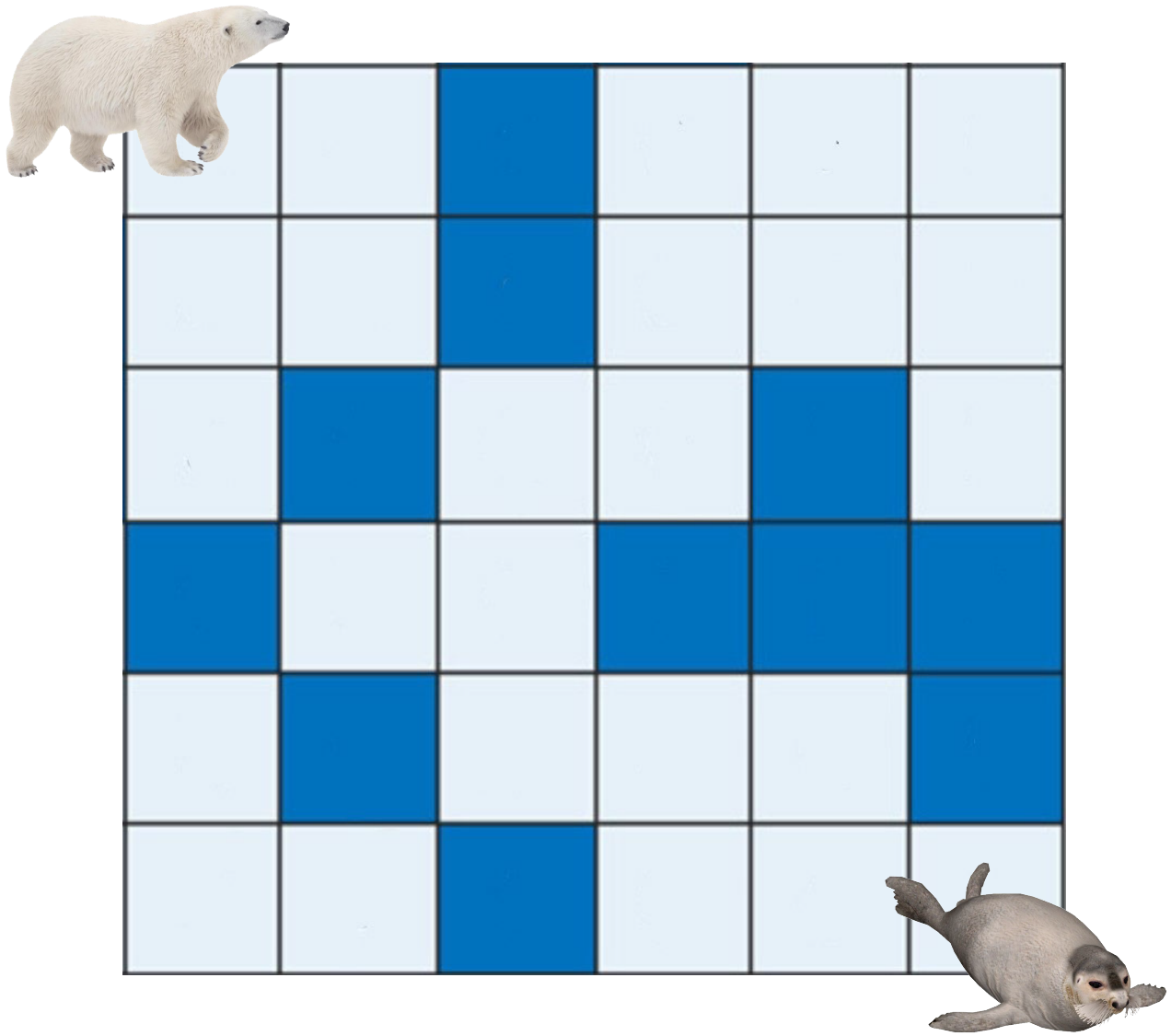

Polar bears expend 5X more energy swimming than walking on sea ice.

As sea ice is lost, how do polar bears optimize their movement to save energy and survive?

https://pluspng.com/img-png/polar-bear-png-polar-white-bear-png-1000.png
https://zt2downloadlibrary.fandom.com/wiki/Bearded_Seal_(Tamara_Henson)

Polar Bear Percolation

To study the importance of ice connectedness, we exaggerate the data by setting the cost of walking on ice to 0 with the cost of swimming still at 5.

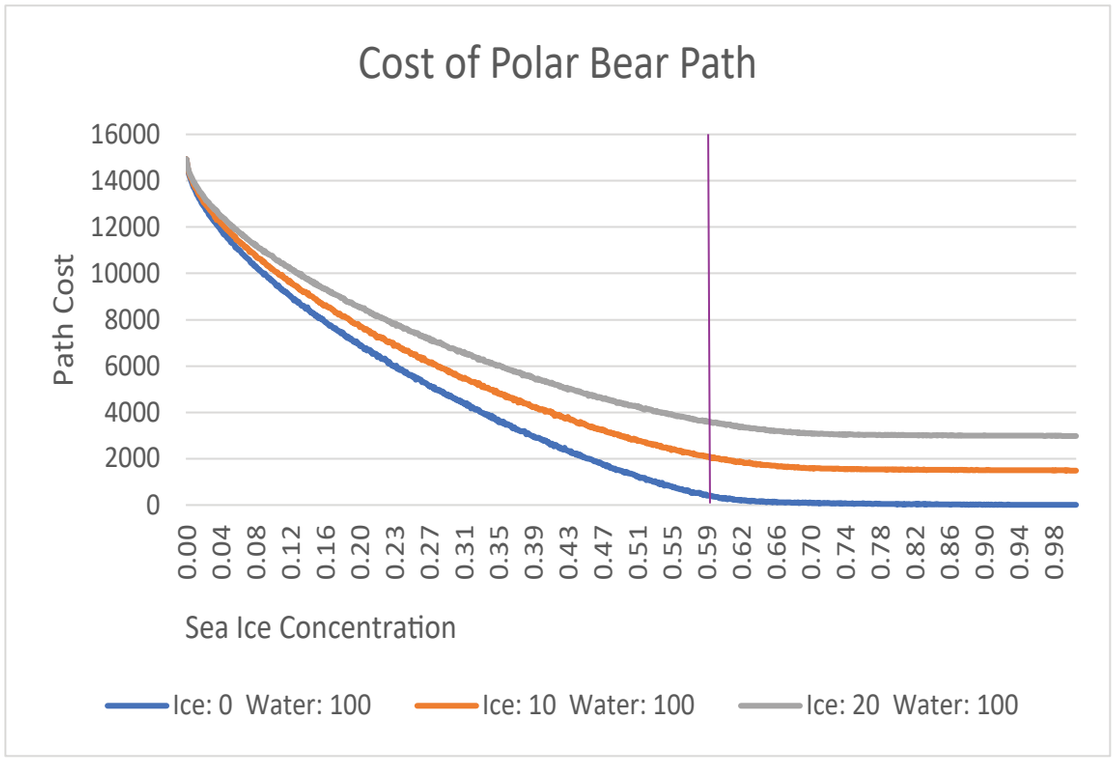

$C(p)$

$h = 0.2$
$h = 0.1$
$h = 0$

$$h = \frac{c_i}{c_w}$$

ratio of local "conductivities"

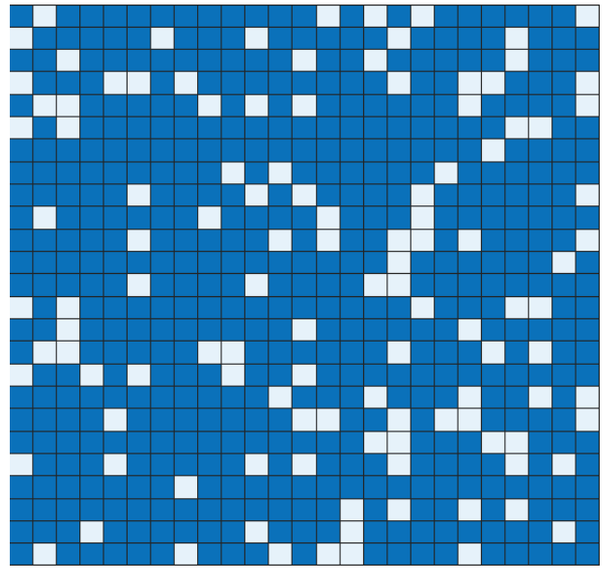

20% Ice

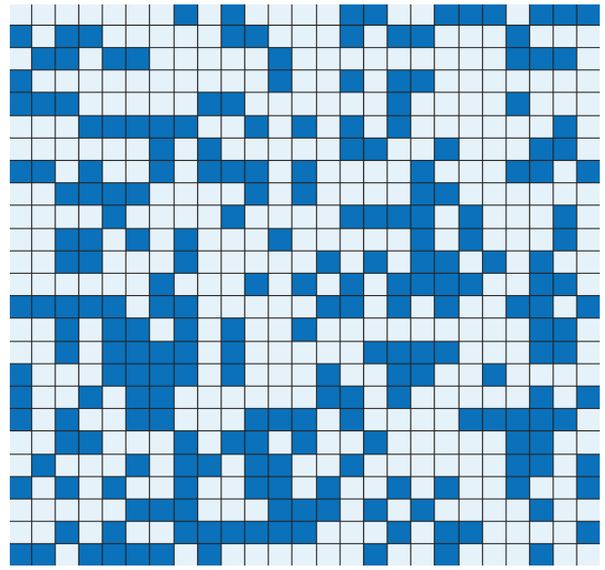

60% Ice

site percolation threshold

$p_c = 0.59 \quad for \quad d = 2$

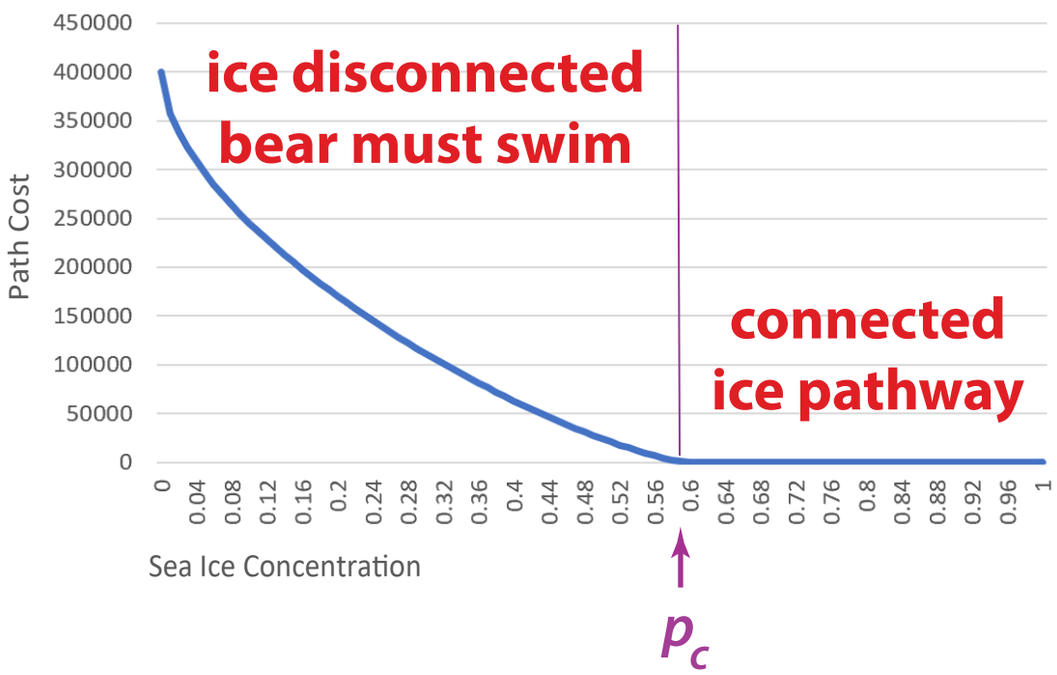

$C(p)$

$h = 0$

Polar Bear Critical Exponent

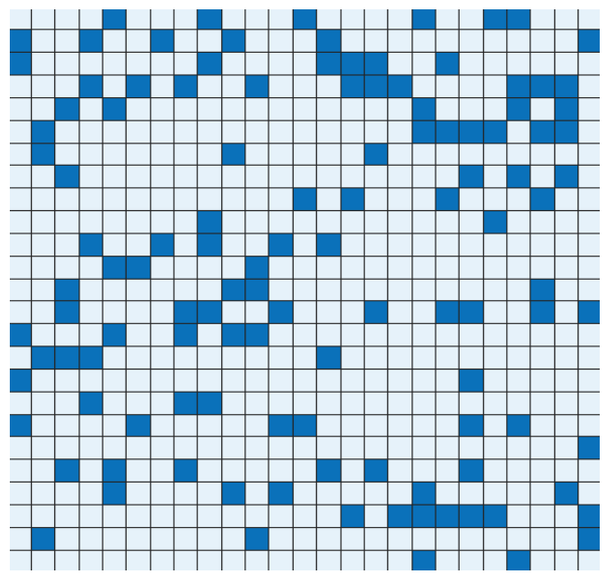

80% Ice

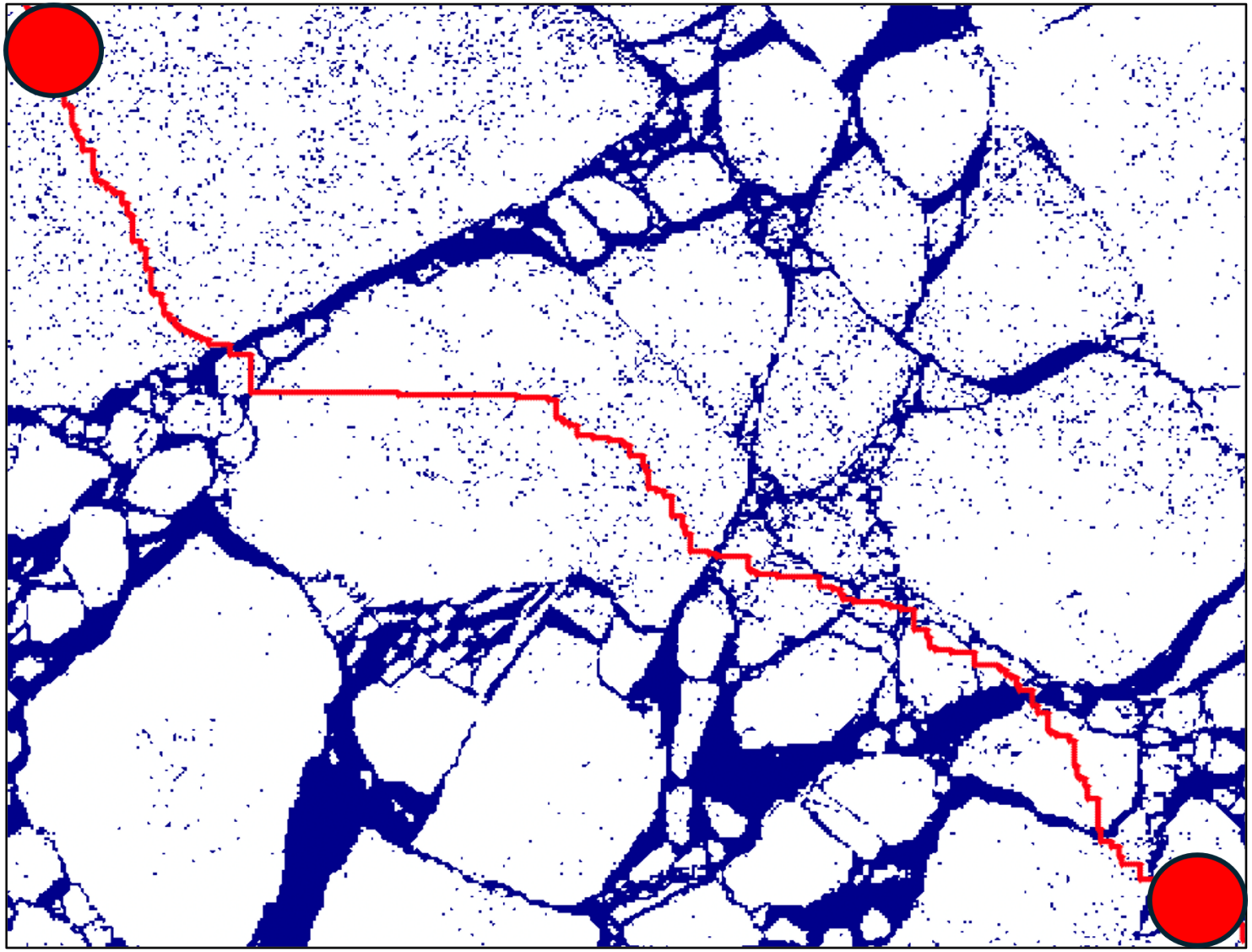

melt pond formation and albedo evolution:

- ***major drivers in polar climate***
- ***key challenge for global climate models***

numerical models of melt pond evolution, including topography, drainage (permeability), etc.

Lüthje, Feltham, Taylor, Worster 2006

Flocco, Feltham 2007

Skyllingstad, Paulson, Perovich 2009

Flocco, Feltham, Hunke 2012

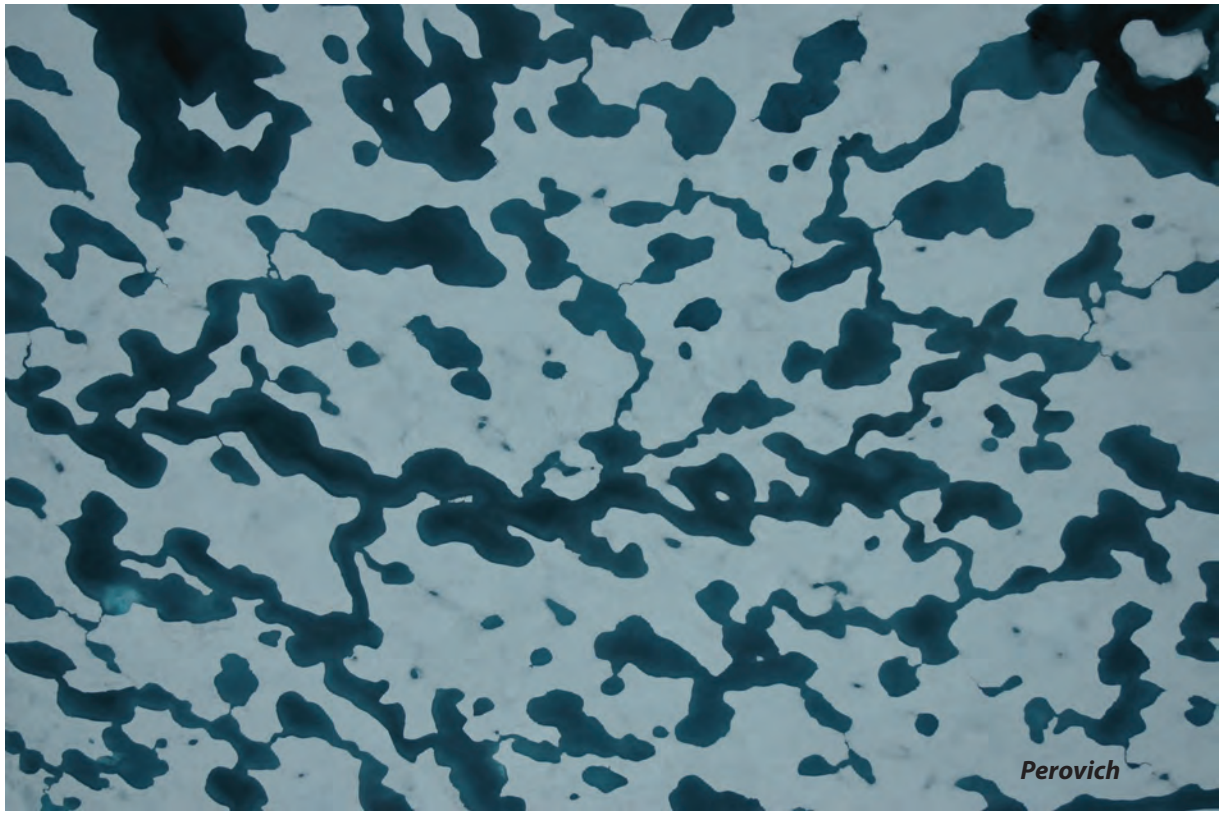

Are there universal features of the evolution similar to phase transitions in statistical physics?

Transition in the fractal geometry of Arctic melt ponds

Christel Hohenegger, Bacim Alali, Kyle Steffen, Don Perovich, Ken Golden

The Cryosphere, 2012

complexity grows with length scale

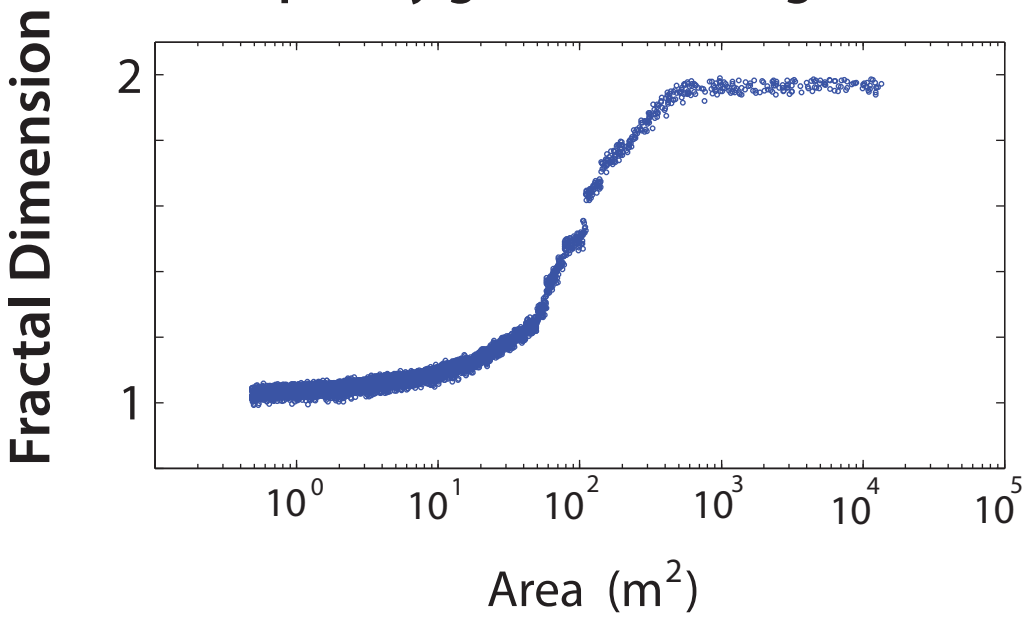

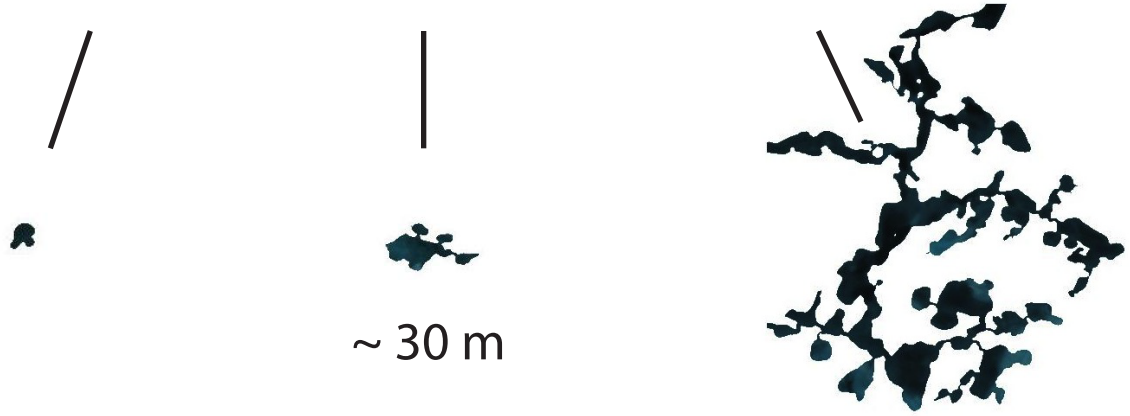

simple pond ***transitional pond*** ***complex pond***

Continuum percolation model for melt pond evolution

level sets of random surfaces

Brady Bowen, Court Strong, Ken Golden, J. Fractal Geometry 2018

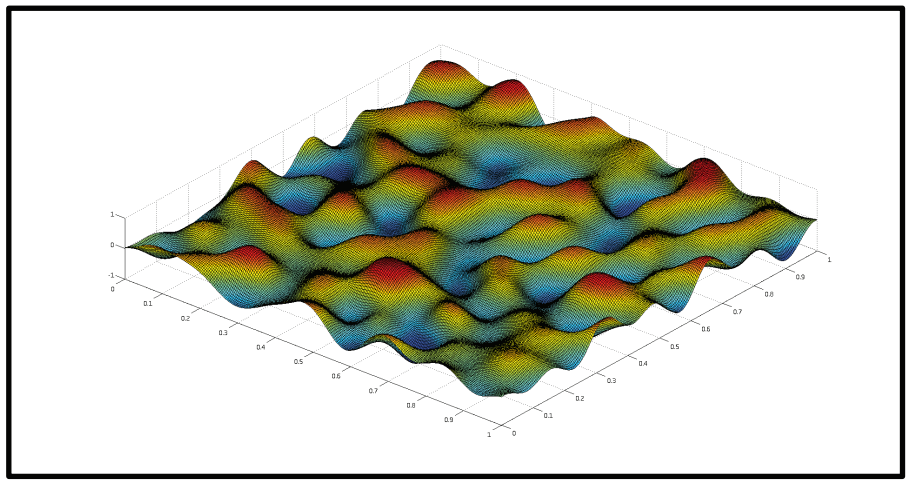

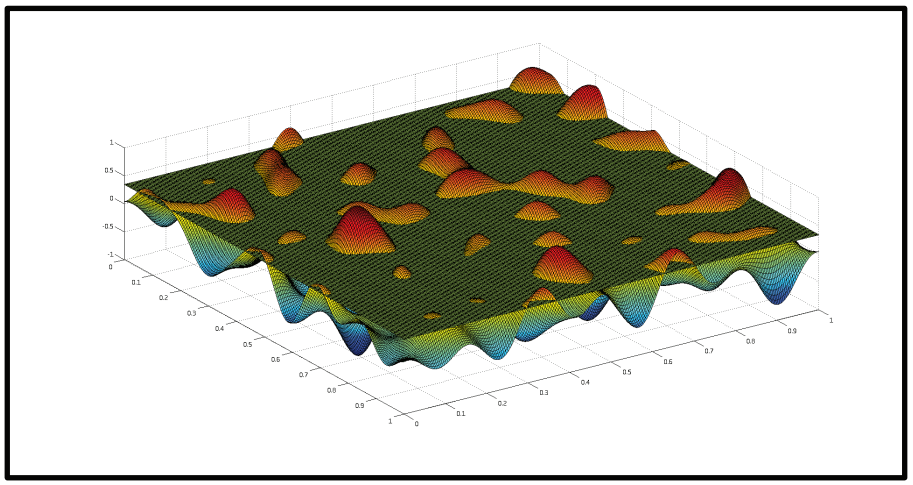

random Fourier series representation of surface topography

intersections of a plane with the surface define melt ponds

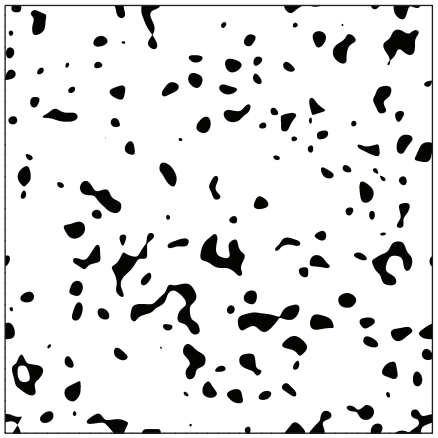

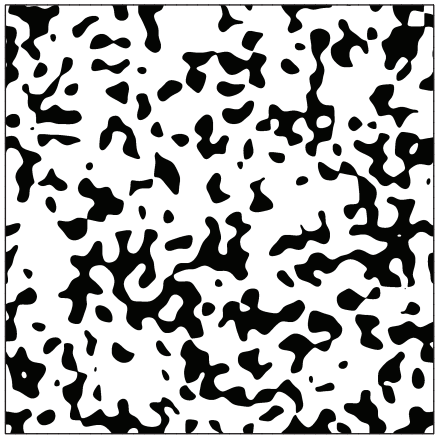

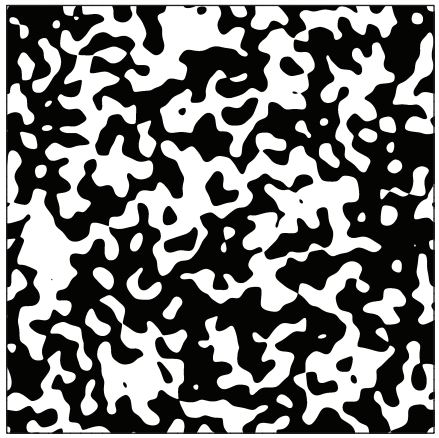

electronic transport in disordered media *diffusion in turbulent plasmas* *Isichenko, Rev. Mod. Phys., 1992*

Topological Data Analysis

Euler characteristic = # maxima + # minima - # saddles

topological invariant

filtration - sequence of nested topological spaces, indexed by water level

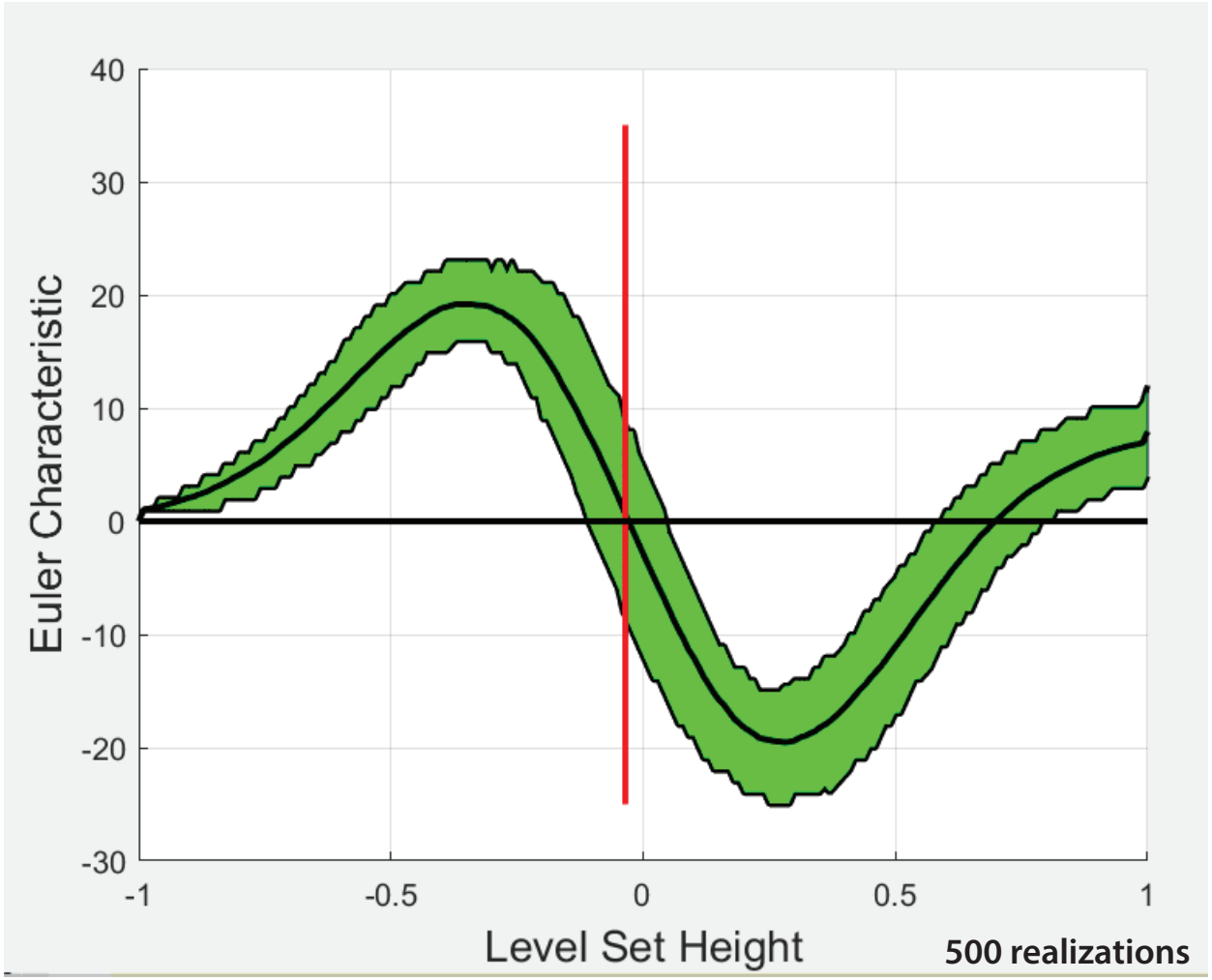

Expected
Euler Characteristic Curve (ECC)

tracks the evolution of the EC of the flooded surface as water rises

zero of ECC ~ percolation

percolation on a torus
creates a giant cycle

Bobrowski & Skraba, 2020

Carlsson, 2009

Vogel, 2002 GRF

image analysis
porous media
cosmology
brain activity

Physical Review Research (invited, in revision), R. Moore, J. Jones, D. Gollero, R. Hardenbrook, C. Strong, K. M. Golden 2024

From magnets to melt ponds

100 year old model for magnetic materials used to explain melt pond geometry

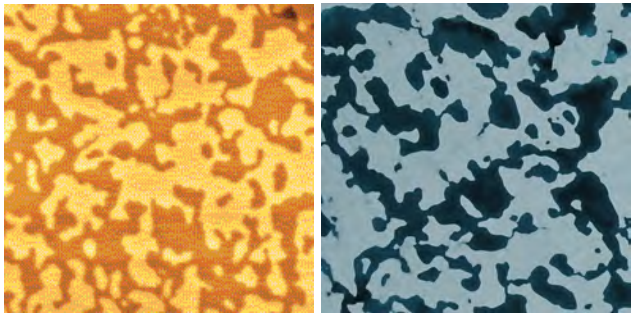

magnetic domains in cobalt

Arctic melt ponds

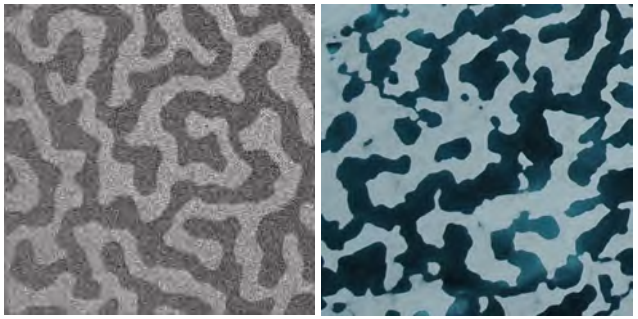

magnetic domains in cobalt-iron-boron

Arctic melt ponds

2D Ising model

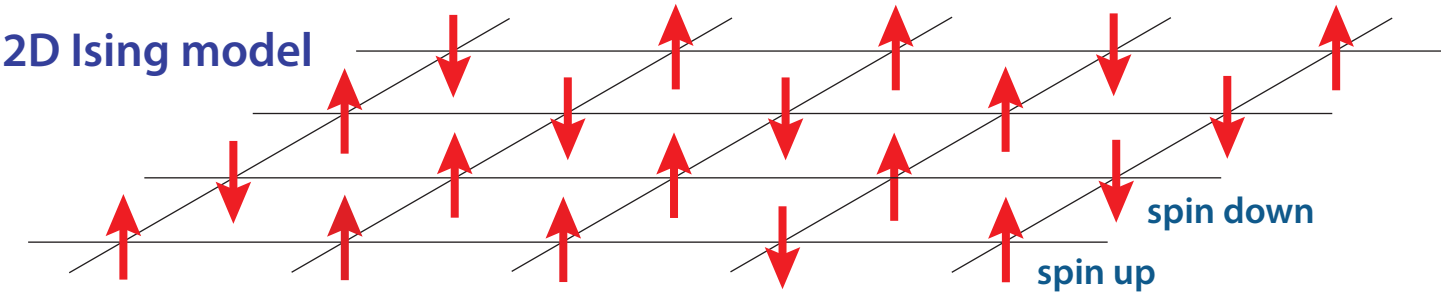

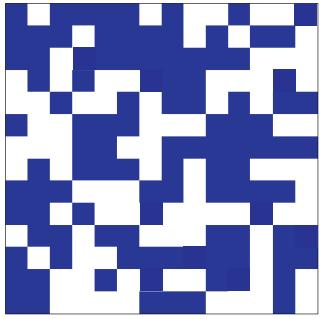

model

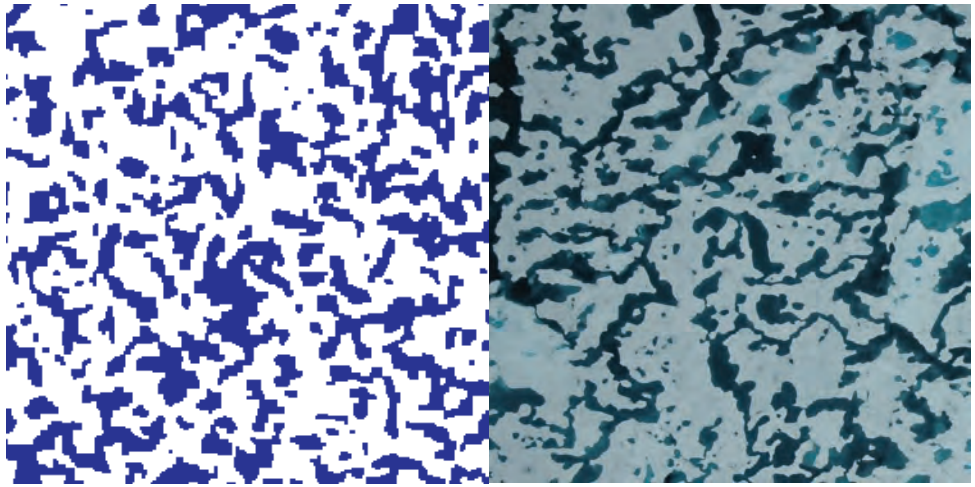

real ponds (Perovich)

Ma, Sudakov, Strong, Golden, *New J. Phys.* 2019

Scientific American, EOS, PhysicsWorld, ...

Time evolution - William Harrison, Tyler Evans, Ken Golden 2024

macroscale

Anomalous diffusion in sea ice dynamics

Ice floe diffusion in winds and currents

observations from GPS data

Lukovich, Hutchings, Barber, *Ann. Glac.* 2015

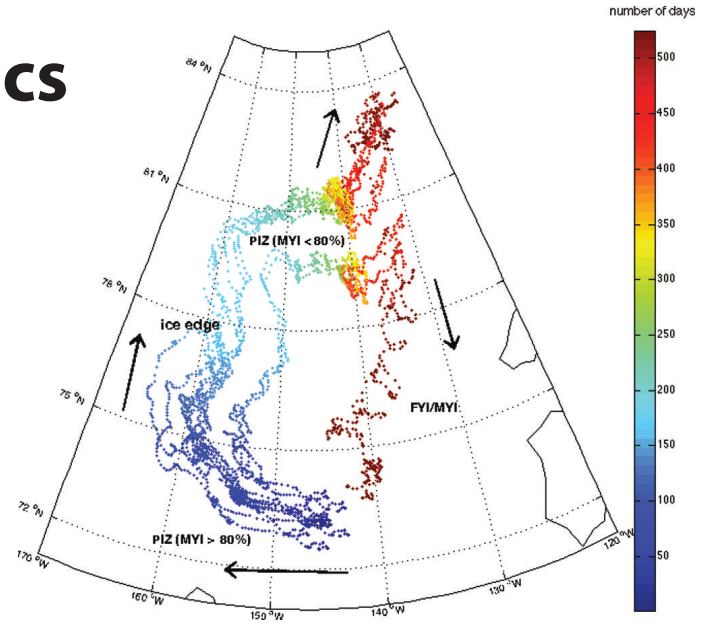

Floe scale model of advection diffusion

Tyler Evans, Huy Dinh, Kaeden George, Ben Murphy, Elena Cherkaev, Ken Golden 2025

$$\left\langle |\mathbf{x}(t) - \mathbf{x}(0) - \langle \mathbf{x}(t) - \mathbf{x}(0) \rangle|^2 \right\rangle \sim t^{\alpha}$$

$\alpha =$ **Hurst exponent**

diffusive $\alpha = 1$

sub-diffusive $\alpha < 1$

super-diffusive $\alpha > 1$

Model Approximations

Power Law Size Distribution: $N(D) \sim D^{-k}$

D. A. Rothrock and A. S. Thorndike Journal of Geophysical Research 1984

Floe-Floe Interactions: Linear Elastic Collisions

Advective Forcing: Passive, Linear Drag Law

Fractional PDE

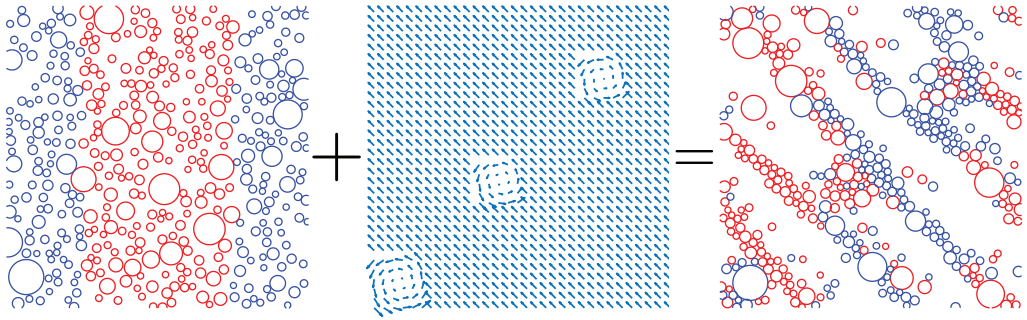

$\psi = 0.3$ **Vorticity Dominated Forcing**

Arctic sea ice pack with tagged particle

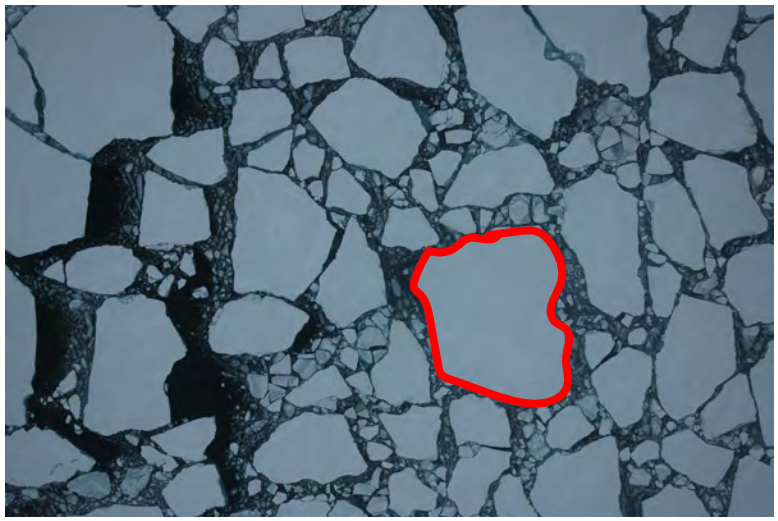

Einstein's pollen grain

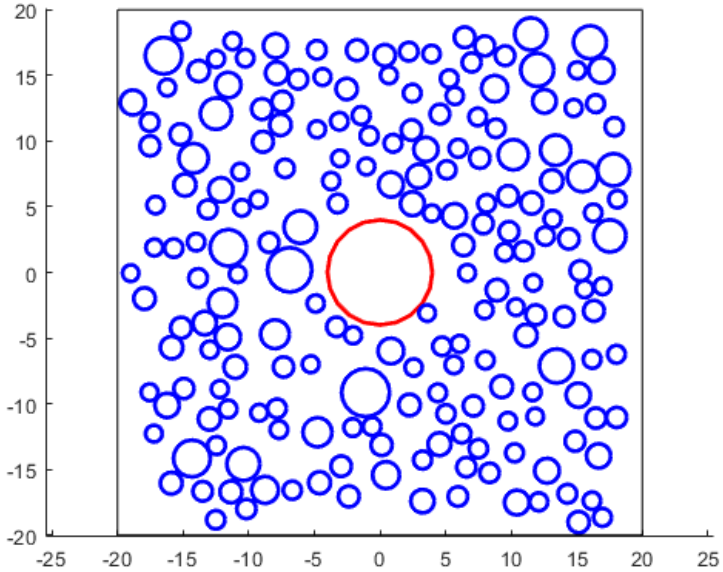

Hurst exponent

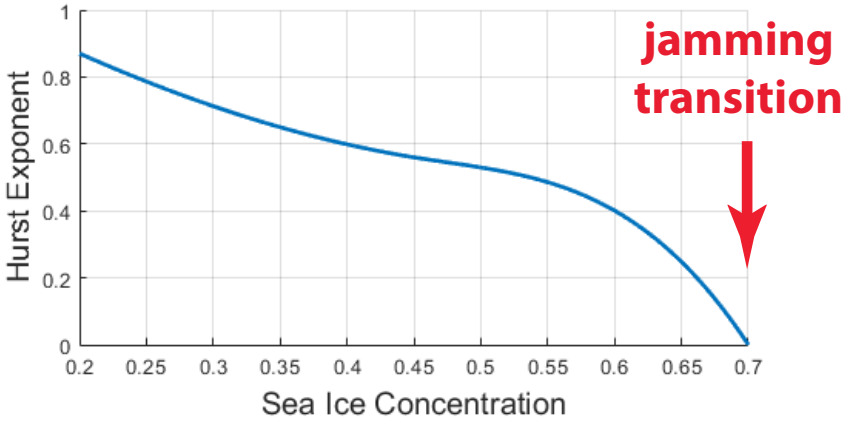

diffusion coefficient

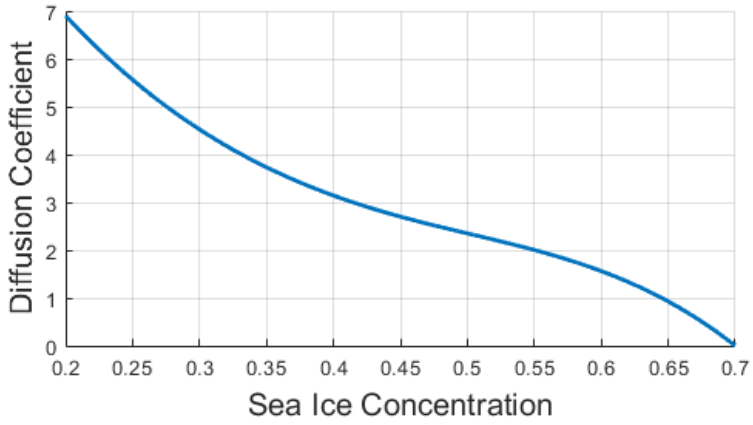

From micro to macro in ice floe dynamics

Delaney Mosier, Tyler Evans, Ben Murphy, Elena Cherkaev, Ken Golden, 2025

homogenization of ice floe advection-diffusion

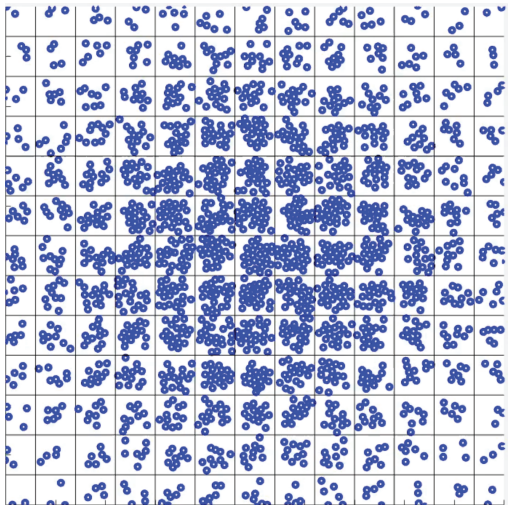

initial sea ice concentration field

Gaussian

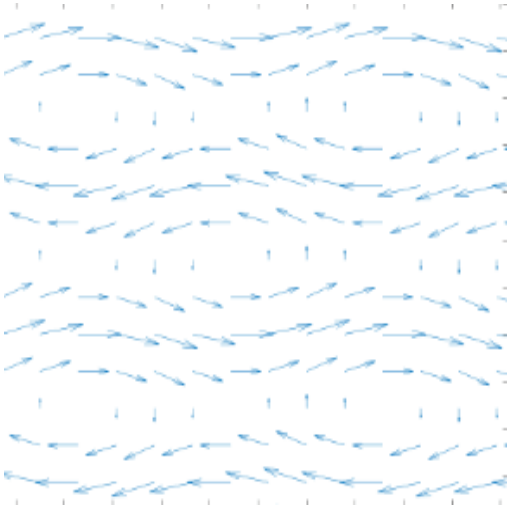

velocity field

BC flow

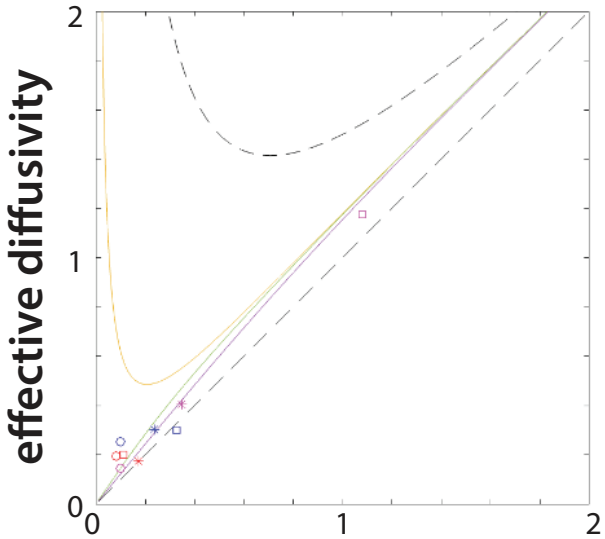

bounds on advection-enhanced diffusivity for ice concentration from STIELTJES INTEGRALS

Arctic Marginal Ice Zone

sea ice concentration

$$0.15 < \psi < 0.80$$

transitional region between dense pack ice and open ocean

- biologically active region
- intense ocean-ice-atmosphere interactions
- significant wave activity

MIZ "WIDTH" ??

fundamental length scale of ecological and climate dynamics

Where the action is!

In processes in geophysics and materials science, a region where solid and liquid phases co-exist is known as a mushy layer.

e.g. in solidification of binary liquids and alloys

solid porous matrix
with liquid inclusions

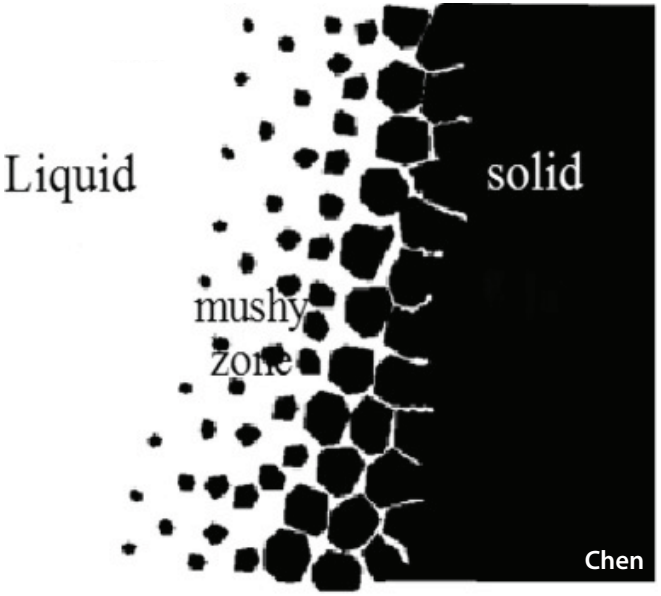

sea ice

cooling metal

Earth's mantle

dendritic interface between
sea ice and sea water

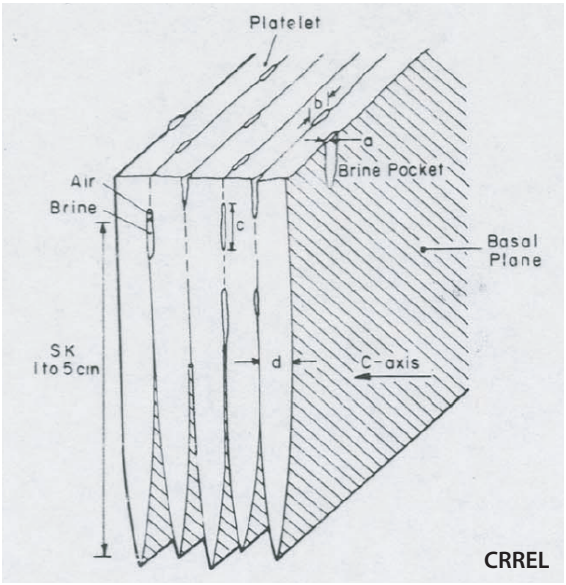

Sea Ice is a mushy layer, Feltham, et al., *GRL* 2006
Phase evolution of young sea ice, Wettlaufer, et al., *GRL* 1997

Multiscale mushy layer model for marginal ice zone dynamics

Strong, Cherkaev, Golden *Scientific Reports* 2024

MIZ - transitional region between dense pack ice and open ocean

OBJECTIVE: model & predict dramatic annual cycle
impacts climate dynamics, polar ecology, human activities

mushy layer physics in the lab

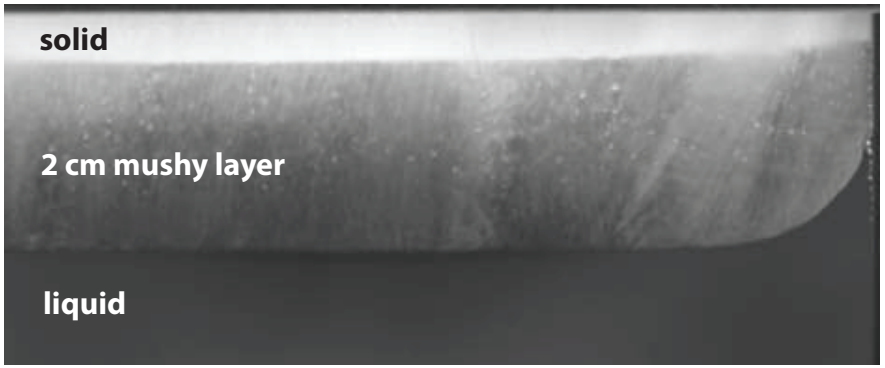

NaCl-H2O in lab
(Peppin et al., 2007, J. Fluid Mech.)

Arctic MIZ as a mushy layer

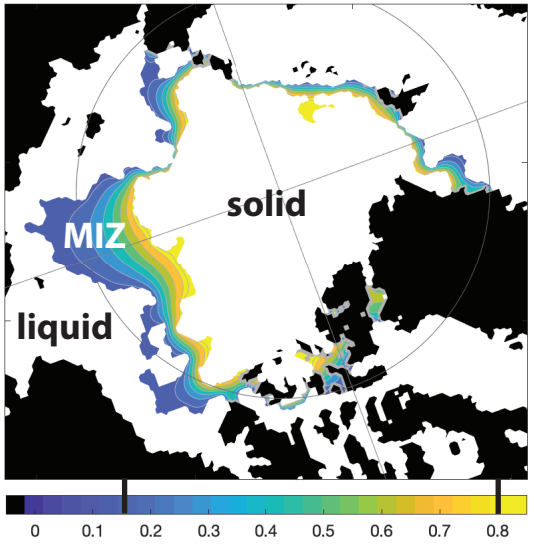

sea ice concentration ψ

Model captures basic physics of

MIZ dynamics & predicts cycle.

Identifying Fractal Geometry in Arctic Marginal Ice Zone Dynamics

Julie Sherman, Court Strong, Ken Golden, *Environ. Res. Lett.* 2025

Compute the fractal dimension of the boundary of the Arctic MIZ by boxcounting methods; analyze seasonal cycle and long term trends.

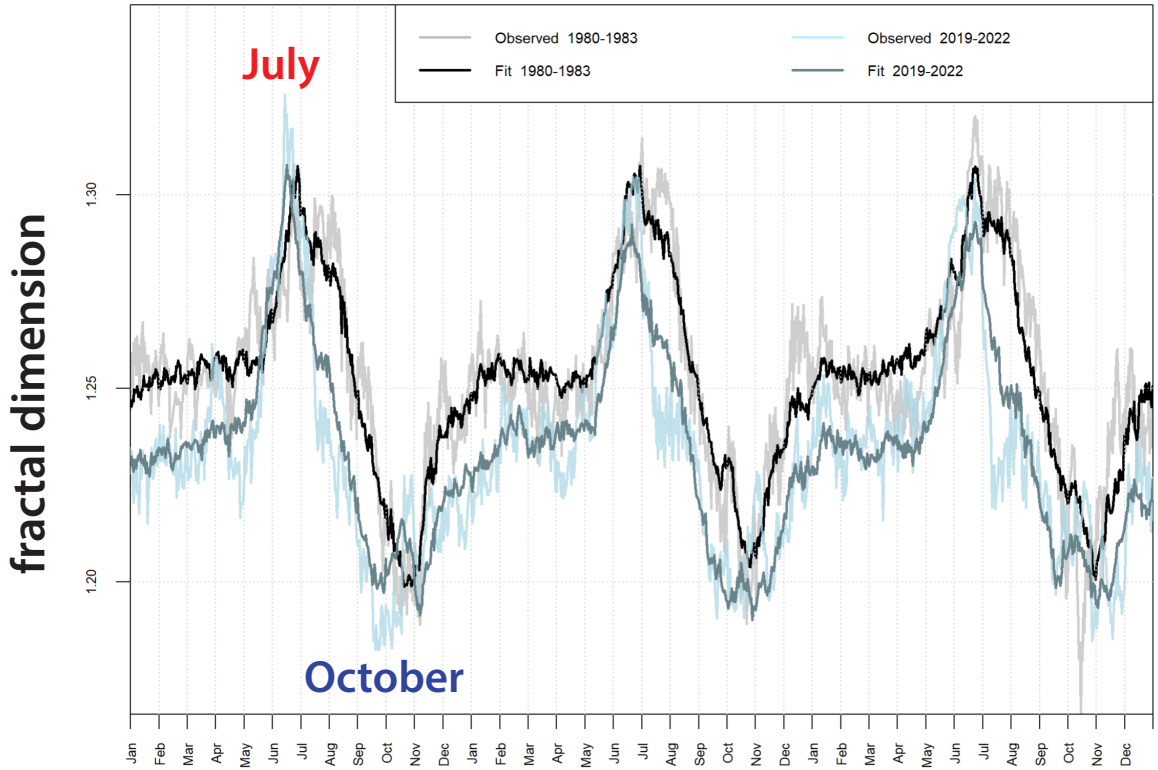

early summer

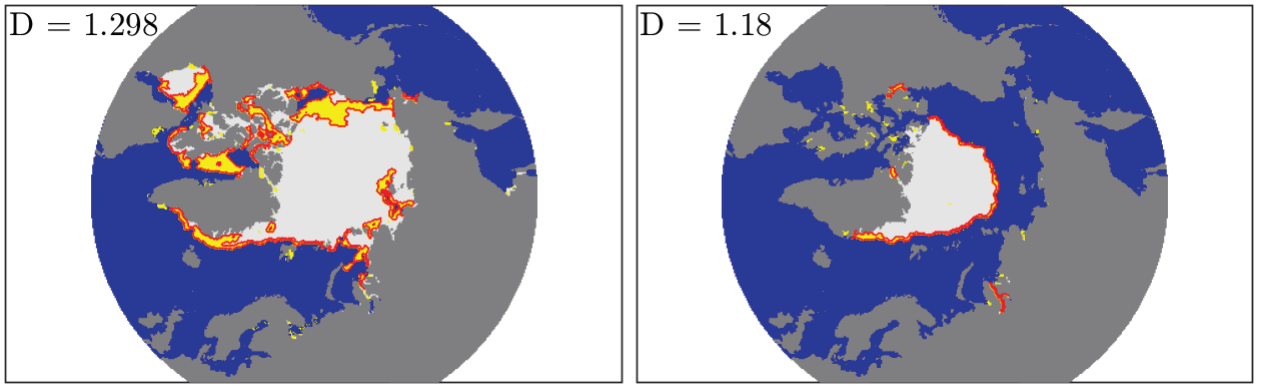

early autumn

wave and thermal interactions with fractal boundary

Filling the polar data gap with partial differential equations

hole in satellite coverage of sea ice concentration field

previously assumed ice covered

Gap radius: 611 km
06 January 1985

Gap radius: 311 km
30 August 2007

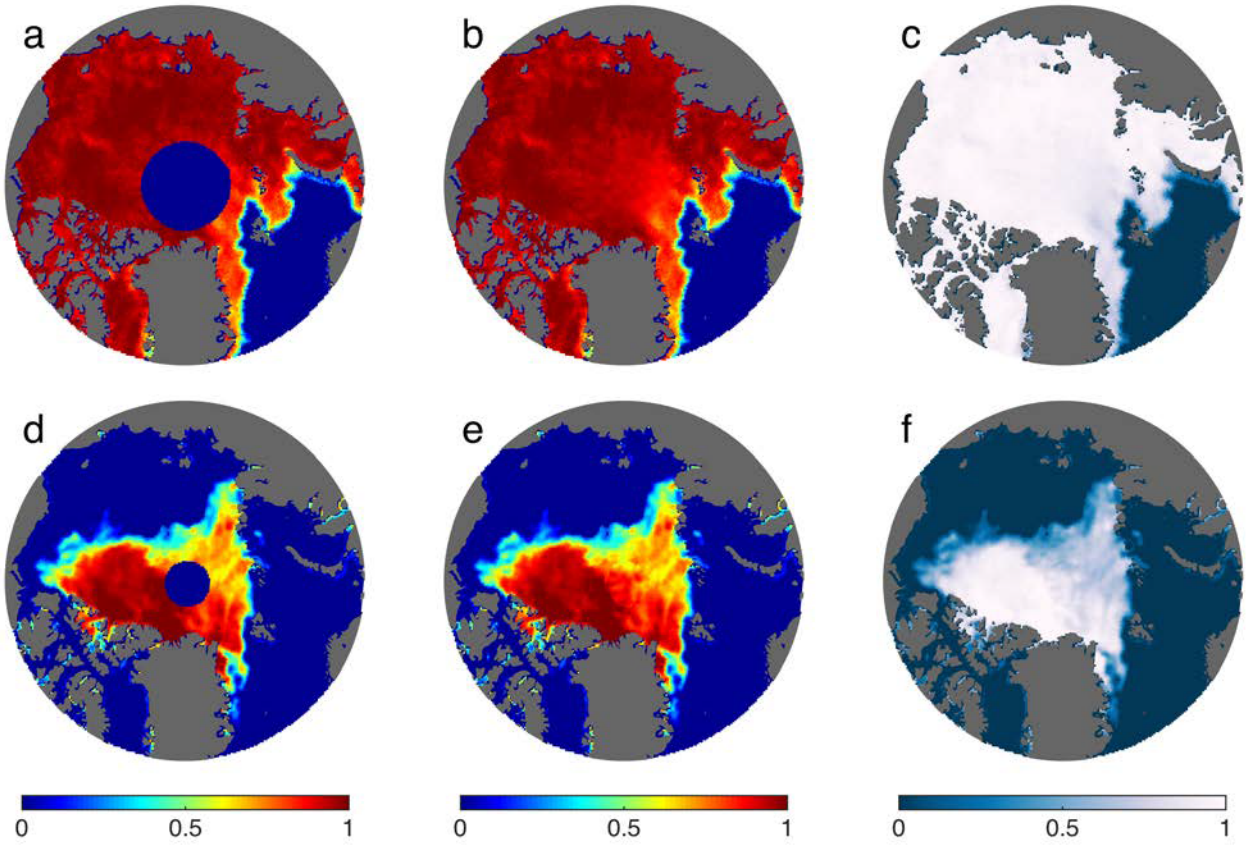

$$\Delta\psi = 0$$

fill = harmonic function satisfying satellite BC's plus learned stochastic term

Strong and Golden, *Remote Sensing* 2016
Strong and Golden, *SIAM News* 2017

Global Sea Ice Concentration Climate Data Records, 2022
Lavergne, Sorensen, et al., Norwegian Met. Inst., ... OSI SAF

Conclusions

Our research is helping to improve projections of the fate of Earth's sea ice packs, and the ecosystems they support.

Mathematics for sea ice advances the theory of composites, inverse problems, and other areas of science and engineering.

Modeling sea ice leads to unexpected areas of math and physics.

ISSN 0002-9920 (print)
ISSN 1088-9477 (online)

Notices

of the American Mathematical Society

November 2020 Volume 67, Number 10

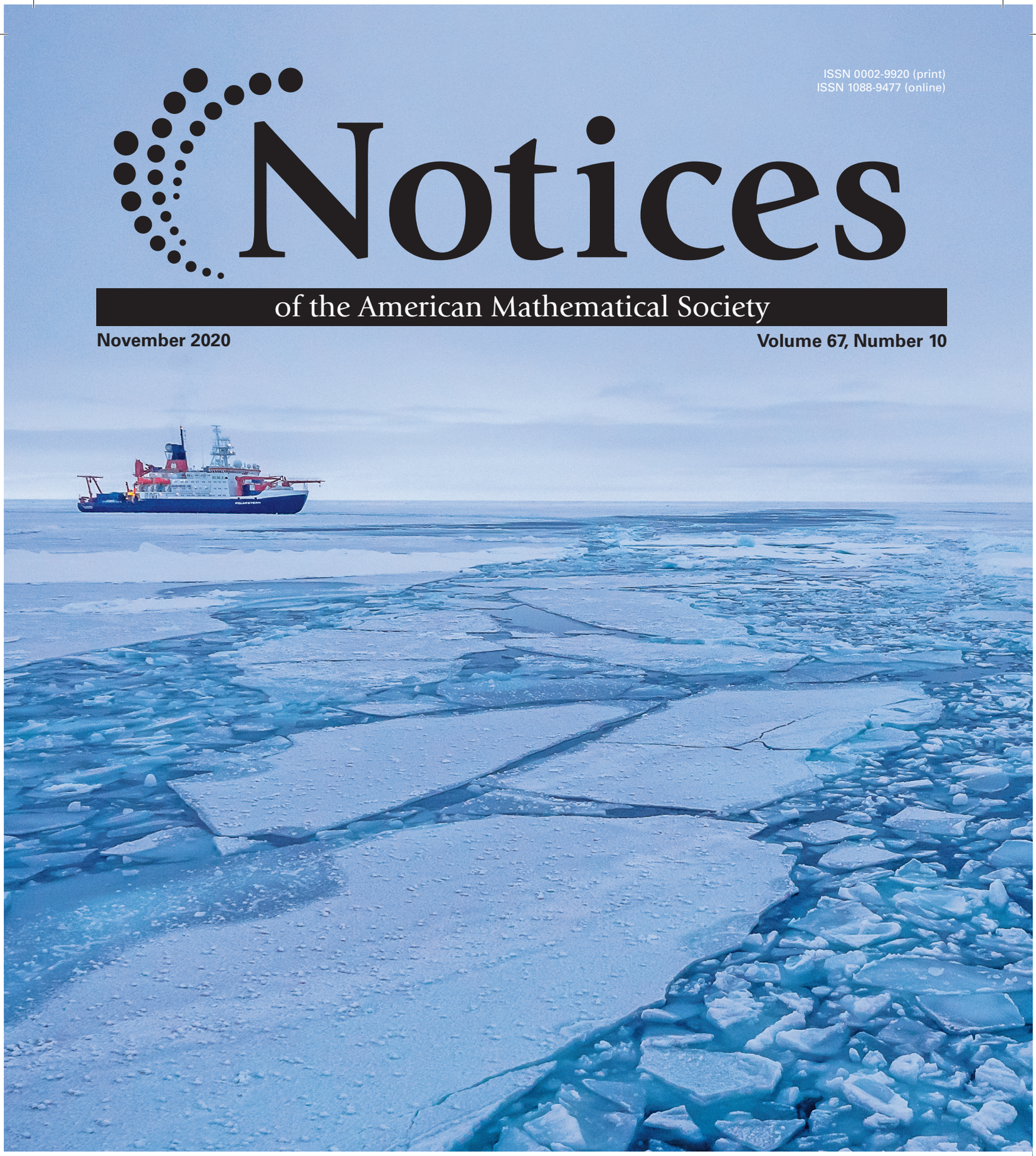

AMS American Mathematical Society
Advancing research. Creating connections.

The cover is based on "Modeling Sea Ice," page 1535.

Arctic Mathpedition 2024

Reimer

Golden

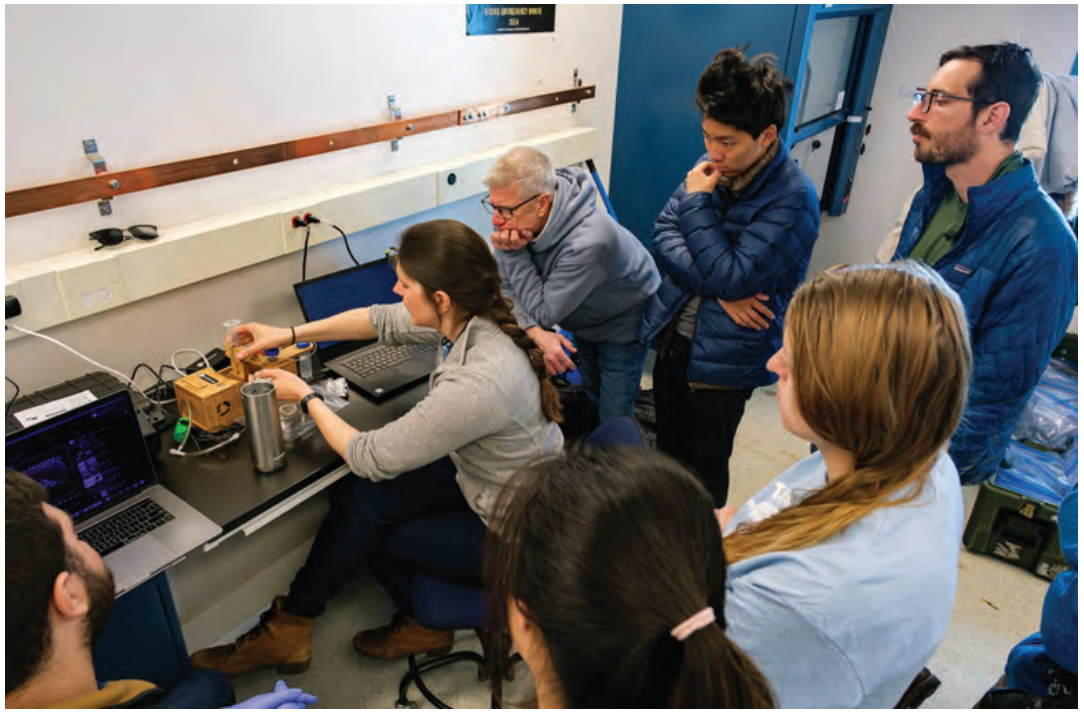


DEWALT
DEWALT

bottom of a sea ice core

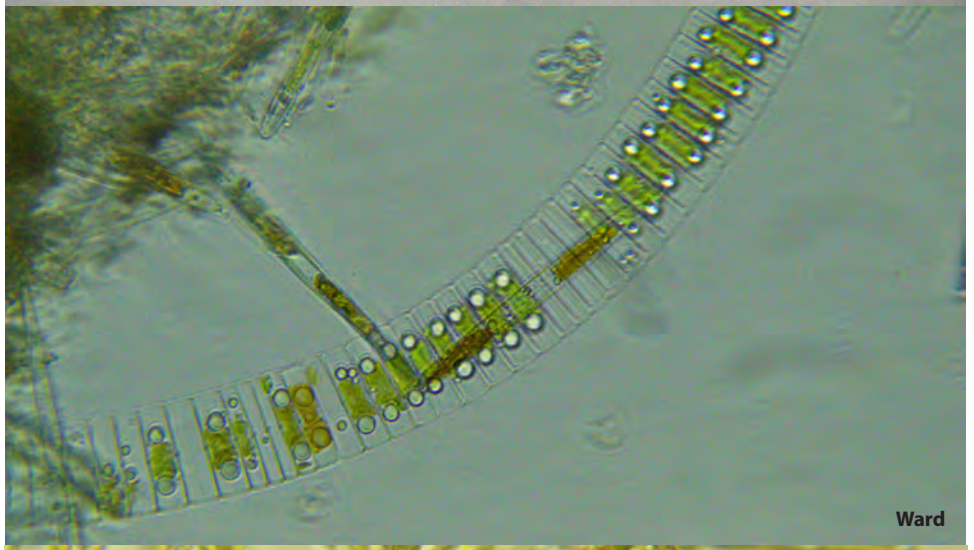

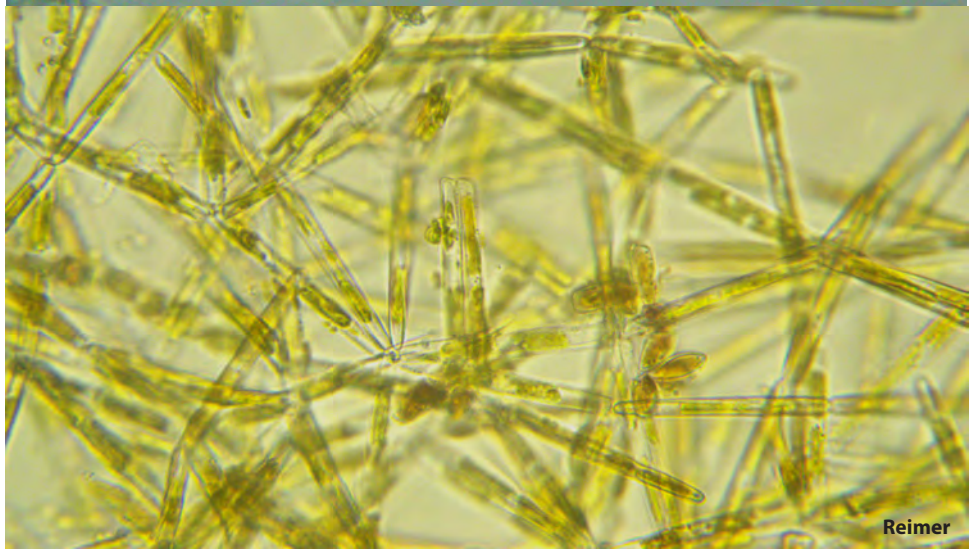

THANK YOU

Office of Naval Research

Applied and Computational Analysis Program

Arctic and Global Prediction Program

National Science Foundation

Division of Mathematical Sciences

Division of Polar Programs

MCRN

Mathematics and Climate Research Network

Australian Government

Department of the Environment and Water Resources

Australian Antarctic Division

ANTARCTIC CLIMATE & ECOSYSTEMS

COOPERATIVE RESEARCH CENTRE

Antarctica New Zealand

UNIVERSITY OF ALASKA FAIRBANKS

THE UNIVERSITY OF UTAH

Buchanan Bay, Antarctica Mertz Glacier Polynya Experiment July 1999

Topography-albedo feedback and the shifting Arctic ice pack

David E. Gluckman, Tyler P. Evans and Kenneth M. Golden, 2025

first-year ice
thinner with
smoother surface

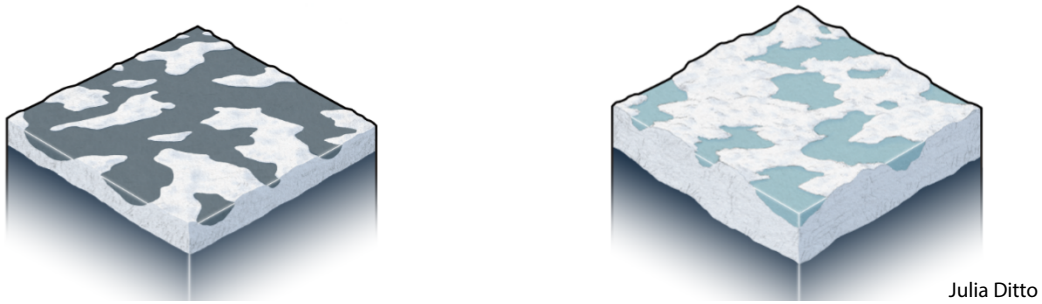

Julia Ditto

multiyear ice
thicker with
hummocky surface

Meter-scale differences in surface topography between MYI and FYI mechanistically alter summertime melt pond formation and coverage, significantly lowering albedo for younger, smoother ice, and forming a self-perpetuating feedback loop.

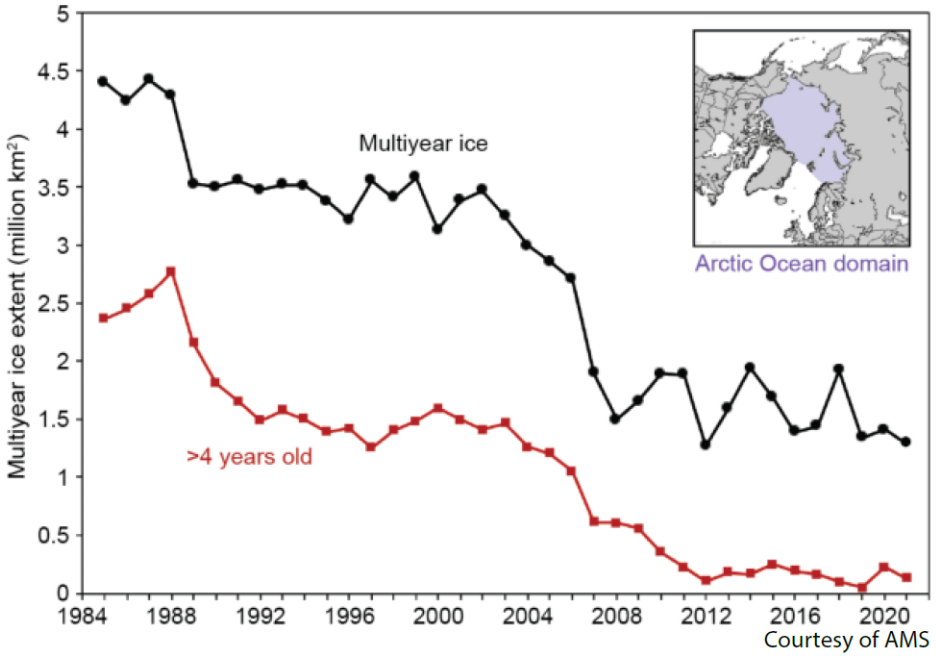

Courtesy of AMS

Topography-albedo feedback and the shifting Arctic ice pack

David E. Gluckman, Tyler P. Evans and Kenneth M. Golden, 2025

Coupled PDE model of topography *H*(x,y,t) and melt pond depth *h*(x,y,t).

Co-evolution of topography and albedo drives stark differences in the state of the ice pack at the end of summer.

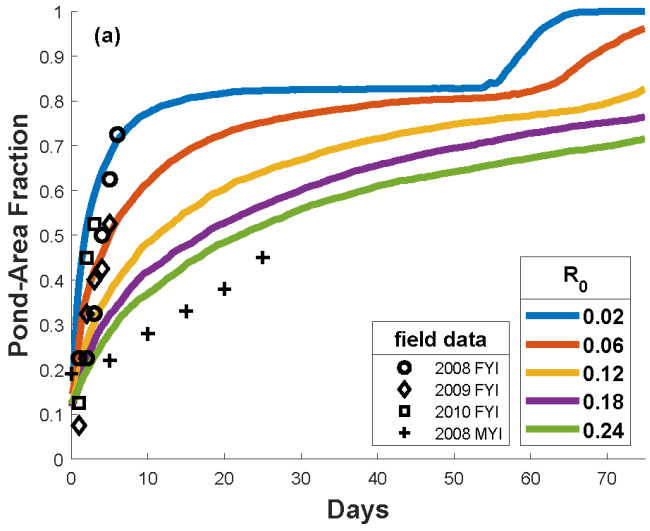

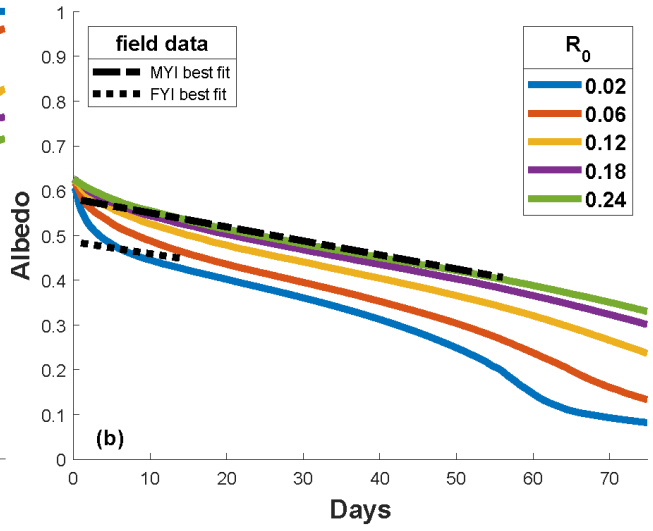

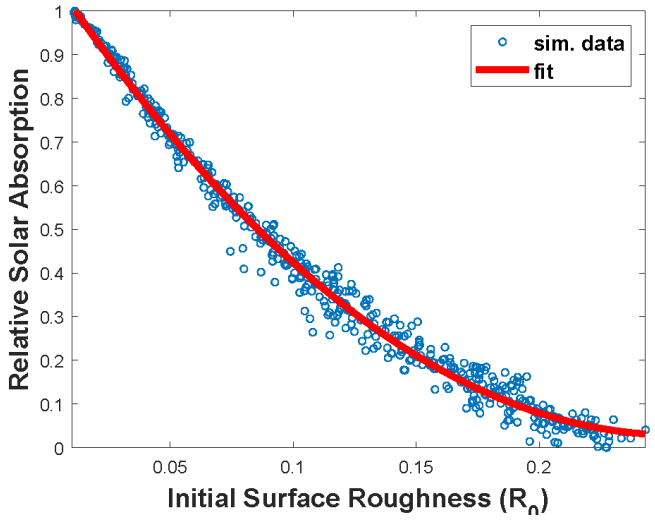

transport in percolation theory

MICRO —lattice homogenization→ **MACRO**

local conductivity (electrical or fluid)

effective conductivity or fluid permeability

bond → $\begin{cases} \sigma_0 & \text{probability } p \\ 0 & \text{probability } 1 - p \end{cases}$

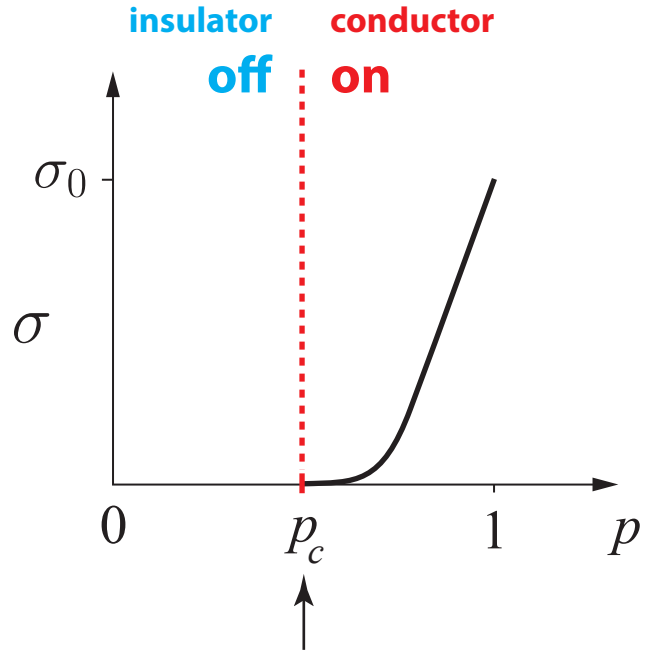

consider local conductivities
1 and *h* > 0
smooths, softens transition

$$\sigma(p) \sim \sigma_0 (p - p_c)^t \quad p \to p_c^+$$

UNIVERSAL critical exponents for lattices -- depend only on dimension

1 ≤ *t* ≤ 2 (for idealized model), Golden, *Phys. Rev. Lett.* 1990 ; *Comm. Math. Phys.* 1992

non-universal behavior in continuum

Ising Model for a Ferromagnet

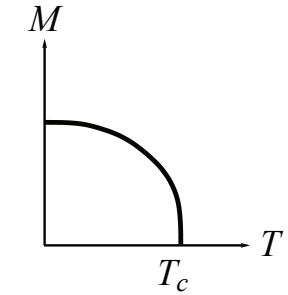

Curie point
critical temperature

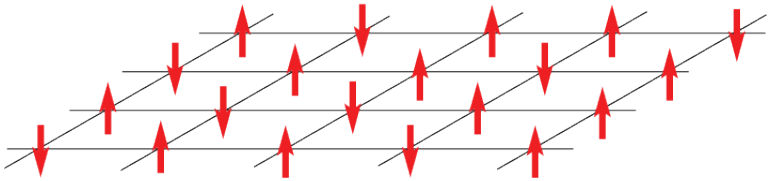

$$s_i = \begin{cases} +1 & \text{spin up} \\ -1 & \text{spin down} \end{cases}$$

blue

white

applied magnetic field H

$$\mathcal{H} = -H\sum_i s_i - J\sum_{<i,j>} s_i s_j$$

nearest neighbor Ising Hamiltonian

islands of like spins

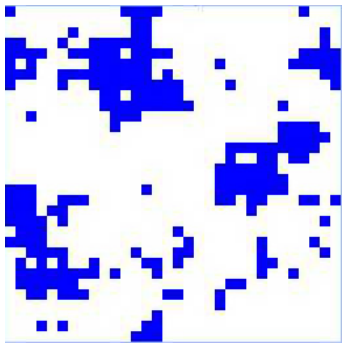

$$M(T,H) = \lim_{N\to\infty} \frac{1}{N}\left\langle \sum_j s_j \right\rangle$$

effective magnetization

energy is lowered when nearby spins align with each other, forming magnetic domains

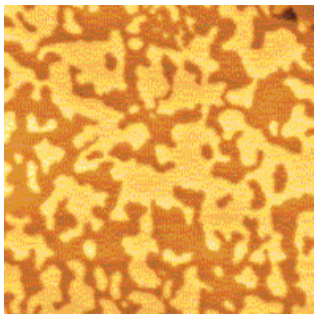

magnetic domains in cobalt

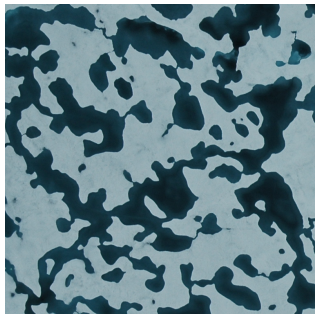

melt ponds (Perovich)

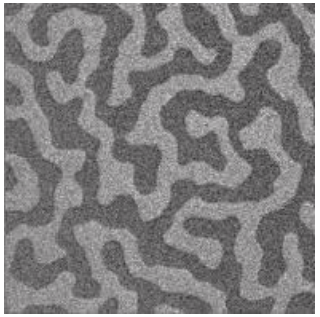

magnetic domains in cobalt-iron-boron

melt ponds (Perovich)

Ising model for ferromagnets → Ising model for melt ponds

Ma, Sudakov, Strong, Golden, *New J. Phys.*, 2019

$$\mathcal{H} = -\sum_{i}^{N} H_i s_i - J \sum_{<i,j>}^{N} s_i s_j \qquad s_i = \begin{cases} +1 & \text{water (spin up)} \\ -1 & \text{ice (spin down)} \end{cases}$$

random magnetic field represents snow topography

magnetization M

pond area fraction ~ *albedo*

$$F = \frac{(M+1)}{2}$$

only nearest neighbor patches interact

Starting with random initial configurations, as Hamiltonian energy is minimized by Glauber spin flip dynamics, system "flows" toward metastable equilibria.

Order from Disorder

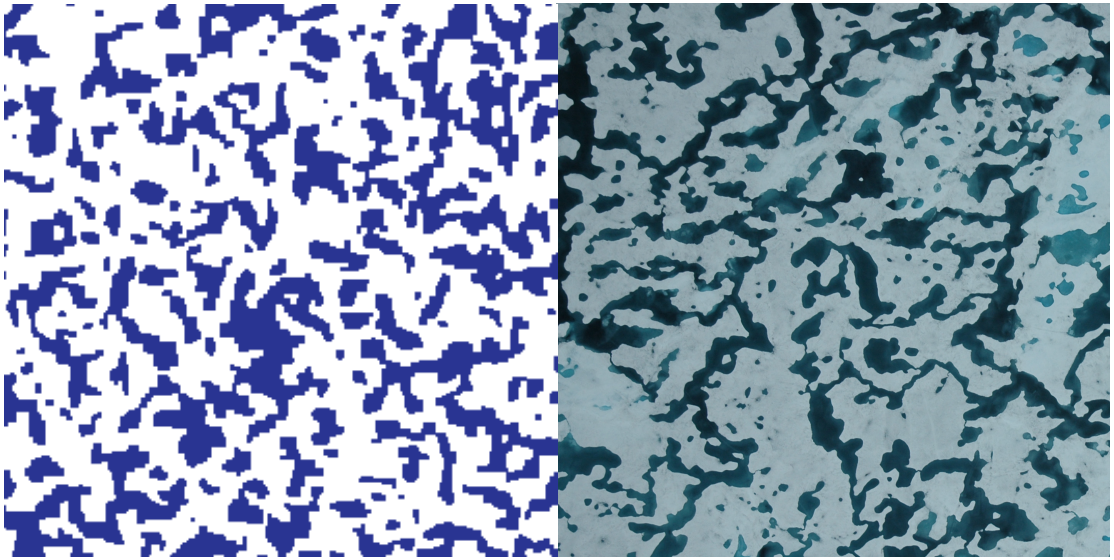

Ising model

melt pond photo (Perovich)

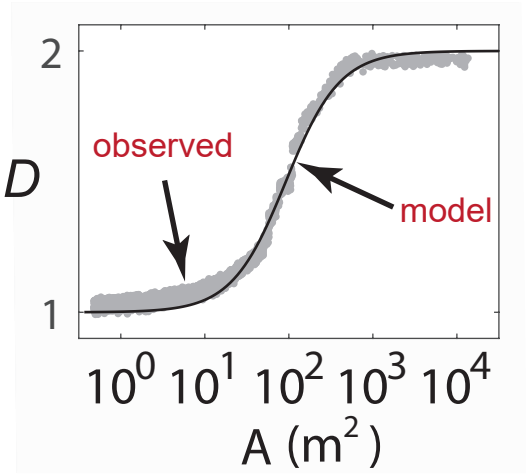

pond size distribution exponent

observed -1.5

(Perovich, *et al.* 2002)

model -1.58

Scientific American
EOS, PhysicsWorld, ...

ONLY MEASURED INPUT = LENGTH SCALE (GRID SIZE) from snow topography data

Order to disorder in quasiperiodic composites

Morison, Murphy, Cherkaev, Golden, Comm. Phys. 2022

sea ice inspired - twisted bilayer composites

tunable quasiperiodic composites with exotic properties

(optical, electrical, thermal) Anderson localization; our Moiré patterned geometries are similar to twisted bilayer graphene

increasing twist angle between two lattices

periodic → quasiperiodic

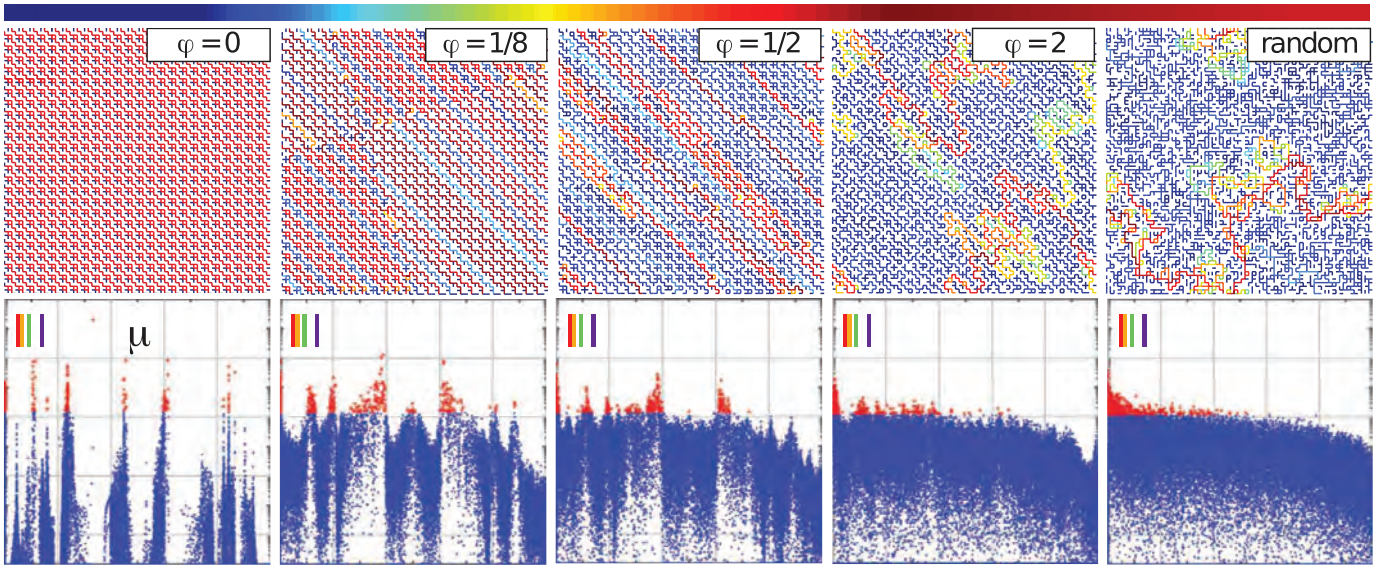

electric field strength

spectral measure

RRN at percolation threshold

twisted bilayer graphene

superconducting magic twist angle

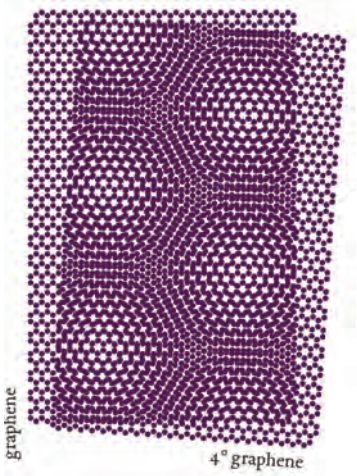

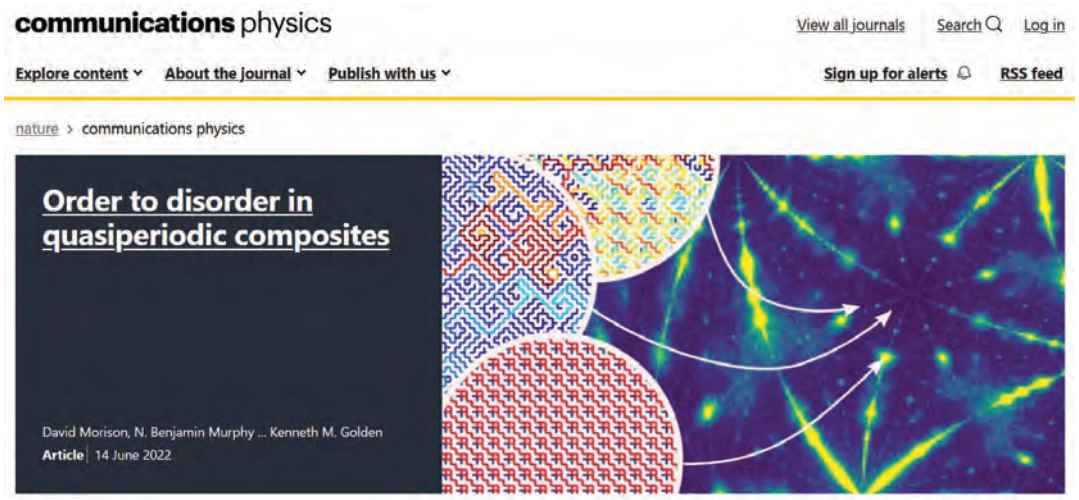

constellation of periodic systems in a sea of randomness

Wide Variety of Microgeometries

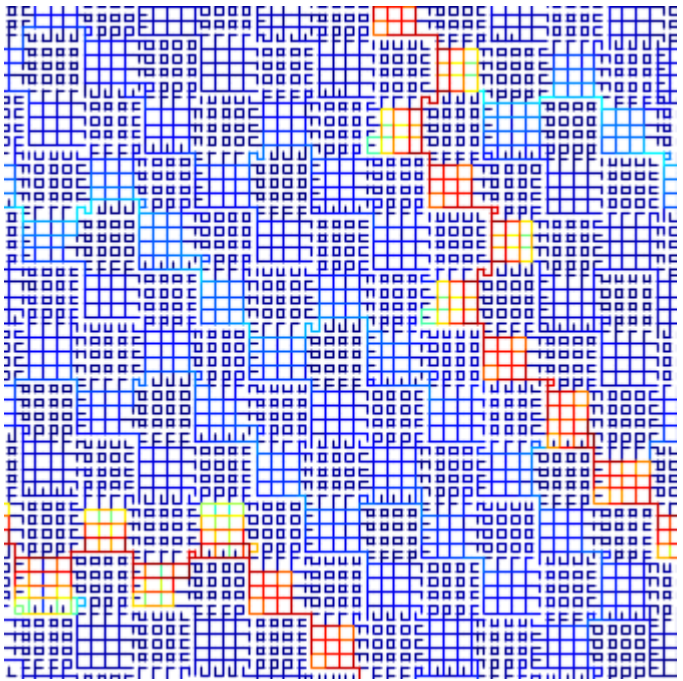

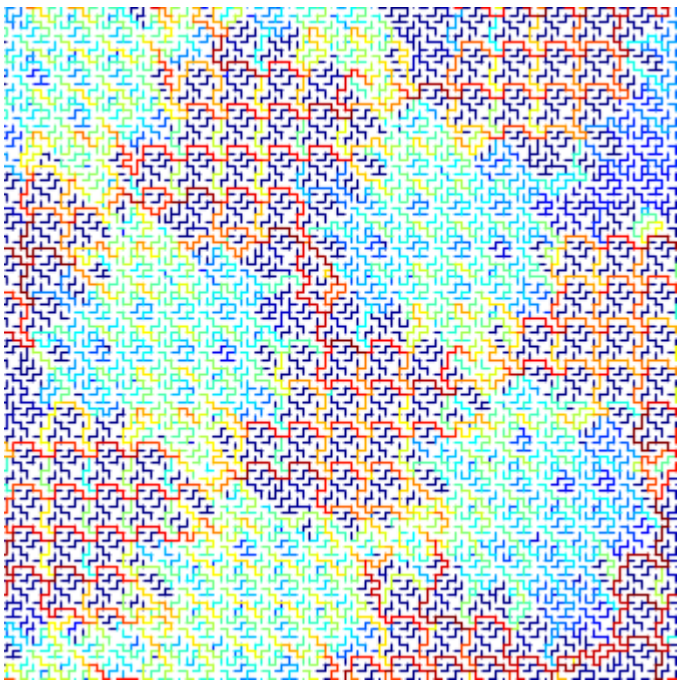

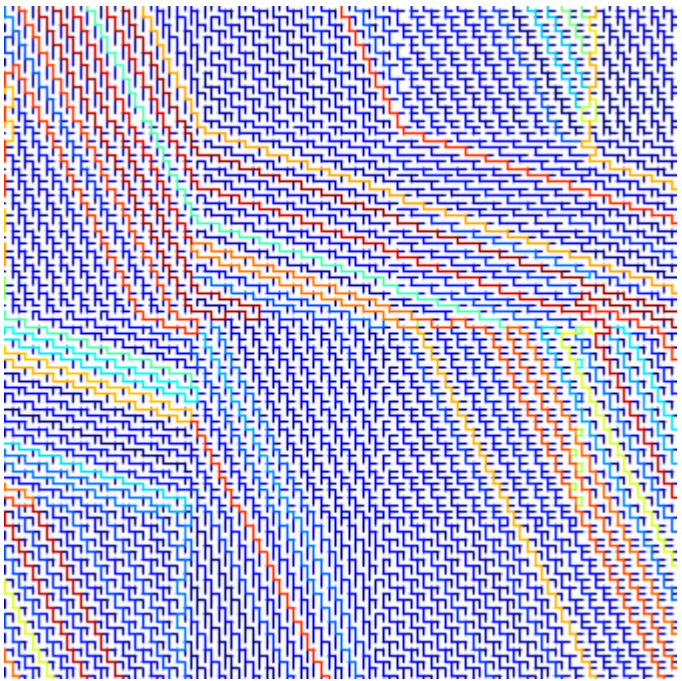

Wide Variety of Microgeometries

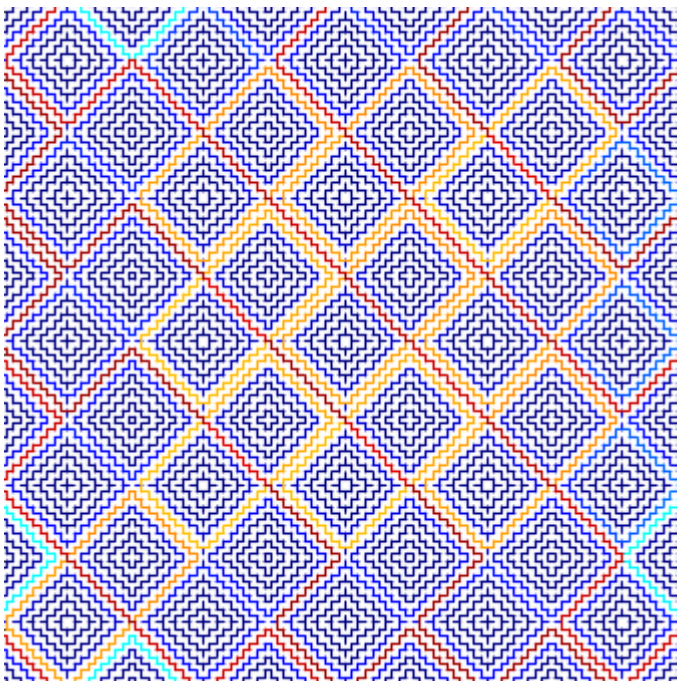

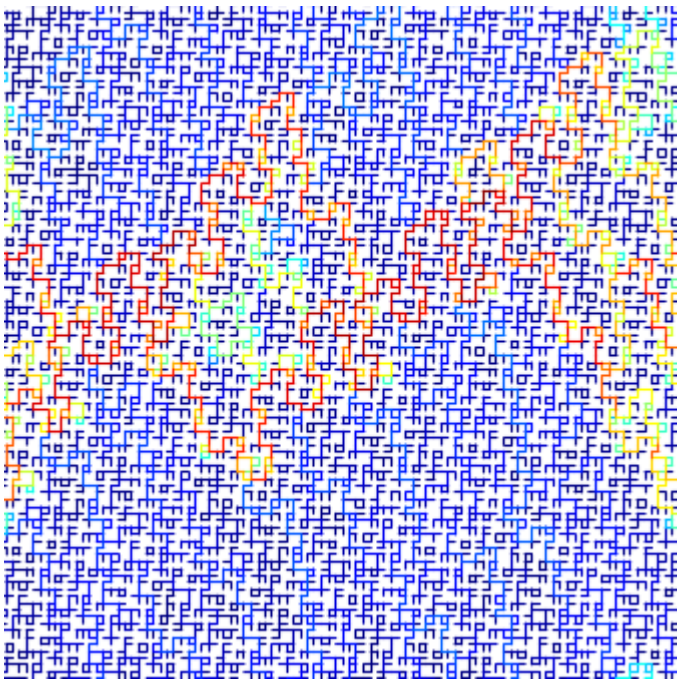

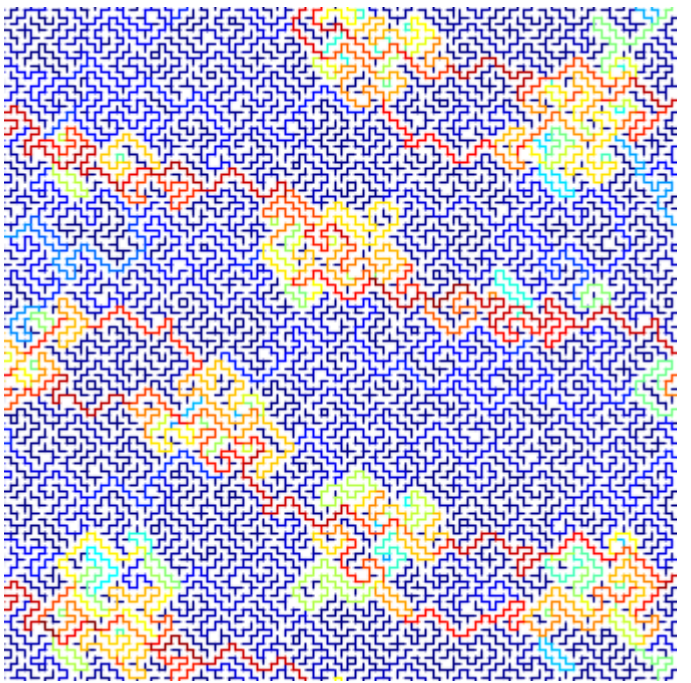

Small Difference in Moiré Parameters

Big Difference in Material Properties

Observed MIZ location and width

Observational analysis of annual cycle in Bering-Chukchi Sea sector 2000-2004

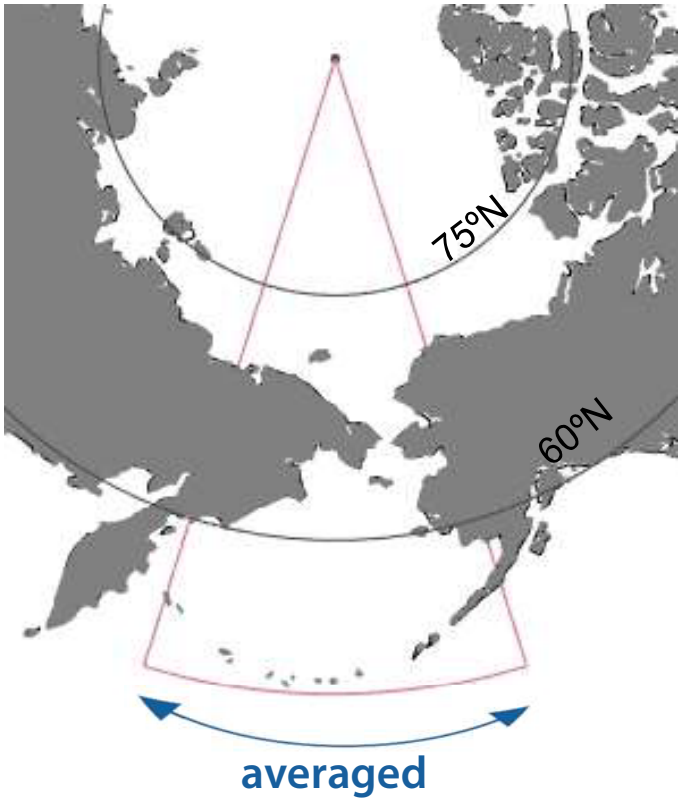

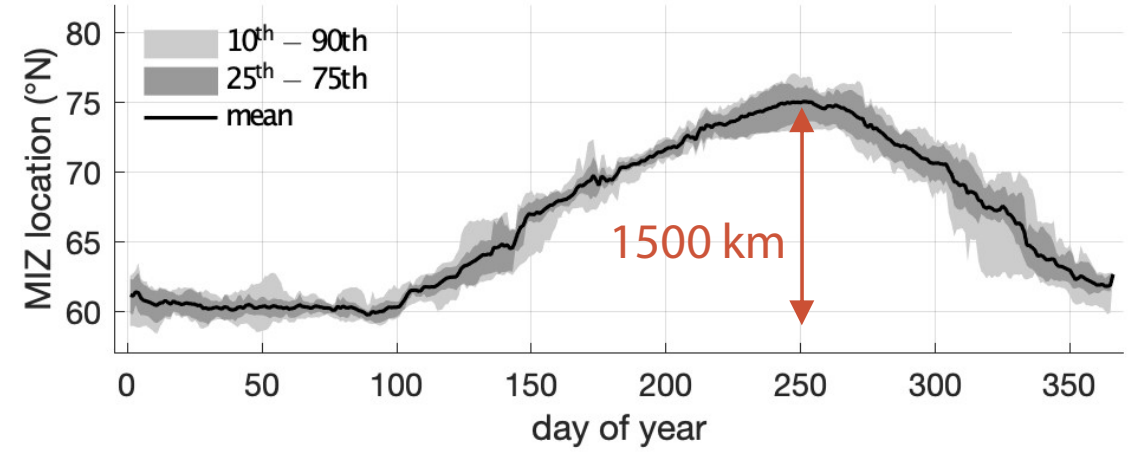

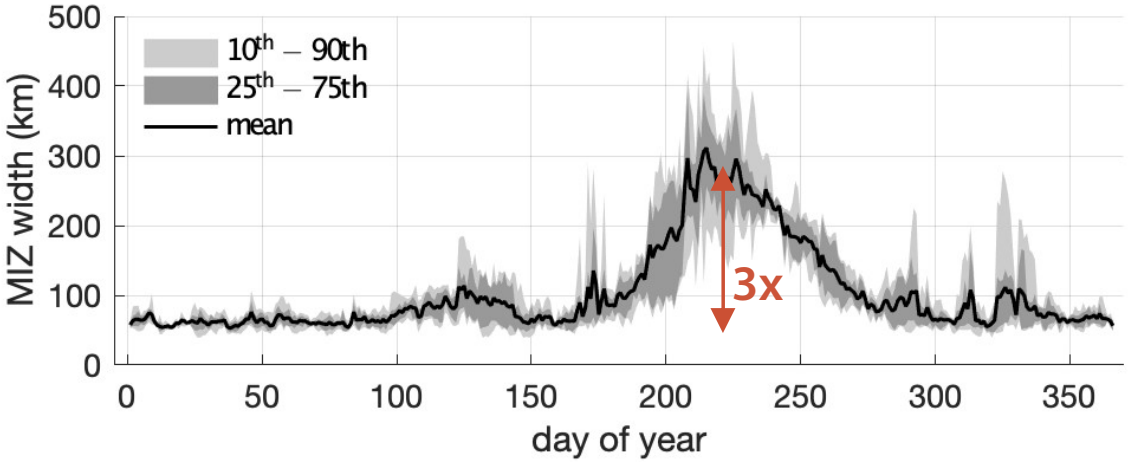

widens by a factor of 3-4 and moves poleward by 1500 km

thermal flow field through the ice cover: multiscale granular composite

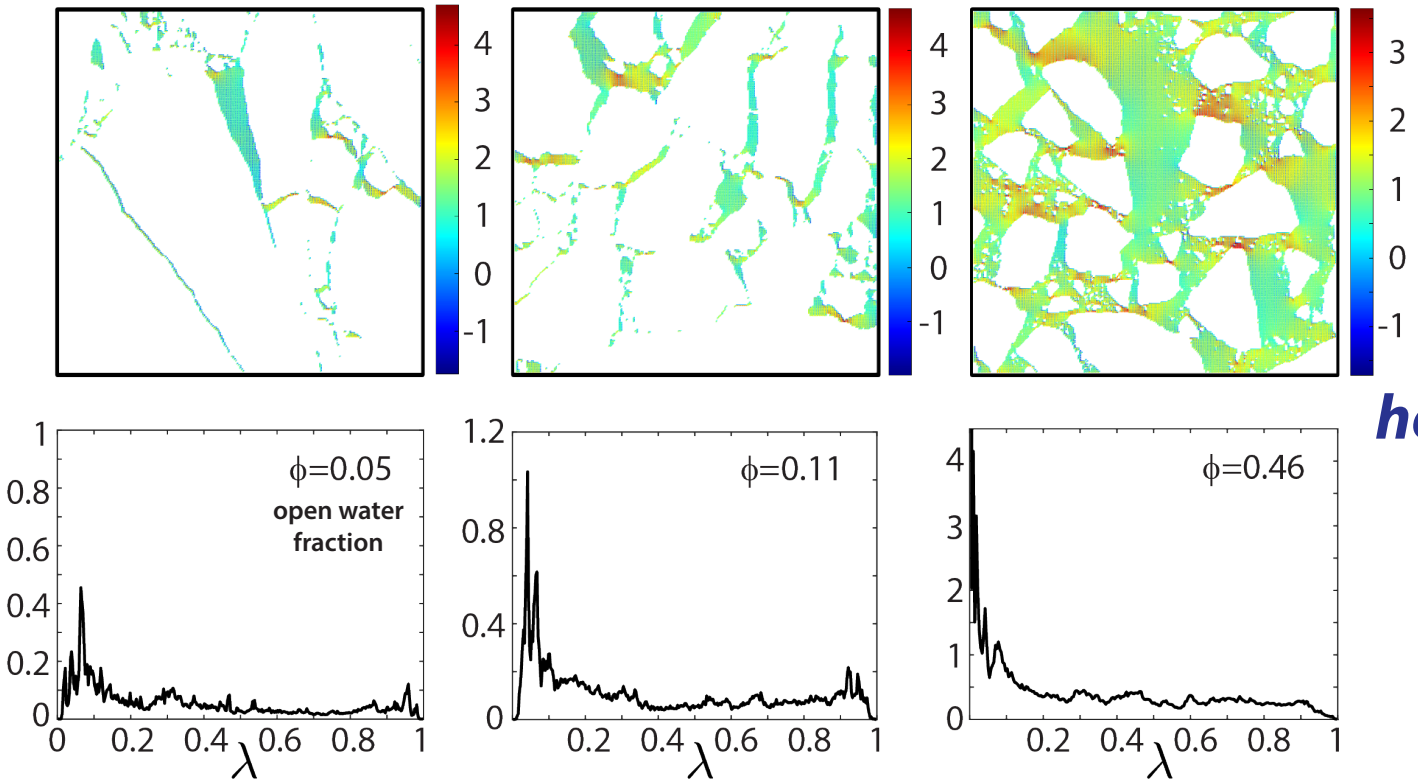

homogenize

spectral measures for 2D horizontal thermal conductivity

homogenized thermal conductivity is a key parameter in MIZ mushy layer model

Where to look to see this behavior exploited in tunable media that display rich transport properties?

Go back to the dawn of ordered, aperiodic materials -

quasicrystals.

Shechtman et al. 1984
Levine & Steinhardt 1984

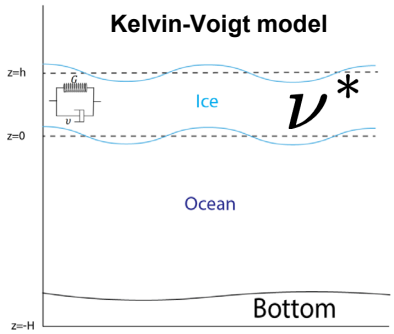

Single effective rheological parameter (Mosig et al. 2015)

$$\nu^* = G - i\omega\rho v$$

Effective complex viscoelasticity

Integral representation

$$\frac{\nu^*}{\nu_2} = ||\epsilon_s^0||^2(1 - F(s))$$

$$F(s) = \int_0^1 \frac{d\mu(\lambda)}{s-\lambda}$$

divergence-free deviatoric stress

$$\nabla \cdot \sigma_s = 0$$

microscale

$$\sigma_s = 2\nu\epsilon_s$$

$$\nu(\vec{x}) = \chi_1\nu_1 + \chi_2\nu_2$$

macroscale

$$\langle\sigma_s\rangle = 2\nu^*\epsilon_s^0$$

$$\langle\epsilon_s\rangle = \epsilon_s^0$$

Forward bounds for the effective viscoelasticity are fitted to well known wave-ice datasets, including *Wadhams et al. 1988, Newyear & Martin 1997, Wang & Shen 2010, Meylan et al. 2014*, and several others!

G	P	C	ρ	v	g	u
shear modulus	pressure	elasticity	density	kinematic viscosity	gravity	displacement

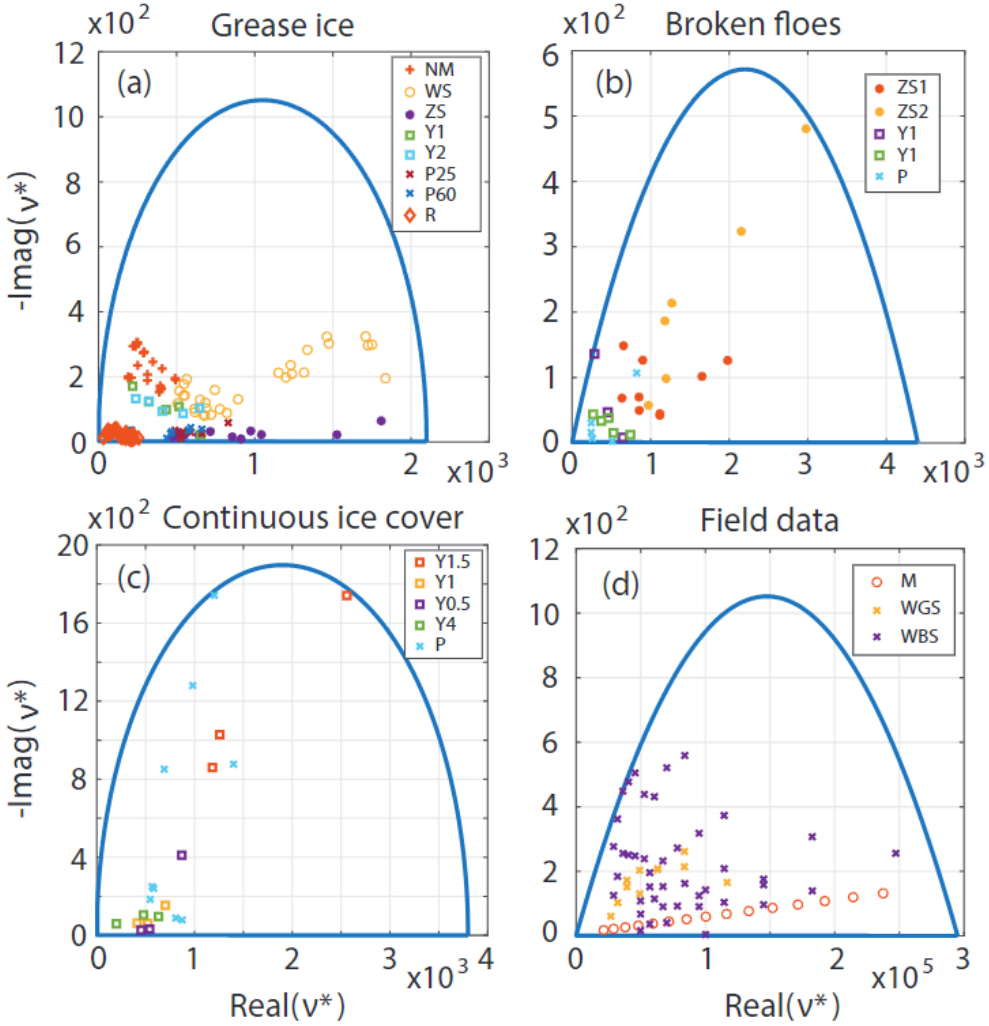

MIZ as a moving phase transition region

$$\rho c \frac{\partial T}{\partial t} = \nabla \cdot (k \nabla T) + S$$

$$S = [\rho(c_l - c_s)T + \rho L] \frac{\partial \psi}{\partial t}$$

$$\psi = 1 - \left(\frac{T - T_s}{T_l - T_s} \right)^{\alpha}$$

$$k_x = \left(\frac{\psi}{k_s} + \frac{1 - \psi}{k_l} \right)^{-1}$$

$$k_z = \psi k_s + (1 - \psi) k_l$$

homogenization

ρ effective density

T temperature

c specific heat

L latent heat of fusion

S models nonlinear phase change

ψ sea ice concentration

k effective diffusivity

l liquid, s solid

Classical small-scale application

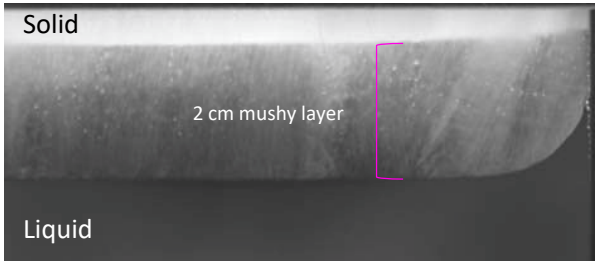

NaCl-H_2O in lab
(Peppin et al., 2007;, J. Fluid Mech.)

Macroscale application

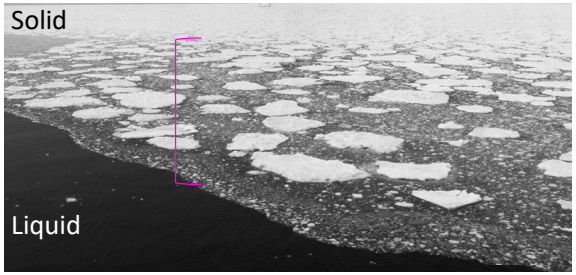

- Develop multiscale PDE model for simulating phase transition fronts to predict MIZ seasonal cycles and decadal trends
- Model simulates MIZ as a large-scale mushy layer with effective thermal conductivity derived from physics of composite materials

MIZ observations

MIZ model vs. observations

location

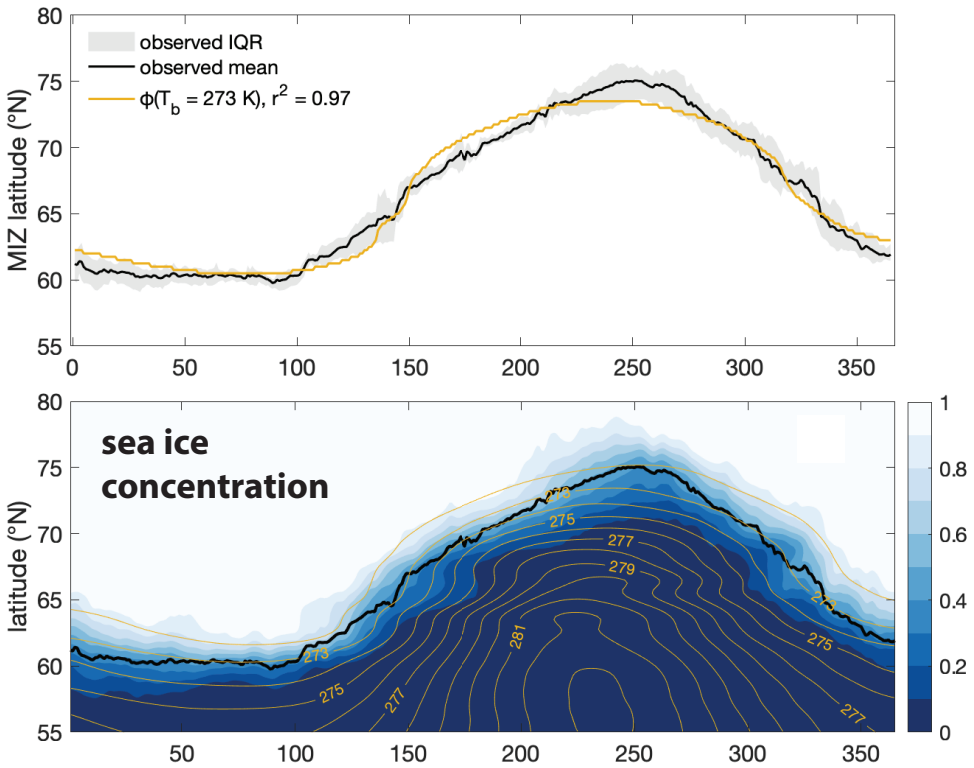

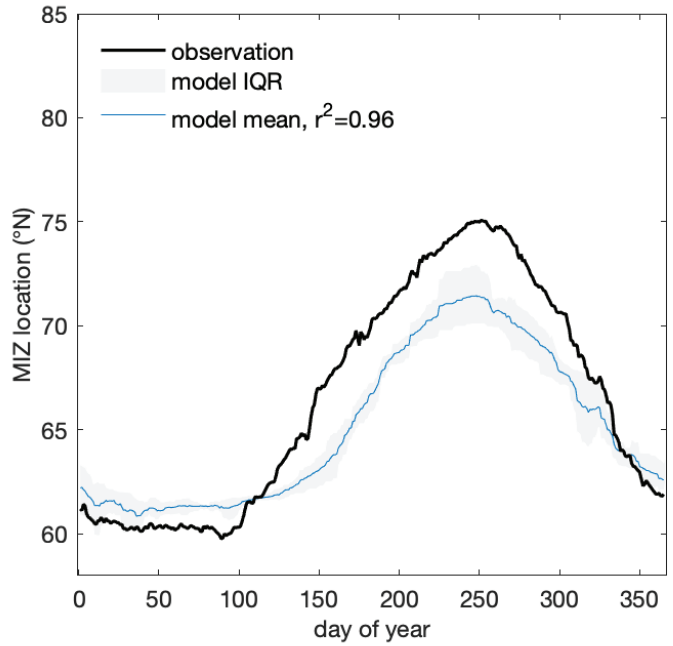

captures 96% annual cycle MIZ location; 78% width

width

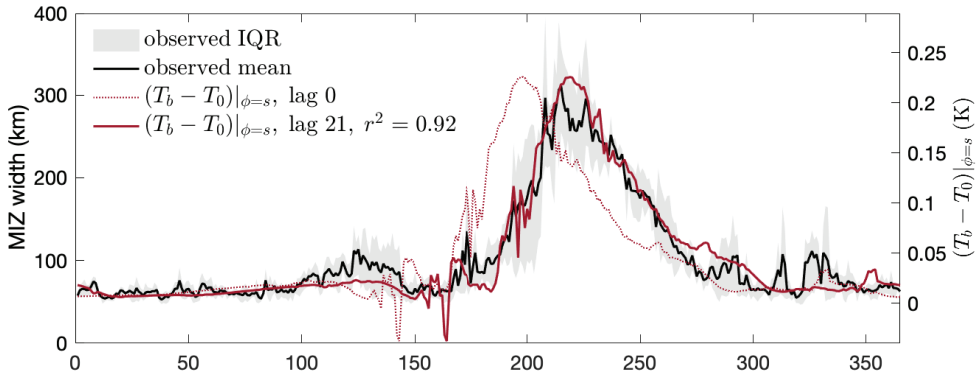

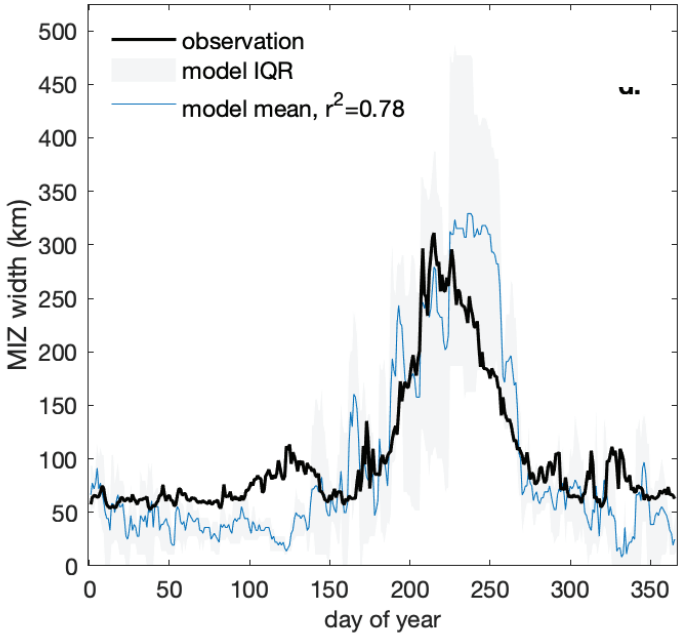

Model captures basic physics of MIZ dynamics.